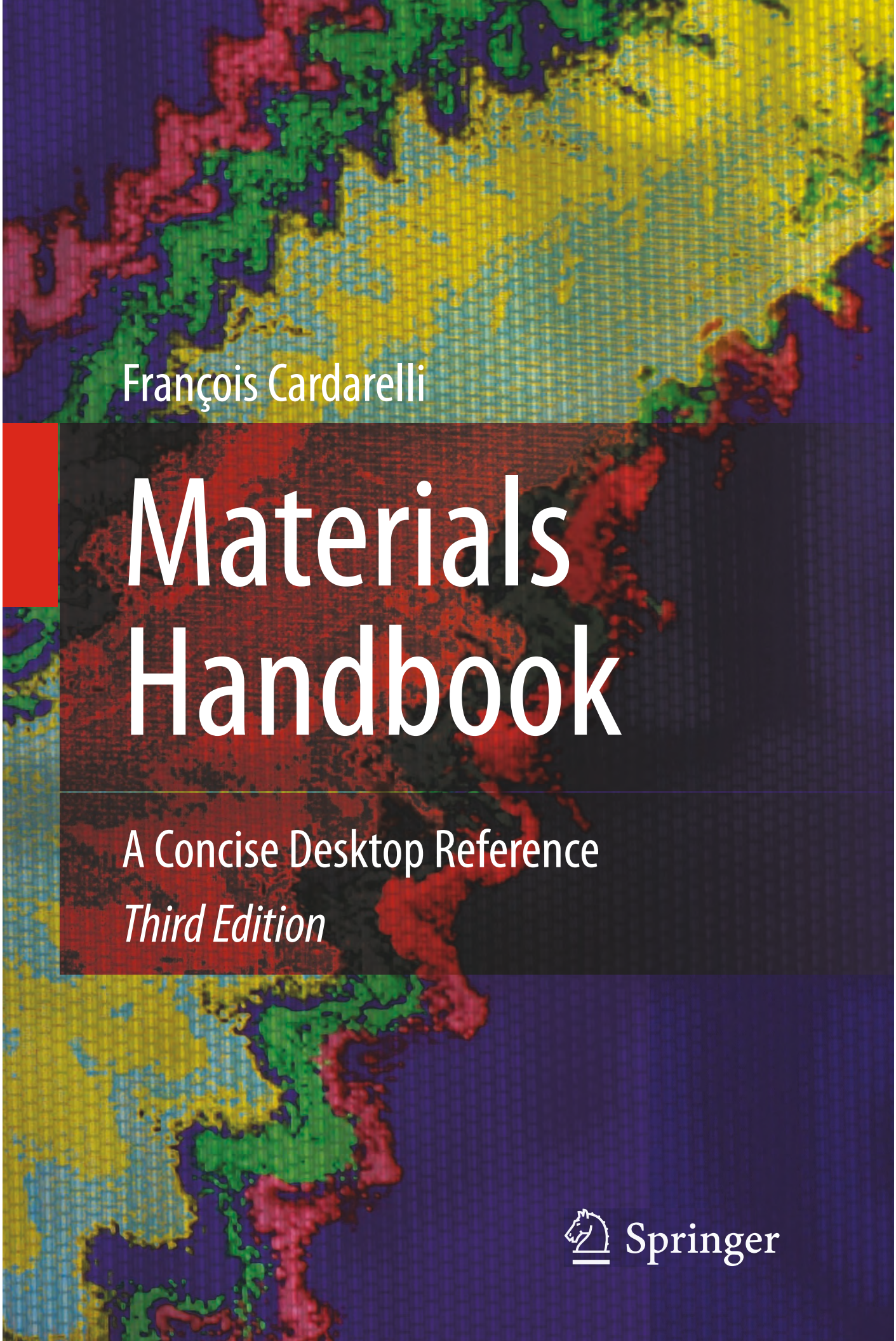
François Cardarelli
Materials Handbook
A Concise Desktop Reference
Third Edition
Springer

François Cardarelli

Materials Handbook

A Concise Desktop Reference

3rd Edition

Springer

François Cardarelli, President & Owner
Electrochem Technologies & Materials Inc.
2037 Aird avenue, Suite 201
Montréal (QC) H1V 2V9, Canada
www.electrochem-technologies.com

Email: contact@electrochem-technologies.com
contact@francoiscardarelli.ca

ISBN 978-3-319-38923-3 ISBN 978-3-319-38925-7 (eBook)
https://doi.org/10.1007/978-3-319-38925-7

Library of Congress Control Number: 2018940467

Printed on acid-free paper

This Springer imprint is published by the registered company Springer International Publishing AG, part of Springer Nature.
The registered company address is: Gewerbestrasse 11, 6330 Cham, Switzerland

Miscellaneous Electrical Materials

F. Cardarelli, *Materials Handbook,* https://doi.org/10.1007/978-3-319-38925-7_9

9.1 Thermocouple Materials

9.1.1 The Seebeck Effect

In 1821, the Estonian physicist Thomas Johann Seebeck observed that when two wires of dissimilar conductors A and B (i.e., metals, alloys, or semiconductors) are joined together at both ends and the two junctions are kept at two different temperatures – that is, cold junction temperature T_c and hot junction temperature T_h (◘ Fig. 9.1) – the temperature differential $\Delta T = (T_h - T_c)$ produces an electric current that flows continuously through the circuit. This phenomenon was called the ***Seebeck effect*** after its discoverer.

When the circuit is open, there appears an electric potential difference called the ***Seebeck electromotive force***, denoted e_{AB} and expressed in volts. This voltage is a complex function of both the temperature difference and the type of conductors [i.e., $e_{AB} = F(\Delta T, A, B)$]. In practice, the Seebeck electromotive force is related to the temperature difference by a polynomial equation, where the polynomial coefficients (i.e., c_0, c_1, c_2, c_3, etc.) are empirical constants determined by experiment and that characterize the thermocouple selected:

$$e_{AB} = c_0 + c_1\Delta T + c_2\Delta T^2 + c_3\Delta T^3 + c_4\Delta T^4 + \ldots.$$

However for a small temperature difference, the Seebeck electromotive force can be assumed to be directly proportional to the temperature difference:

$$e_{AB} = \Delta\alpha\Delta T = \Delta\alpha(T_h - T_c),$$

where the algebraic physical quantity $\Delta\alpha$ is called the ***relative Seebeck coefficient*** or the ***thermoelectric power***, denoted Q_{AB} and expressed in V/k. Thermoelectric power corresponds to the difference between the ***absolute Seebeck coefficients*** of the conductors:

$$\Delta\alpha = Q_{AB} = \alpha_A - \alpha_B.$$

In practice, the thermoelectric power of a conductor A is usually reported for a temperature difference of 100 °C between the hot and cold junctions and for a fixed second material B. The second material used as the standard is most often pure platinum and less frequently copper or even lead. Hence, the thermoelectric power is reported in modern tables in millivolts versus platinum or millivolts versus copper. Therefore, to convert a thermoelectric power measured with a given scale to another scale, the following simple equations can be used:

$$Q_{APt} = Q_{ACu} + Q_{CuPt}, \quad \text{with } Q_{CuPt} = +0.75\,\text{mV vs Pt } (0 - 100\,^\circ\text{C}),$$
$$Q_{APt} = Q_{APb} + Q_{PbPt}, \quad \text{with } Q_{PbPt} = +0.44\,\text{mV vs Pt } (0 - 100\,^\circ\text{C}).$$

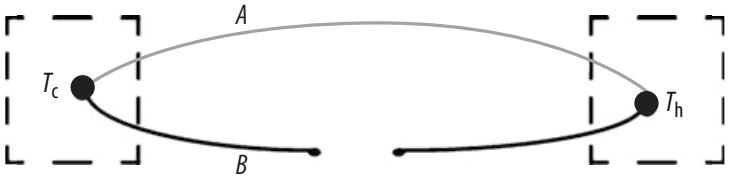

◘ **Fig. 9.1** Thermocouple basic circuit

Table 9.1 Thermoelectric power Q_{AB} of selected elements and commercial alloys (A) versus pure platinum (B is Pt) for $\Delta T = 100\,°C$ (mV vs Pt)

A	Q_{AB}	A	Q_{AB}	A	Q_{AB}	A	Q_{AB}	A	Q_{AB}	A	Q_{AB}	A	Q_{AB}
Li	+1.82	Be	n. a.	Al	+0.39	C	+0.22	As	n. a.	Se	n. a.	Ru	n. a.
Na	−0.20	Mg	+0.42	Ga	n. a.	Si	+44.8	Sb	+4.89	Te	+50.0	Rh	+0.65
K	−0.83	Ca	−0.51	In	+0.69	Ge	+33.9	Bi	−7.34	Cr	n. a.	Pd	−0.47
Rb	+0.46	Sr	n. a.	Tl	+0.58	Sn	+0.42	V	n. a.	Mo	+1.45	Os	n. a.
Cs	+0.50	Ba	n. a.	Sc	n. a.	Pb	+0.44	Nb	n. a.	W	+0.80	Ir	+0.66
Cu	+0.75	Zn	+0.76	Y	n. a.	Ti	n. a.	Ta	+0.41	Fe	+1.98	Pt	0.00
Ag	+0.73	Cd	+0.91	La	n. a.	Zr	+1.17	Mn	+0.70	Ni	−1.48	U	n. a.
Au	+0.70	Hg	+0.06	Ce	+1.14	Hf	n. a.	Re	n. a.	Co	−1.33	Th	−0.13

Commercial alloys (mV vs Pt): beryllium–copper (97.3Cu-2.7Be), +0.67; yellow brass (70Cu-30Zn), +0.60; nickel–chrome (80Ni-20Cr), +1.14; stainless steel (Fe-18Cr-8Ni), +0.44; lead solder (50Sn-50Pb), +0.46; phosphor bronze (96Cu-3.5Sn-0.3P), +0.55; Manganin (84Cu-12Mn-4Ni), +0.61; constantan (45Ni-55Cu), −3.51; Alumel (95Ni-2Mn-2Al), −1.29; Chromel (90Ni-9Cr), +2.81

n. a. not available

The thermoelectric power is commonly in the range of several mV/K for semiconductors and of several μV/K for most metals and alloys (■ Table 9.1). On the other hand, for semiconductors, the theoretical thermoelectric power can be assessed by means of the following equation:

$$Q_{AB} = -C_v/3eN_e,$$

where N_e is the electronic density in the conductor and C_v is the molar heat capacity at constant volume.

9.1.2 Thermocouple

A thermocouple is a particular temperature-sensing device consisting, in its simplest design, of two wires made of two dissimilar conductors, A and B, that are joined by two junctions. The cold junction is maintained at a well-known temperature (e.g., the ice point), while the other junction serves as a probe. The electromotive force measured with a high-precision voltmeter is then proportional to the temperature of the hot junction. The signal can even be amplified by the connecting in series of n identical thermocouples (■ Fig. 9.2).

The resulting overall electromotive force ΔV is the sum of all the individual electromotive forces of each thermocouple and is easier to measure with accuracy:

$$\Delta V = Q_{AB}\Delta T + Q_{AB}\Delta T_2 + Q_{AB}\Delta T_3 + Q_{AB}\Delta T_4 + \ldots + Q_{AB}\Delta T_n = Q_{AB}\sum_k \Delta T_k.$$

9.1.3 Properties of Common Thermocouple Materials

See ■ Tables 9.2–9.4.

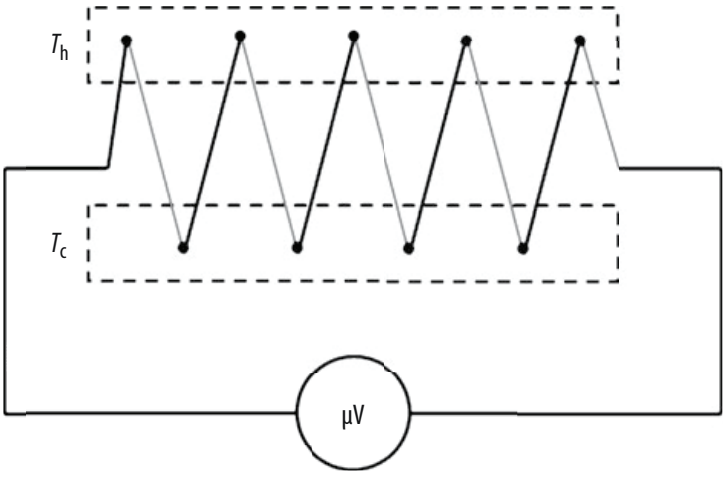

■ **Fig. 9.2** Thermocouples in series

Table 9.2 Standard thermocouple types and common uses

Type	Description
J	Suitable in reducing, vacuum, or inert atmospheres but limited use in oxidizing atmosphere at high temperature. Not recommended for low temperatures
K	Clean and oxidizing atmospheres. Limited use in vacuum or reducing atmospheres. Wide temperature range
S	Oxidizing or inert atmospheres. Beware of contamination. For high temperatures
R	Oxidizing or inert atmospheres. Beware of contamination. For high temperatures
N	Stabler than type K at high temperature
B	Oxidizing or inert atmospheres. Beware of contamination. For high temperatures
E	Oxidizing or inert atmospheres. Limited use in vacuum or reducing atmospheres. Highest thermoelectric power
C	Suitable in reducing, vacuum, or inert atmospheres. Beware of embrittlement. Not suitable for oxidizing atmospheres and not practical below 400 °C
T	Suitable in mid-oxidizing, reducing, vacuum, or inert atmospheres. Good for cryogenic applications

9.2 Resistors and Thermistors

Resistors are special conductive metals and alloys, such as Manganin®, each having an accurate and well-known electrical resistivity combined with an extremely low temperature coefficient, and for that reason they are currently used in high-precision electric and electronic instruments and devices such as calibrated resistances, shunts, and rheostats. Two major classes must be distinguished depending on their end use:

1. ***Resistance alloys*** are special conductive metals and alloys having a uniform and stable electrical resistivity combined with a constant temperature coefficient and a low thermoelectric power versus copper; Manganin and pure platinum are well-known examples.
2. ***Heating alloys*** are metals or alloys having a high electrical resistivity combined with a high melting point; hence, they are selected as heating elements in resistance furnaces; nickel–chromium is a typical example.

9.2.1 Electrical Resistivity

Electrical resistivity is an intrinsic property of a resistor material that allows the calculation of the electrical resistance, R, expressed in ohms, of a homogeneous conductor with a regular cross-sectional area, A, expressed in square meters, and a length, L, expressed in meters. R is given by the following equation, where the proportionality quantity, ρ, is the electrical resistivity of the material, expressed in ohm meters:

$$R = \rho(L/A).$$

Table 9.3 Physical properties of selected thermocouple materials

Thermocouple type (ANSI)	Metal and alloy trade names	Average chemical composition (wt%)	Junction polarity	Mass density (ρ/kg · m^{-3})	Yield strength 0.2% proof (σ_{YS}/MPa) (annealed)	Ultimate tensile strength (σ_{UTS}/MPa) (annealed)	Elongation (Z/%)	Temperature range (°C)	Thermoelectric power (μV · K^{-1})	Melting range (°C)	Coefficient of linear thermal expansion (α/10^{-6} K^{-1})	Specific heat capacity (c_p/J · kg^{-1} · K^{-1})	Thermal conductivity (k/W · m^{-1} · K^{-1})	Electrical resistivity (ρ/μΩ · cm)	Temperature coefficient of resistance (0–100 °C)
Type J	Iron	Fe	JP	7860	n. a.	234	40	0–760	50.2 (0 °C)	1539	11.7	447.7	67.78	9.67	0.0065
	Constantan	45Ni-55Cu	JN	8890	n. a.	552	32			1270	14.9	397.5	22.18	48.9	0.00002
Type K	Chromel®	90Ni-9Cr	KP	8730	n. a.	655	27	−270 to 1372	39.4 (0 °C)	1350	13.1	447.7	19.25	70	0.0032
	Alumel®	95Ni-2Mn-2Al	KN	8600	n. a.	586	32			1400	12.0	523	29.71	32	0.00188
Type N	Nicrosil®	84.3Ni-14Cr-1.4Si-0.1Mg	NP	8520	415	760	30	−270 to 1260	26.2 (0 °C)	1410	13.3	15.06	130	93	0.00011
	Nisil®	95.5Ni-4.4Si-0.1Mg	NN	8700	380	655	35			1400	12.1	26.61	230	37	0.00078
Type T	Copper OFHC	Cu (99.9 wt%)	TP	8930	69	221	46	−200 to 370	38 (0 °C)	1083	16.6	384.9	376.8	1.74	0.0043
	Constantan	45Ni-55Cu	TN	8890	n. a.	552	32			1270	14.9	397.5	22.18	48.9	0.00002
Type E	Tophel®	90Ni-10Cr	EP	8730	n. a.	670	n. a.	−200 to 870	58.5 (0 °C)	1430	13.1	447.7	19.25	70	0.00032
	Constantan	45Ni-54Cu-1Mn	EN	8890	450	552	32			1270	14.9	397.5	22.18	48.9	0.00002
Type R	Platinum–13 rhodium	87Pt-13Rh	RP	19,550	190	331	32	−50 to 1768	11.5 (600 °C)	1860	9.0	n. a.	36.81	19.6	0.0016
	Platinum	Pt	RN	21,450	70	166	38			1769	9.1	133.9	71.54	10.4	0.00393
Type S	Platinum–10 rhodium	90Pt-10Rh	SP	19,950	180	317	32	−50 to 1768	10.3 (600 °C)	1830	10.0	n. a.	37.66	18.9	0.0017
	Platinum	Pt	SN	21,450	70	166	38			1769	9.1	133.9	71.54	10.4	0.00393
Type B	Platinum–30 rhodium	70Pt-30Rh	BN	17,520	n. a.	510	26	800–1820	6.0 (600 °C)	1910	n. a.	n. a.	n. a.	19.0	0.0020
	Platinum–6 rhodium	94Pt-6Rh	BP	20,510	n. a.	255	34			1810	n. a.	n. a.	n. a.	17.5	0.0014

Table 9.3 (*continued*)

Thermocouple type (ANSI)	Metal and alloy trade names	Average chemical composition (wt%)	Junction polarity	Mass density (ρ/kg · m^{-3})	Yield strength 0.2% proof (σ_{YS}/MPa) (annealed)	Ultimate tensile strength (σ_{UTS}/MPa) (annealed)	Elongation (Z/%)	Temperature range (°C)	Thermoelectric power (μV · K^{-1})	Melting range (°C)	Coefficient of linear thermal expansion (α/10^{-6} K^{-1})	Specific heat capacity (c_p/J · kg^{-1} · K^{-1})	Thermal conductivity (k/W · m^{-1} · K^{-1})	Electrical resistivity (ρ/μΩ · cm)	Temperature coefficient of resistance (0–100 °C)
Alloy 19/20	Alloy 19	Ni-1Co	P	8900	170	415	35	0–1260	n. a.	1450	13.6	n. a.	50	8	n. a.
	Alloy 20	Ni-18Mo	N	9100	515	895	35			1425	11.9	n. a.	15	165	n. a.
Pt-Mo	Platinum-5 molybdenum	Pt-5Mo	P	n. a.	n. a.	n. a.	n. a.	1100–1500	29	1788	n. a.	n. a.	n. a.	n. a.	n. a.
	Platinum-molybdenum	Pt-0.1Mo	N	n. a.	n. a.	n. a.	n. a.			1770	n. a.	n. a.	n. a.	n. a.	n. a.
Platinel I	Palladium alloy	83Pd-14Pt-3Au	P	n. a.	n. a.	n. a.	n. a.	n. a.	41.9	1580	n. a.	n. a.	n. a.	n. a.	n. a.
	Gold-palladium	65Au-35Pd	N	n. a.	n. a.	n. a.	n. a.			1426	n. a.	n. a.	n. a.	n. a.	n. a.
Platinel II	Palladium alloy	55Pd-31Pt-14Au	P	n. a.	n. a.	n. a.	n. a.	n. a.	42.4	1500	n. a.	n. a.	n. a.	n. a.	n. a.
	Gold-palladium	65Au-35Pd	N	n. a.	n. a.	n. a.	n. a.			1426	n. a.	n. a.	n. a.	n. a.	n. a.
W-Re	Tungsten	W	P	19,900	n. a.	552	3	0–2760	16.7	3410	n. a.	n. a.	n. a.	n. a.	0.0048
	Tungsten-rhenium	W-26Re	N	19,700	n. a.	1517	10			3120	n. a.	n. a.	n. a.	n. a.	n. a.
W-Re	Tungsten-rhenium	W-3Re	P	19,400	n. a.	1241	10	0–2760	17.1	3360	n. a.	n. a.	n. a.	9.14	0.0003
	Tungsten-rhenium	W-25Re	N	19,700	n. a.	1448	10			3130	n. a.	n. a.	n. a.	27.43	0.0012
Type C	Tungsten-rhenium	W-5Re	P	19,400	n. a.	1379	10	0–2760	19.5 (600 °C)	3350	n. a.	n. a.	n. a.	11.63	n. a.
	Tungsten-rhenium	W-26Re	N	19,700	n. a.	1517	10			3120	n. a.	n. a.	n. a.	28.3	n. a.

N negative, *n. a.* not available, *OFHC* oxygen-free high conductivity, *P* positive

Table 9.4 NIST polynomial equations for thermocouples

Thermocouple type	Polynomial equation with NIST coefficients and electromotive force in volts
E	$T_E(°C) = +0.104967248 + 17{,}189.45282\,\Delta E - 282{,}639.0850\,\Delta E^2 + 1.26953395 \times 10^7\,\Delta E^3 - 4.487030846 \times 10^8\,\Delta E^4 + 1.10866 \times 10^{10}\,\Delta E^5 - 1.76807 \times 10^{11}\,\Delta E^6 + 1.71842 \times 10^{12}\,\Delta E^7 - 9.19278 \times 10^{12}\,\Delta E^8 + 2.06132 \times 10^{13}\,\Delta E^9$
J	$T_J(°C) = -0.048868252 + 1.987314503 \times 10^4\,\Delta E - 2.186145353 \times 10^5\,\Delta E^2 + 1.156919978 \times 10^7\,\Delta E^3 - 2.649175314 \times 10^8\,\Delta E^4 + 2.018441314 \times 10^8\,\Delta E^5$
K	$T_K(°C) = +0.226584602 + 2.4152109 \times 10^4\,\Delta E + 6.72334248 \times 10^4\,\Delta E^2 + 2.210340682 \times 10^6\,\Delta E^3 - 8.609639149 \times 10^8\,\Delta E^4 + 4.83506 \times 10^{10}\,\Delta E^5 - 1.18452 \times 10^{12}\,\Delta E^6 + 1.38690 \times 10^{13}\,\Delta E^7 - 6.33708 \times 10^{13}\,\Delta E^8$
R	$T_R(°C) = +0.263632917 + 1.79075491 \times 10^5\,\Delta E - 4.884034137 \times 10^7\,\Delta E^2 + 1.90002 \times 10^{10}\,\Delta E^3 - 4.82704 \times 10^{12}\,\Delta E^4 + 7.62091 \times 10^{14}\,\Delta E^5 - 7.20026 \times 10^{16}\,\Delta E^6 + 3.71496 \times 10^{18}\,\Delta E^7 - 8.03104 \times 10^{19}\,\Delta E^8$
S	$T_S(°C) = +0.927763167 + 1.69526515 \times 10^5\,\Delta E - 3.156836394 \times 10^9\,\Delta E^2 + 8.990730663 \times 10^9\,\Delta E^3 - 1.63565 \times 10^{12}\,\Delta E^4 + 1.88027 \times 10^{14}\,\Delta E^5 - 1.37241 \times 10^{16}\,\Delta E^6 + 6.17501 \times 10^{17}\,\Delta E^7 - 1.56105 \times 10^{19}\,\Delta E^8 + 1.69535 \times 10^{20}\,\Delta E^9$
T	$T_T(°C) = +0.10086091 + 2.572794369 \times 10^4\,\Delta E - 7.673458295 \times 10^5\,\Delta E^2 + 7.802559581 \times 10^7\,\Delta E^3 - 9.247486589 \times 10^9\,\Delta E^4 + 6.97688 \times 10^{11}\,\Delta E^5 - 2.66192 \times 10^{13}\,\Delta E^6 + 3.94078 \times 10^{14}\,\Delta E^7$

9.2.2 Temperature Coefficient of Electrical Resistivity

Over a narrow range of temperatures, the electrical resistivity, ρ, varies linearly with temperature according to the following equation:

$$\rho(T) = \rho(T_0)[1 + \alpha(T - T_0)],$$

where α is the ***temperature coefficient*** of electrical resistivity expressed in ohm meters per kelvin ($\Omega \cdot m \cdot K^{-1}$).

The temperature coefficient of electrical resistivity is an algebraic physical quantity (i.e., negative for semiconductors and positive for metals and alloys) defined as follows:

$$\alpha = 1/\rho_0(\partial\rho/\partial T).$$

It is important to note that in theory the temperature coefficient of electrical resistivity is different from that of the electrical resistance denoted a and defined as follows:

$$R(T) = R(T_0)[1 + a(T - T_0)],$$

where $a = 1/R_0(\partial R/\partial T)$.

Electric resistance, as defined in the previous paragraph, also involves the length and the cross-sectional area of the conductor, so the dimensional change of the conductor due to temperature change must also be taken into account. We know that both dimensional quantities vary with temperature according to their coefficient of linear thermal expansion (α_L) and the

coefficient of surface thermal expansion (α_S) respectively, in addition to that of electrical resistivity. Hence, the exact equation giving the variation of the resistance with temperature is

$$R = \rho_0[1 + \alpha(T - T_0)]\{L_0[1 + \alpha_L(T - T_0)]\}/A_0[1 + \alpha_S(T - T_0)].$$

However, in most practical cases, the two coefficients of thermal expansion are generally much smaller than the temperature coefficient of electrical resistivity. Therefore, if dimensional variations are negligible, the values of the temperature coefficient of electrical resistivity and that of electrical resistance can be assumed to be identical.

However, the exact relationship between the temperature coefficients of electrical resistance and resistivity and the thermal expansion coefficient can be obtained with use of the total differential of the electrical resistance considered a function of the three variables: $R = F(\rho, L, A)$ as follows:

$$dR = (\partial R/\partial\rho)d\rho + (\partial R/\partial L)dL - (\partial R/\partial A)dA = (L/A)d\rho + (\rho/A)dL - (\rho L/A^2)dA.$$

Thus, dividing the preceding exact differential by an arbitrarily chosen reference resistance, denoted R_0, we obtain the relative variation of the electrical resistance:

$$dR/R_0 = d\rho/\rho_0 + dL/L_0 - dA/2A_0$$

Therefore, the relative temperature coefficient is simply obtained:

$$a = (1/R_0)dR/dT = (1/\rho_0)d\rho/dT + (1/L_0)dL/dT - (1/2A_0)dA/dT,$$

where can easily recognize the mathematical equations for the temperature coefficient of electrical resistivity (α), the linear thermal expansion coefficient (α_L), and the surface thermal expansion coefficient (α_S). Hence, we obtain the following straightforward equation:

$$a = \alpha + \alpha_L - \alpha_S/2.$$

Because for isotropic materials the surface thermal expansion coefficient is exactly twice the linear coefficient, in this particular case only the temperature coefficients of resistance and resistivity are equal.

Sometimes, in practice, electrical engineers use another dimensionless physical quantity to characterize the variations of the electrical resistivity between room temperature and a given operating temperature T, which is simply termed the coefficient of temperature, denoted C_T and defined as a dimensionless ratio:

$$C_T = \rho(T)/\rho(T_0).$$

Therefore, the relationship between the temperature coefficient of electrical resistivity and the coefficient of temperature is

$$\alpha = [(C_T - 1)/(T - T_0)].$$

Example For pure platinum metal, the temperature coefficient of resistivity, α, is 0.003927 K^{-1}. This is why platinum is used extensively in high-precision devices for accurate temperature measurement called ***resistance temperature detectors*** (RTD). To calibrate these devices, the temperature coefficient of resistance for a reference resistance, denoted R_0, equal to 100 Ω between the ice point (0 °C) and the boiling point of water (100 °C) is adopted internationally as $a_{IEC} = 0.00385\ K^{-1}$ (a RTD of class B according to standard IEC-751/DIN 43760), while in the American standard (ANSI), used mostly in North America, the temperature coefficient of resistance for the same temperature range is $a_{ANSI} = 0.00392\ K^{-1}$. In Japan, $a_{JIS} = 0.003916\ K^{-1}$ (JIS-C-1604-81).

See ◘ Tables 9.5–9.7.

9.3 Electron-Emitting Materials

To extract an electron from an atom with kinetic energy K, **ionizing energy** E (i.e., thermal, mechanical, chemical, electrical, or optical) is required that is greater than the **binding energy** of the electron, B. The kinetic energy released to the ionized electron is given by $K = E - B$. In a solid, electron extraction implies the provision of electrons with sufficient energy to reach the difference between the Fermi level (i.e., the electrochemical potential of an electron inside the solid crystal lattice) and the surface potential energy at the vacuum level and absolute zero. This energy difference is called the ***electron work function***, denoted W_S, and it is expressed in joules (or electronvolts). The thermal emission of electrons, ***thermoelectronic*** or ***thermoionic emission***, is characterized by electrons leaving the surface of a material because of thermal activation. Electrons having sufficient kinetic energy on account of their thermal motion escape from the material surface, so an increase in the temperature at the surface of a material will increase the flow of electrons (i.e., electric current). The electric current density, expressed in amperes per square meter ($A \cdot m^{-2}$), as a function of the absolute temperature of the material surface is given by the ***Richardson–Dushman*** equation as follows:

$$J_S = AT^2(1 - r)\exp(-W_S/kT),$$

where A is the ***Richardson constant*** ($A \cdot m^{-2} \cdot K^{-2}$) and r is the dimensionless reflection coefficient of the surface for zero applied electric field (i.e., usually negligible). In theory, the Richardson constant would be equal to 1.2 $MA \cdot m^{-2} \cdot K^{-2}$, but in practice, because the work function is also a function of temperature, A varies over a wide range. The theoretical value of A is given in quantum theory and is

$$A = 4\pi mk^2e/h^3.$$

Electron-emitting materials (commonly referred to as thermoionic emitters) can be classified as pure-metal emitters (e.g., W, Ta), monolayer-type emitters, oxide emitters, chemical-compound emitters, and alloy emitters. Thermoionic properties of selected materials are listed in ◘ Table 9.8.

Table 9.5 Resistors used in electrical and electronic devices (shunts and rheostats)

Resistor material and composition	Mass density (ρ/kg · m^{-3})	Yield strength (σ_{YS}/MPa)	Ultimate tensile strength (σ_{UTS}/MPa)	Elongation (Z/%)	Thermal conductivity (k/W · m^{-1} · K^{-1})	Specific heat capacity (c_p/J · kg^{-1} · K^{-1})	Coefficient of linear thermal expansion up to 1000 °C (α/10^{-6} K^{-1})	Electrical resistivity (ρ/μΩ · cm)	Temperature coefficient of electrical resistivity (0–100 °C) (α/10^{-6} K^{-1})	Maximum operating temperature (T/°C)	Major uses
Alkrothal® 14 (93.8Fe-15Cr-0.7Si-0.5Mn)	7280	445–455	600–630	22	16	460	15	125		1100	Electrical resistance wire for low-temperature applications
Constantan (45Ni-54Cu-1Mn)	8890	450	552	32		410	19.5	48.9	–20	600	Wire-wound precision resistors, potentiometers, volume-control devices, winding heavy-duty industrial rheostats, and electric motor resistances
Kanthal® 52 (52Ni-48Fe)	8200	340	610	30	17	500	10	37	3300		Low-resistivity material with a high temperature coefficient of resistance used in voltage regulators, timing devices, temperature-sensitive resistors, temperature-compensating devices, and low-temperature heating applications
Kanthal® 70 (70Ni-30Fe)	8450	340	640	30	17	520	15	21	3500	600	
Manganin® (84Cu-12Mn-4Ni)	8410	275	620		20		18.7	48.2	15		Material with low coefficient of resistance used in shunts
Manganin® shunt (86Cu-10Mn-4Ni)	8420	345	690				18.7	38	10		
MnLow	8410		420–690	25				43			Precision electrical measuring apparatus and resistors
Nichrome® 80-20	8300	300–420	725–810	30	15	460	18	109	50	1100	Heaters
Resistor alloy 30	8900	290	640	25				30		400	General resistance wires, cores of low-temperature heaters, resistance elements of heaters for electrical circuit breakers/fuses
Resistor alloy 15	8900	340	690	25				15		400	
Resistor alloy 10	8900	230	680	25				10		400	
Resistor alloy 5	8900	220	440	25				5		400	

Table 9.6 (*continued*)

Class	Resistor material and composition	Density (ρ/kg · m^{-3})	Yield strength (σ_{YS}/MPa)	Ultimate tensile strength (σ_{UTS}/MPa)	Elongation (Z/%)	Thermal conductivity (k/W · m^{-1} · K^{-1})	Specific heat capacity (c_p/J · kg^{-1} · K^{-1})	Coefficient of linear thermal expansion up to 1000 °C (α/10^{-6} K^{-1})	Electrical resistivity (ρ/μΩ · cm)	Temperature coefficient of electrical resistivity (0–100 °C) (α/10^{-5} K^{-1})	Melting point (°C)	Maximum operating temperature (°C)	Applications
Medium temperature (up to 1400 °C)	Nichrome® 35-20 (42Fe-35Ni-20Cr-2Si-1Mn)	7900	450	750	30	13	500	19	104	230	1390	1000	Industrial furnaces, heating elements of cooking equipment
	Nichrome® 40-20 (40Ni-38Fe-20Cr-1Mn-1Si)	7900	300–450	650–750	30	13	500	19	96–105	230	1390	1050	Domestic heating appliances, industrial furnaces (carburizing or semireducing atmosphere)
	Nichrome® 60-15 (60Ni-20Fe-18Cr-1Mn-1Si)	8200	300–370	700–730	30–35	13	480	17	112	110	1390	1150	Industrial furnaces, electrically heated equipment, high-resistance and potentiometer resistors
	Nichrome® 80-20 (78Ni-20Cr-1Fe-1Si)	8300	300–420	725–810	30	15	460	18	109	50	1400	1200	Industrial furnaces, electric cooking equipment, precision resistors (oxidizing, reducing, or vacuum atmosphere)
	Nichrome® 70-30 (68Ni-30Cr-1Mn-1Si)	8100	425–430	800–820	30	14	460	17	118	50	1380	1250	Industrial furnaces, precision resistors
	Kanthal® AE (Fe-22Cr-5.3Al-0.7Si-0.4Mn-0.08C)	7150	520	720	20	11	460	15	139	60	1500	1300	Heating elements for ceramic glass top hobs and quartz tube heaters
	Kanthal® AF (Fe-22Cr-5.3Al-0.7Si-0.4Mn-0.08C)	7150	475–500	680–700	18–23	11	460	15	139	60	1500	1300	Heating elements in industrial furnaces and in electrical appliances
	Kanthal® A (Fe-22Cr-5.3Al-0.7Si-0.08C)	7150	550	725	22		460	15	139	60	1500	1350	

Table 9.6 (*continued*)

Class	Resistor material and composition	Density (ρ/kg · m^{-3})	Yield strength (σ_{YS}/MPa)	Ultimate tensile strength (σ_{UTS}/MPa)	Elongation (Z/%)	Thermal conductivity (k/W · m^{-1} · K^{-1})	Specific heat capacity (c_p/J · kg^{-1} · K^{-1})	Coefficient of linear thermal expansion up to 1000 °C (a/10^{-6} K^{-1})	Electrical resistivity (ρ/μΩ · cm)	Temperature coefficient of electrical resistivity (0–100 °C) (a/10^{-5} K^{-1})	Melting point (°C)	Maximum operating temperature (°C)	Applications
Medium temperature (up to 1400 °C)	Kanthal® A-1 (Fe-22Cr-5.8Al-0.7Si-0.08C)	7100	475–545	680–780	18–20	26	460	15	145	40	1500	1400	High-temperature furnaces for heat treatment and firing of ceramics; oxidizing and carburizing atmospheres
	Kanthal® APM (Fe-22Cr-5.8Al-0.7Si-0.4Mn-0.08C)	7100	470	680	20	26	460	16	145	40	1500	1425	High-temperature furnaces in electronics industries and in diffusion furnaces
High temperature (up to 1700 °C)	Silicon carbide (SiC)	3200		28				4.7	99–199		2410	1650	Oxidizing atmosphere
	Platinum (Pt)	21,450				71.6	132	9.1	9.81	3920	1772	1600	Oxidizing, reducing, or vacuum atmosphere
Super high temperature (1900–3000 °C)	Molybdenum disilicide ($MoSi_2$)	6240		185				9.2–13.1	27–37		2050	1950	Oxidizing atmosphere to maintain protective silica layer
	Ziconia, yttria stabilized (ZrO_2-8 mol% Y_2O_3)											1500–2000	Secondary resisting coil requires a preheater to reach 800 °C
	Molybdenum (Mo)	10,220				142	251	5.43	5.2	4350	2621	2000	Reducing or vacuum atmosphere
	Tantalum (Ta)	16,654				58	140	6.6	12.45	3820	2996	2300	Reducing or vacuum atmosphere
	Graphite (C)	1600		1.8		350	709	1.3	910		3650	3000	Reducing or vacuum atmosphere
	Tungsten (W)	19,300				71	136	4.59	5.65	4800	3413	3000	Reducing or vacuum atmosphere

Table 9.7 Upper temperature limits (°C) for selected high-temperature resistors in various furnace atmospheres

High-temperature resistor	Ar	CO	He	N_2	CO_2	NH_3	CH_4	H_2
Graphite	3000	3000	3000	2200	900	2200	3000	2700
Molybdenum	1650	1400	1650	1650	1200	2200	1100	1650
Tantalum	2800	1000	2800	2000	1250	400	900	1000
Tungsten	3000	800	3000	2300	1200	3000	900	3000

Table 9.8 Thermoionic properties of selected materials

Material	Electron work function (W_S/eV)	Richardson constant (A/kA · m^{-2} · K^{-1})	Material	Electron work function (W_S/eV)	Richardson constant (A/kA · m^{-2} · K^{-1})
Ferrous metals			**Refractory carbides**		
Iron (ferrite)	4.5	260	Carbon	5.0	150
Cobalt	5.0	410	TaC	3.14	3
Nickel	4.61	300	TiC	3.35	250
Common nonferrous metals			ZrC	2.18	3
Copper	4.65	1200	SiC	3.5	640
Other metals			ThC_2	3.5	5500
Beryllium	4.98	3000	**Refractory borides**		
Barium	2.52	600	CeB_6	2.6	36
Caesium	2.14	1600	LaB_6	2.7	290
Platinum group metals			ThB_6	2.9	5
Osmium	5.93	1,100,000	CaB_6	2.9	26
Rhodium	4.98	330	BaB_6	3.5	160
Iridium	5.27	1200	**Refractory oxides**		
Platinum	5.65	320	ThO_2	2.6	50
Refractory metals (groups IVB, VB, and VIB)			CeO_2	2.3	10
Titanium	4.53	n. a.	La_2O_3	2.5	9
Zirconium	4.05	3300	Y_2O_3	2.4	10
Hafnium	3.60	220	BaO-SrO	1.0	10
Niobium	4.19	1200	**Uranides**		
Tantalum	4.25	1200	Uranium	3.27	60
Molybdenum	4.15	550	Thorium	3.38	700
Tungsten	4.55	600			

n. a. not available

9.4 Photocathode Materials

When monochromatic electromagnetic radiation with frequency v, expressed in hertz, illuminates the surface of a solid, some electrons (i.e., photoelectrons) can be emitted if the incident photon energy, hv, is equal to or greater than the binding energy of the electron in the atom of the solid. Because the energy transfer occurs between photons and electrons, this behavior is called the ***photoelectric effect***. More precisely, Einstein demonstrated in the early twentieth century that the ***maximum kinetic energy***, K_{max}, released by electromagnetic radiation to photoelectrons is given by the energy difference between the incident photon energy and the electron binding energy in the atoms of a solid: $K_{max} = hv - hv_0$, where $B = hv_0$ is the ***binding energy*** of the electron inside the solid, which corresponds to the ***electron work function*** in the emitting material (i.e., $e\Phi$). For a given incident radiation energy, the ratio between the number of photoelectrons and the number of incident photons is called the ***photoelectric quantum yield*** or ***efficiency***. Owing to magnitude of the binding electronic energies, the photoelectric effect occurs in metals for electromagnetic radiation having a frequency higher than that of near ultraviolet. Even if all solid materials exhibit a photoelectric effect under irradiation by appropriate electromagnetic radiation (e.g., UV, X-rays, gamma rays), the common metals exhibiting the photoelectric effect for low-energy photons and currently used as photocathodes are the alkali and alkaline earth metals and some of their alloys deposited onto an antimony coating. For instance, rhenium metal, with an electronic work function of roughly 5.0 eV, requires at least UV radiation with a wavelength of 248 nm for emission of photoelectrons, while cesium requires only irradiation by visible light with a wavelength of 652 nm or lower. Selected properties of some common photocathode materials are listed in ◘ Table 9.9. As a general rule, photocathode materials are extensively used in photocells and photomultiplier tubes.

It is important to make a clear distinction between the photoelectric effect, which occurs during the extraction of electrons of an atom that are part of a crystal lattice in a solid by incident electromagnetic radiation, and ***photoemission***, which consists of the extraction of electrons (i.e., ionization) of a free atom in a vapor by incident electromagnetic radiation.

9.5 Secondary Emission

When a flux of electrons is incident on a surface of a solid, secondary electrons are produced and emitted in a vacuum. These secondary electrons can be grouped into several types according to their origin: true secondary electrons with a kinetic energy of about 10 eV independent of that of the primary energy, and primary electrons scattered both elastically (i.e., coherent scattering) and inelastically (i.e., incoherent scattering). The dimensionless ratio of secondary electrons to other primary electrons is called the ***secondary emission coefficient***, denoted δ. The secondary emission coefficient reaches a maximum value, δ_{max}, for a definite maximum energy of incident electrons, E_{max}, and afterward decrease slowly for higher kinetic energies (see ◘ Table 9.10).

9.6 Electrolytes

Electrolytes are distinguished from pure electronic conductors by the fact that the passage of an electric current is only ensured by displacement of charged species called ions and hence is accompanied by a transfer of matter. Therefore, electrolytes are entirely ionic electrical conductors without exhibiting any electronic conductivity (i.e., no free electrons). They can be found in

Table 9.9 Photocathode metals and alloys

Photocathode materials	Electron work function (W_S/eV)	Wavelength (λ/nm)	Photoelectric quantum yield
Lithium	2.4	517	10^{-4}
Sodium	2.2	564	10^{-4}
Potassium	2.2	564	10^{-4}
Rubidium	2.1	591	10^{-4}
Cesium	1.9	653	10^{-4}
Calcium	2.9	428	10^{-4}
Strontium	2.7	459	10^{-4}
Barium	2.5	496	10^{-4}
Na_3Sb	3.1	400	0.02
K_3Sb	2.6	478	0.07
Rb_3Sb	2.2	564	0.10
Cs_3Sb	2.05	605	0.25
NaK_3Sb	2.0	620	0.30
$CsNaK_3Sb$	1.55	800	0.40

The correspondence between the energy of the incident photon expressed in electronvolts and the wavelength expressed in nanometers of the associated electromagnetic radiation is given by the Duane and Hunt relation: λ(nm) = 1239.85207/E(eV)

the solid state (e.g., fluorite, beta aluminas, yttria-stabilized zirconia, and silver iodide), liquid state (e.g., aqueous solutions, organic solvents, molten salts, and ionic liquids), and gaseous state (e.g., ionized gases and plasmas). The ions (i.e., anions or cations) ensure the proper ionic conductivity by moving under the electrical field imposed by the electrodes. Usually, electrolytes can be grouped into three main classes:

1. **Pure electrolytes.** This class is entirely represented by molten or fused salts (e.g., molten cryolite, Na_3AlF_6) and usually requires high temperatures – largely above the melting or liquidus temperature of the salt – to provide sufficient ionic conductivity.
2. **Ionic solutions.** This class is represented by electrolytic solutions and is also split into two subclasses according to ionic conductivity and dissociation constant.
   (a) **Strong electrolytes** (ionophores)**.** Potassium chloride (KCl) is the main example of the class of ionophores – that is, pure ionic compounds (solids, liquids, or gases) already made of anions and cations. The dissolution of these ionophores simply involves the dispersion of preexisting ions of the crystal lattice in an appropriate solvent, followed by reorganization of solvent molecules around ions (i.e., the solvation process). This phenomenon strongly depends on the relative electric permittivity ε_r (i.e., formerly the dielectric constant) of the solvent. In ionizing solvents – those, such as water (ε_r = 78.36 at 298.15 K), having a high electric permittivity – the coulombic interaction between ions is strongly decreased. Hence, ions maintain a certain independence in their displacement, and they are totally dissociated (i.e., ionized). By contrast, in inert solvents (e.g., benzene) – those exhibiting the low electric permittivity – ionic entities such as

Table 9.10 Secondary emission characteristics of selected materials

Material	Maximum incident energy (E_{max}/eV)	Maximum secondary emission coefficient (δ_{max})	Material	Maximum incident energy (E_{max}/eV)	Maximum secondary emission coefficient (δ_{max})
Ferrous metals			**Halides**		
Iron	200	1.30	CsCl	n. a.	6.50
Cobalt	500	1.35	LiF	n. a.	5.60
Nickel	450	1.35	NaF	n. a.	5.70
Common nonferrous metals			NaBr	n. a.	6.30
Copper	600	1.28	NaCl	600	6.80
Other metals			KCl	1500	8.00
Beryllium	200	0.50	**Oxides and sulfides**		
Barium	300	0.85	BeO	400	8.00
Caesium	400	0.72	MgO	1600	15
Platinum group metals			Al_2O_3	1300	3.00
Palladium	550	1.65	Cu_2O	440	1.20
Ruthenium	570	1.40	SiO_2	300	2.20
Iridium	700	1.50	ZnS	350	1.80
Platinum	720	1.60	MoS_2	n. a.	1.10
Reactive and refractory metals (groups IVB, VB, and VIB)					
Titanium	280	0.90	Niobium	350	1.20
Zirconium	350	1.10	Tantalum	600	1.25
Chromium	400	1.10	Molybdenum	350	1.20
Tungsten	650	1.35	Thorium	800	1.10

n. a. not available

pairs or clusters form, losing their freedom. For instance, in a series of solvents of decreasing permittivity, ions form double, triple, and quadruple associations such as $LiBF_4$ in dimethoxyethane ($\varepsilon_r = 7.15$ at 298.15 K).

(b) **Weak electrolytes.** In this case the solute is only partially ionized (e.g., NH_4Cl in water). Salts obtained by the neutralization of a weak acid by a strong base (e.g., $CH_3COO^-Na^+$), a weak base by a strong acid (e.g., NH_4Cl), or a weak acid by a weak base (e.g., $CH_3COO^-NH_4^+$) are typical examples of weak electrolytes.

3. **Solid electrolytes.** These correspond to solid materials in which the ionic mobility is ensured by various intrinsic and extrinsic defects and are called ***solid ion conductors***. Common examples are ion-conducting solids with rock salt or halite-type solids with a B1 structure (e.g., α-AgI), oxygen-conducting solids with a fluorite-type C1 structure ($A^{II}O_2$), for instance, CaF_2 and yttria-stabilized zirconia (ZrO_2 with 8 mol% Y_2O_3), or a pyrochlore structure ($A_2B_2O_7$),

perovskite-type oxides ($A^{II}B^{IV}O_3$), $La_2Mo_2O_9$, or solids with a spinel-type structure such as beta aluminas ($NaAl_{11}O_{17}$), for which the ionic conduction is ensured by Na^+ mobility.

See ◘ Table 9.11.

9.7 Electrode Materials

9.7.1 Electrode Materials for Batteries and Fuel Cells

In power sources (i.e., primary and secondary batteries, and fuel cells) the electrode material of both the cathode and the anode must exhibit a high standard electrode potential, expressed in volts (V). An anode material must be highly electropositive (i.e., reducing), while a cathode material must be highly electronegative (i.e., oxidizing). The second important physical quantity required to select the most appropriate electrode material is its electrochemical equivalence. The ***electrochemical equivalence*** of an electrode material expresses the available electric charge stored per unit mass of material, and hence it is expressed in coulombs per kilogram ($C \cdot kg^{-1}$) or ampere hours per gram ($Ah \cdot g^{-1}$) and is calculated with the following equation:

$$\text{Eq} = nF/vM,$$

where n is the number of electrons required to oxidize or reduce the electrode material, F is the Faraday constant (96,485.309 $C \cdot mol^{-1}$), v is the dimensionless stoichiometric coefficient of the electrochemical reduction or oxidation, and M is the atomic or molecular mass of the electrode material in kilograms per mole or grams per mole. Sometimes the electrochemical equivalence per unit volume is used, and it is expressed as the electric charge stored per unit volume of material ($Ah \cdot m^{-3}$); in this particular case, it can be calculated by multiplication of the specific electrochemical equivalence by the density of the electrode material (see ◘ Table 9.12).

In addition, in primary and rechargeable batteries, apart from the two previous parameters, several technological requirements must be considered when one is selecting the most appropriate electrode. These requirements are high electrical conductivity, chemical inertness, ease of fabrication, involvement of nonstrategic materials, low cost, and commercial availability. As a general rule, metals and alloys are the major anode materials in batteries, except for the case of hydrogen in fuel cells, while metallic oxides, hydroxides, chlorides, and sulfides are the major anodic materials, except for the case of oxygen in fuel cells.

9.7.2 Intercalation Compounds

Insertion, also called intercalation, is a topotactic reaction that consists of the insertion of a species, atom, or molecule inside the interstitial crystal lattice of a solid host material, with or without charge transfer. Historically, the first intercalation compounds were the graphites (1841), for which the intercalation of cations of alkali metals occurred between the graphene lamellar planes and the hydrogen–palladium system (1866). Later, in 1959, the phenomenon was recorded in lamellar dichalcogenides, and since the 1970s hundreds of new compounds have been reported, several of them now being used in rechargeable batteries such as nickel–metal hydride or lithium batteries.

Table 9.11 Ionic electrical conductivity of various electrolytes

Molten oxide	Ionic conductivity (κ/S · m^{-1})	Molten-salt electrolyte or eutectic mixture (melt temperature)	Ionic conductivity (κ/S · m^{-1})	Aqueous electrolyte	Ionic conductivity (κ/S · m^{-1})	Solid-state ionic conductor	Ionic conductivity (κ/S · m^{-1})
FeO (1370 °C)	12,200	LiF (1000 °C)	920	H_2O (distilled)	5.5×10^{-6}	Yttria-stabilized zirconia (8–10 mol% Y_2O_3)	0.2 (800 °C)
TiO_2 (1850 °C)	10,000	LiCl (801 °C)	659	HNO_3 (31 wt%)	78.10		0.3 (900 °C)
MgO (2800 °C)	3500	LiF-NaF (800 °C)	580	HCl (20.2 wt%)	76.15		1.0 (1000 °C)
CaO (2580 °C)	4000	NaF (1000 °C)	494	H_2SO_4 (30 wt%)	73.88	Ceria-stabilized zirconia	0.6 (1200 °C)
Al_2O_3 (2050 °C)	1500	NaCl (1000 °C)	416	KOH (29.4 wt%)	54.34	Fluorite (CaF_2)	n. a.
SiO_2 (1710 °C)	0.1	CaF_2 (1500 °C)	410	NaOH (15 wt%)	34.90	Silver iodide (AgI)	10 (150 °C)
		KF (980 °C)	392	LiOH (7.5 wt%)	29.99	Beta aluminas ($NaAl_{11}O_{17}$)	3–5
		KOH (600 °C)	369	KCl (21 wt%)	28.10	Titania-rich chloride slag (1600 °C)	30
		NaOH (450 °C)	327	K_2CO_3 (30 wt%)	22.22	Semigraphite	1.125×10^5
		Na_2CO_3 (950 °C)	322	NaCl (26 wt%)	21.51		
		$CaCl_2$ (1000 °C)	266	$CaCl_2$ (25 wt%)	17.81		
		KCl (1200 °C)	265	LiCl (20 wt%)	16.76		
		Na_2SO_4 (1050 °C)	264	$MgCl_2$ (20 wt%)	14.02		
		NaCl-KCl (750 °C)	249	Na_2SO_4 (15 wt%)	8.86		
		K_2CO_3 (1000 °C)	232	K_2SO_4 (10 wt%)	8.60		
		LiCl-KCl (520 °C)	197	$FeCl_2$ (14.4 wt%)	8.43		
		K_2SO_4 (1100 °C)	184	$MgSO_4$ (15 wt%)	4.80		
		$MgCl_2$ (1000 °C)	158	$FeSO_4$ (18.97 wt%)	4.61		
		NaOH-KOH (178 °C)	43.6				

In the particular case of lithiation or delithiation of cathode materials used in lithium secondary batteries, the calculation of the electrochemical equivalent involves an additional parameter related to the reaction of intercalation of lithium cations into the crystal lattice of the host cathode materials. Consider the theoretical reversible reaction of intercalation of lithium into a crystal lattice of a solid host material (e.g., oxide, sulfide):

$$x\mathrm{Li}^+ + y\mathrm{M} + xe^- \longleftrightarrow \mathrm{Li}_x\mathrm{M}_y,$$

where Li^+ represents lithium cations, M represents the solid host cathode material, x and y represent dimensionless stoichiometric coefficients, and x also represents the dimensionless number of electrons exchanged.

Hence, during the lithiation reaction (i.e., charge), x moles of lithium cations are reduced and intercalated into y moles of the solid host material, and a quantity of electricity, xF, must be supplied to the cell. Conversely, during delithiation (i.e., discharge), x moles of lithium cations are produced and a quantity of electricity, xF, is supplied to the external circuit of the cell. Therefore, the quantity of electricity, Q, expressed in coulombs (or ampere hours), delivered following the deintercalation of lithium from a mass, m_{M}, of the solid host material or a mass, $m_{\mathrm{Li}_x\mathrm{M}_y}$, of the final intercalated compound is given by the following relations:

$$Q = m_{\mathrm{M}}(xF/yM_{\mathrm{M}}) = m_{\mathrm{Li}_x\mathrm{M}_y}(xF/M_{\mathrm{Li}_x\mathrm{M}_y}),$$

where is m_{M} the mass of the solid host material (kg), $m_{\mathrm{Li}_x\mathrm{M}_y}$ is the mass of the intercalated compound (kg), x and y are dimensionless stoichiometric coefficients, M_{M} is the molar mass of the solid host material ($\mathrm{kg \cdot mol^{-1}}$), $M_{\mathrm{Li}_x\mathrm{M}_y}$ is the molar mass of the intercalated compounds ($\mathrm{kg \cdot mol^{-1}}$), x is also the dimensionless number of electrons exchanged, and F is the Faraday constant (96,485.309 $\mathrm{C \cdot mol^{-1}}$).

From the preceding equation it is possible to define two types of electrochemical equivalents. The first electrochemical equivalent, denoted Eq(M), is the quantity of electricity consumed per unit mass of the solid host material, M, during the lithiation reaction (i.e., charging) and is defined by the following equation:

$$\mathrm{Eq(M)} = xF/yM_{\mathrm{M}}.$$

The second electrochemical equivalent, denoted $\mathrm{Eq(Li}_x\mathrm{M}_y)$, is the quantity of electricity released per unit mass of the intercalated compound, $\mathrm{Li}_x\mathrm{M}_y$, during the delithiation reaction (i.e., discharging) and is defined by the following equation:

$$\mathrm{Eq(Li}_x\mathrm{M}_y) = xF/M_{\mathrm{Li}_x\mathrm{M}_y}.$$

The two electrochemical equivalents of some selected solid host cathode materials and corresponding intercalated compounds used in rechargeable lithium batteries are presented in Table 9.13.

Table 9.12 Electrochemical equivalents of common anode and cathode materials used in primary and secondary cells (293.15 K and 101.325 kPa)

Electrode material		Electrochemical half-reaction	E^0_{298} (V vs SHE)	M_r[a] ($^{12}C = 12$)	Density[b, c, d] ($kg \cdot m^{-3}$)	Eq ($Ah \cdot kg^{-1}$)	Eq ($Ah \cdot dm^{-3}$)
Anode materials (negative)	Al	$Al^0 \rightarrow Al^{3+} + 3e^-$	−1.676	26.981538	2699	2980	8043
	Ca	$Ca^0 \rightarrow Ca^{2+} + 2e^-$	−2.840	40.078	1550	1337	2073
	Cd	$Cd^0 \rightarrow Cd^{2+} + 2e^-$	−0.403	112.411	8650	477	4125
	Fe	$Fe^0 \rightarrow Fe^{2+} + 2e^-$	−0.440	55.845	7874	960	7558
	$H_2(g)$	$H_2(g) \rightarrow 2H^+ + 2e^-$	0.000	2.01594	0.084	26,590	2234
	Li	$Li^0 \rightarrow Li^+ + e^-$	−3.040	6.941	534	3861	2062
	Mg	$Mg^0 \rightarrow Mg^{2+} + 2e^-$	−2.356	24.3050	1738	2205	3833
	Na	$Na^0 \rightarrow Na^+ + e^-$	−2.713	22.989770	971	1166	1132
	Pb	$Pb^0 \rightarrow Pb^{2+} + 2e^-$	−0.126	207.2	11,350	259	2936
	Zn	$Zn^0 \rightarrow Zn^{2+} + 2e^-$	−0.760	65.409	7133	820	5846

Table 9.12 (*continued*)

Electrode material		Electrochemical half-reaction	E^0_{298} (V vs SHE)	M_r[a] ($^{12}C = 12$)	Density[b, c, d] ($kg \cdot m^{-3}$)	Eq ($Ah \cdot kg^{-1}$)	Eq ($Ah \cdot dm^{-3}$)
Cathode materials (positive)	Ag_2O	$Ag^+ + e^- \rightarrow Ag^0$	+0.7991	231.7358	7200	231	1665
	AgO	$AgO + 2H^+ + e^- \rightarrow Ag^0 + H_2O$	+1.772	123.8676	7500	433	3246
	$Cl_2(g)$	$Cl_2 + 2e^- \rightarrow 2Cl^-$	+1.360	70.906	2948	756	2229
	HgO	$HgO + 2H^+ + 2e^- \rightarrow Hg^0 + H_2O$	+0.926	216.5894	11,140	248	2757
	$I_2(s)$	$I_2(s) + 2e^- \rightarrow 2I^-$	+0.5356	253.80894	4933	212	1045
	MnO_2	$MnO_2 + 4H^+ + e^- \rightarrow Mn^{3+} + 2H_2O$	+0.950	86.936849	5080	308	1566
	NiOOH	$2NiOOH + 2H^+ + 2e^- \rightarrow 2Ni(OH)_2$	+0.490	91.70017	7400	292	2160
	$O_2(g)$	$O_2 + 4H^+ + 4e^- \rightarrow 2H_2O$	+1.229	31.9988	1330	3350	4456
	PbO_2	$PbO_2 + 4H^+ + 2e^- \rightarrow Pb^{2+} + H_2O$	+1.460	239.1988	9640	224	2160
	$SO_2(l)$	$2SO_2 + 2e^- \rightarrow S_2O_4^{2-}$	n. a.	64.0638	1370	419	n. a.
	$SOCl_2(l)$	$2SOCl_2 + 4e^- \rightarrow S + SO_2 + 4Cl^-$	n. a.	118.9704	1631	901	1470
	V_2O_5	$VO_2^+ + 2H^+ + e^- \rightarrow VO^{2+} + H_2O$	1.000	181.880	3350	147	494

n. a. not available, *SHE* standard hydrogen electrode

[a] Standard relative atomic masses from Loss, R.D. (2003) *Atomic Weights of the Elements 2001. Pure Appl. Chem.*, **75**(8), 1107–1111

[b] Densities of pure elements from Cardarelli, F. (2001) *Materials Handbook. A Concise Desktop Reference.* Springer, Berlin Heidelberg New York

[c] Densities of inorganic compounds from Lide, D.R. (ed.) (1997–1998) *CRC Handbook of Chemistry and Physics,* 78th ed. CRC Press, Boca Raton, FL, pp. 4–35 to 4–9

[d] Densities for ideal gases calculated with the equation $\rho = PM/RT$ at 293.15 K and 101.325 kPa

Table 9.13 Electrochemical equivalents of solid host materials and intercalated compounds for rechargeable lithium batteries

Host cathode material	Insertion reaction(lithiation/delithiation)	E^0_{298} (V vs Li^+)	M_r[a]		Density[b] ($kg \cdot m^{-3}$) (M)	Eq (Li_xM_y) ($Ah \cdot kg^{-1}$)	Eq(M) ($Ah \cdot kg^{-1}$)
			Li_xM_y	M			
C	$Li^+ + 6C + e^- \leftrightarrow LiC_6$		79.0070	12.011	2200	339	372
FeS_2	$Li^+ + FeS_2 + e^- \leftrightarrow LiFeS_2$		126.9180	119.9770	5020	211	223
$FePO_4$	$Li^+ + FePO_4 + e^- \leftrightarrow LiFePO_4$		157.7574	150.8164		167	178
$Li_{1.2}V_3O_8$	$2.8Li^+ + Li_{1.2}V_3O_8 + 2.8e^- \leftrightarrow Li_4V_3O_8$		308.5837	289.1489		243	260
$Li_{0.5}CoO_2$	$0.5Li^+ + Li_{0.5}CoO_2 + 0.5e^- \leftrightarrow LiCoO_2$	3.7	97.8730	94.4025		137	142
$Li_{0.5}NiO_2$	$0.5Li^+ + Li_{0.5}NiO_2 + 0.5e^- \leftrightarrow LiNiO_2$	3.5	97.6332	94.1627		137	142
$Li_4Ti_5O_{12}$	$3Li^+ + Li_4Ti_5O_{12} + 3e^- \leftrightarrow Li_7Ti_5O_{12}$	1.5	484.9148	464.0918		167	173
MnO_2	$0.7Li^+ + MnO_2 + 0.7e^- \leftrightarrow Li_{0.7}MnO_2$	3.0	91.7956	86.9369	5080	204	216
MoS_2	$0.8Li^+ + MoS_2 + 0.8e^- \leftrightarrow Li_{0.8}MoS_2$	1.7	165.6248	160.0720	5060	130	134
TiS_2	$Li^+ + TiS_2 + e^- \leftrightarrow LiTiS_2$	2.1	118.940	112.999	3370	225	237
V_2O_5	$1.2Li^+ + V_2O_5 + 1.2e^- \leftrightarrow Li_{1.2}V_2O_5$	2.8	190.2092	181.8800	3350	170	177
VO_x	$2.5Li^+ + VO_x + 2.5e^- \leftrightarrow Li_{2.5}VO_x$	2.3					
WO_2	$Li^+ + WO_2 + e^- \leftrightarrow LiWO_2$		222.7798	215.8388	10,800	120	124

[a] Standard relative atomic masses from Loss, R.D. (2003) *Atomic Weights of the Elements 2001. Pure Appl. Chem.*, **75**(8), 1107–1111

[b] Densities taken from Lide, D.R. (ed.) (1998–1999) *CRC Handbook of Chemistry and Physics*, 78th ed. CRC Press, Boca Raton, FL, pp. 4–35 to 4–98

9.7.3 Electrode Materials for Electrolytic Cells

Today, in modern the chemical-process industry, electrochemistry occupies an important place. Electrochemical processes are widely used in inorganic syntheses.[1] They are the only method for preparing and recovering several pure elements (e.g., aluminum, magnesium, alkali and alkaline earth metals, chlorine, and fluorine).[2] Furthermore, electrochemistry occupies an important place in hydrometallurgy for electrowinning and electrorefining metals of groups IB (e.g., Cu, Ag, Au), IIB (e.g., Zn, Cd), and IVA (e.g., Sn, Pb).[3, 4] In addition, its development also concerns organic synthesis, where some processes reach industrial scale (e.g., Monsanto, Nalco, and Philips processes).[5] Apart from electrochemical processes for preparing inorganic and organic compounds, other electrolytic processes are also used in various fields: in extractive hydrometallurgy (e.g., the electrolytic recovery of zinc[6]), in zinc electroplating (e.g., high-speed electrogalvanizing of steel plates[7]), in electrodialysis (e.g., the salt-splitting regeneration of sulfuric acid and sodium hydroxide from sodium sulfate waste brines,[8, 9] the regeneration of the leaching solutions of uranium ores, the electrolytic regeneration of spent pickling solutions[10]), and in processes for a cleaner environment, where electrochemistry is used to achieve the electrooxidation of organic pollutants (i.e., electrolytic mineralization or electroincineration), and in the removal of hazardous metal cations from liquid waste effluents.[11]

Electrochemical processes are performed in an electrolytic cell[12] (i.e., ***electrolyzer***). The electrolyzer is a reactor vessel, filled with an electrolytic bath or ***electrolyte***, in which the electrodes are immersed and electrically connected via bus bars to a power supply. When the electrolyzer is split into two compartments by a ***separator*** (e.g., diaphragm, membrane), the electrolyte has two different compositions (i.e., ***anolyte*** and ***catholyte***). The electrodes are the main parts of an electrolyzer and consist of the ***anode*** (i.e., positive) where the oxidation reaction occurs, while at the ***cathode*** (i.e., negative) a reduction reaction occurs. Among the several issues encountered by engineers in the design of an industrial electrochemical reactor, one of them consists in reducing the specific electric energy consumption (i.e., electric energy per unit mass of product). The specific energy consumption can be minimized in two ways: increasing the current efficiency and lowering the operating cell voltage. Other issues in the

1 Srinivasan, V.; Lipp, L. (2003) Report on the electrolytic industries for the year 2002. *J. Electrochem. Soc.*, **150**(12), K15–38.
2 Pletcher, D.; Walsh, F.C. (1990) *Industrial Electrochemistry*, 2nd ed. Chapman & Hall, London.
3 Kuhn, A.T. (1977) *Electrochemistry of Lead.* Academic, London.
4 Gonzalez-Dominguez, J.A.; Peters, E.; Dreisinger, D.B. (1991) The refining of lead by the Betts process. *J. Appl. Electrochem.*, **21**(3), 189–202.
5 Baizer, M.M.; Lund, H. (1983) *Organic Electrochemistry: An Introduction and a Guide*, 2nd ed. Marcel Dekker, New York.
6 Karavasteva, M.; Karaivanov, St. (1993) Electrowinning of zinc at high current density in the presence of some surfactants. *J. Appl. Electrochem.*, **23**(7), 763–765.
7 Hardee, K.L.; Mitchell, L.K.; Rudd, E.D. (1989) *Plat. Surf. Finish.*, **76**(4), 68.
8 Thompson, J.; Genders, D. (1992) Process for producing sodium hydroxide and ammonium sulfate from sodium sulfate. US Patent 5,098,532; March 24, 1992.
9 Pletcher, D.; Genders, J.D.; Weinberg, N.L.; Spiegel, E.F. (1993) Electrochemical methods for production of alkali metal hydroxides without the co-production of chlorine. US Patent 5,246,551; September 21, 1993.
10 Schneider, L. (1995) Process and apparatus for regenerating an aqueous solution containing metal ions and sulfuric acid. US Patent 5,478,448; December 26, 1995.
11 Genders, D.; Weinberg, N.L. (eds.) (1992) *Electrochemistry for a Cleaner Environment.* Electrosynthesis Co., Lancaster, NY.
12 Wendt, S.; Kreysa, G. (1999) *Electrochemical Engineering.* Springer, Berlin Heidelberg New York.

design of electrochemical cells are discussed in more detail elsewhere in the literature.[13, 14, 15] The overall cell voltage at a given current density, ΔU_{cell}, can be classically described as the following algebraic sum:

$$\Delta U_{\text{cell}} = \sum_k (E_{\text{a,th}} - E_{\text{c,th}}) + \sum_k (\eta_{\text{a},k} - \eta_{\text{c},k}) + i \sum_k R_k + \Delta U_{\text{t}} = \Delta U_{\text{th}} + \Delta\eta + iR_{\text{tot}} + \Delta U_{\text{t}},$$

where the first term corresponds to the Nernstian theoretical or thermodynamic cell voltage and consists of the algebraic difference between the thermodynamic potentials of the anode and cathode respectively (i.e., Nernst electrode potentials), the second term is the summation of all the ***electrode overpotentials*** (e.g., activation, concentration, passivation, etc.), the third term is the summation of all the ***ohmic drops*** (e.g., electrolytes, both anolyte and catholyte, separators, connectors, and bus bars), and the cell potential drift is due to the aging of electrodes (e.g., corrosion, deactivation, and passivation) and/or separator materials (e.g., fooling, degradation, and swelling).

Hence, the operating cell voltage could be reduced in several ways.[16] First, an appropriate counter electrode reaction minimizes the reversible cell voltage. Second, a narrow interelectrode gap and electrode–membrane gap in association with a highly conductive electrolyte and separator and highly conductive metals for bus bars, feeders, and connectors diminish the overall ohmic drop. Third, turbulent promoters should be used to enhance convection and hence the mass transfer coefficient so as to reduce the concentration overpotential. Finally, the activation overpotential could be reduced by use of an efficient and appropriate electrocatalyst. The selection of the catalyst is an important problem to solve, particularly in the case of oxygen or chlorine anodes. Theoretical aspects of electrocatalysis are reviewed extensively in more detail by Trasatti.[17] Because of the complex behavior of electrodes, the selection of an electrocatalyst for a given process cannot be made simply on the basis of electrochemical kinetic considerations (i.e., exchange current density, Tafel slopes). An experimental approach is compulsory. The prediction of an electrode's service life requires real standardized tests (i.e., accelerated service-life tests). Several scientific and technical criteria must be considered when the practicing engineer is selecting an appropriate electrode material. Electrode materials must exhibit the following requirements:

1. High exchange current density (j_o) and a large electron transfer coefficient (α or β) for the selected electrochemical reaction to decrease the activation overpotential
2. Good electronic conductivity to decrease the ohmic drop and the Joule heating
3. Good corrosion resistance to both chemical and electrochemical reactions, combined with no passivating and blistering behavior, leading to abnormal electrode degradation and consumption
4. A good set of mechanical properties suited for industrial use (i.e., low density, high tensile strength, stiffness)
5. Ease of fabrication (i.e., machining, joining, and cleaning) allowing one to obtain clean and intricate shapes

13 Pickett, D.J. (1979) *Electrochemical Reactor Design*. Elsevier, Amsterdam.
14 Rousar, I.; Micka, K.; Kimla, A. (1985) *Electrochemical Engineering,* Vols. 1 and 2. Elsevier, Amsterdam.
15 Hine, F. (1985) *Electrode Processes and Electrochemical Engineering*. Plenum, New York.
16 Couper, A.M.; Pletcher, D.; Walsh, F.C. (1990) Electrode materials for electrosynthesis. *Chem. Rev.*, **90**(5), 837–865.
17 Trasatti, S. In: Lipkowski, J.; Ross, P.N. (eds.) (1994) *The Electrochemistry of Novel Materials.* VCH, New York, Chap. 5, pp. 207–295.

6. Low cost combined with commercial availability and a wide variety of products (e.g., rod, sheet, expanded metal)
7. Nonhazardous, nontoxic, and environmentally friendly material.

It is important to note that the combination of criteria 3 and 4 is essential for the dimensional stability of an electrode and its service life.

9.7.3.1 Industrial Cathode Materials

Generally speaking, the selection of a cathode material is easier for the electrochemist or the electrochemical engineer than the selection of an anode material. Given that the most important factor in selecting a cathode material is the overpotential for the evolution of hydrogen, there are a wide range of electronically conductive materials with the desired overpotential for both acid and alkaline electrolytes. For instance, some metals exhibit a high overpotential (e.g., Cd, Pb, Hg), while other materials are characterized by a low overpotential (e.g., Pt, Cu, Ag, platinized C, and Ni). The second most important factor is the stability of the cathode material toward nascent hydrogen gas evolved during the cathodic polarization of the material. Several refractory metals used as cathodes (e.g., Ti, Nb, Ta, Fe, and steels) are prone to hydrogen pickup and hence are extremely sensitive to hydrogen embrittlement, which leads to the blistering or even spalling of the metal, affecting its dimensional stability. Therefore, these metals are not suited for the type of industrial cathodes that must be used in aqueous electrolytes.

Low-Carbon Steel Cathodes

Low-carbon steel exhibits a low hydrogen overpotential and a low cost (US$ 0.65 per kilogram) and can be obtained in a wide variety of mill products. In addition, with its ease of fabrication, joining, and cleaning, it is the standard cathode material in the chlor-alkali industry in either the membrane process or the diaphragm process. If cathodically polarized during shutdowns and carefully handled, it offers an unlimited service life. When the hydrogen overpotential must be decreased, nickel- and cobalt-based coatings can be applied on it by electrochemical or thermal decomposition techniques. Sometimes a Ni-Zn or Ni-Al coating is deposited and the zinc or aluminum is later removed by an alkaline hot leach with 50 wt% NaOH, leaving a Raney nickel catalyst, greatly enhancing the active surface area. Recently, noble metal coatings, combined with the introduction of a catalyst into the electrolyte, have also been reported in the literature.

Aluminum Cathodes

Aluminum metal and, to a lesser extent, aluminum alloys are suitable materials for the manufacture of industrial cathodes. Pure aluminum metal has a low density (2690 $kg \cdot m^{-3}$) and high thermal conductivity (237 $W \cdot m^{-1} \cdot K^{-1}$), is a good electrical conductor (2.6548 $\mu\Omega \cdot cm$), does not form a hydride with nascent hydrogen, and is passivated when polarized anodically. All these characteristics, along with a reasonable average cost of US$ 2.00 per kilogram (for 99.7 wt% Al), are major assets for its wide use, especially in zinc electrowinning.

Industrial applications In zinc electrowinning, zinc is directly plated onto aluminum cathodes, while oxygen is evolved at the Pb-Ag anode. Once the zinc electrodeposit reaches a desired thickness, the aluminum cathodes are removed from the cells, followed by either manual or automatic stripping of the zinc deposit. On the other hand, molten aluminum is used as a liquid cathode during the electrowinning of aluminum in the Hall–Héroult process.

Failure modes In zinc electrowinning, when the cathodes are lifted from the electrolyte, removed from the cells, and stripped, some corrosive sulfate electrolyte remains on the surface of the cathodes despite the water rinsing treatment. As a result, the cathodes, especially in the area close to the edges of the cathode, are corroded to various degree, depending on the amount and concentration of the acid in contact with the cathode. Evaporation of the electrolyte is also observed at the surface of the cathode, resulting in precipitation of insoluble zinc sulfate salts and other impurities, causing an increase in the corrosion rate of the aluminum cathode. The overall effect of this corrosion attack can be seen on the smoothness of the aluminum cathode (i.e., patches of rough areas appear at times on the surface of the aluminum). Because of the unevenness in the surface of the cathode and of the presence of impurities, the zinc deposition process is affected, resulting in the formation of rough zinc deposits. Usually, these areas are seen as "puffed" sections of the deposits that, because of their closer proximity to the anode, tend to affect the current distribution in the electrolysis cell. As the zinc electrowinning process is sensitive to variations in current density, the uneven current distribution observed with puffed zinc deposits causes a decrease in the current efficiency of zinc deposition. Under these conditions, higher corrosion rates of the Pb-Ag anode are observed that result in an increase in the lead content of the zinc deposits. Another effect of the impurities on the surface of the aluminum cathode is the formation of pinholes on the zinc deposit. This also results in lower current efficiency of zinc deposition. A known method of preventing the occurrence of puffed zinc deposits consists of mechanically or manually buffing the aluminum cathodes using metal or plastic brushes. Mechanical buffing is performed with automated machines that apply a scrubbing action at the surface of the cathode. As a result, the surface of the cathode is maintained free of deposited impurities. However, because of the presence of edge strips located at the sides and bottom of the aluminum cathode to prevent electrodeposition of zinc on the sides of the cathode and facilitate the stripping of the deposits, the mechanical buffing machines are not efficient in treating the entire surface of the cathode. Furthermore, mechanical or manual buffing of the affected cathodes does not completely remove the deposited impurities and insoluble zinc sulfate salts from the surface of the electrode as the treated areas become affected after about 3 weeks, necessitating rebuffing of the electrode. To facilitate removal of impurities and insoluble zinc sulfate salts from an aluminum cathode used in zinc electrowinning, a chemical treatment has been developed consisting of a mild HCl cleaning and water rinsing.

Titanium Cathodes

Titanium metal is a light metal with nearly half the density of copper (4540 $kg \cdot m^{-3}$), exhibits an excellent strength-to-density ratio, allowing one to use thinner and lightweight anode plates without sacrificing the mechanical stiffness of the cathode, and has an excellent corrosion resistance to various corrosive environments. The only drawbacks of titanium are its high electrical resistivity (42 $\mu\Omega \cdot cm$) and the high cost of the mill products (e.g., sheet, plate, rods), which can reach US$ 80.00 per kilogram in some cases.

Titanium grades The common titanium grades used in electroplating as cathodes are chemically pure titanium such as ASTM grade 1 or grade 2, while for more demanding applications, especially when corrosion resistance to reducing acid is a requirement, titanium when alloyed with palladium (Ti-0.15Pd), such as ASTM grades 7 and 11, or recently with ruthenium (Ti-0.10Ru), such as ASTM grades 26 and 27, is recommended despite being more expensive than commercially pure titanium.

Industrial applications Electrorefining of copper is based on the unsupported process using permanent titanium cathode plates and an associated stripping machine. Electrolytic iron is also electrodeposited from ferrous chloride or ferrous sulfate baths onto titanium cathodes owing to the great ease of removal of the iron plate by mechanical stripping. Usually titanium must be etched with hot 20 wt% HCl or a cold mixture of a fluoronitric mixture ($HF–HNO_3$) before the cathodic electrodeposition is performed so as to remove the passivating rutile layer.

Failure modes Commercially pure titanium metal and its alloys are susceptible to hydrogen pickup,[18] and hence are extremely sensitive to embrittlement by nascent hydrogen gas;[19] moreover, in corrosive electrolytes the cathode must be polarized cathodically during shutdowns.

Zirconium Cathodes

Zirconium metal (6510 $kg \cdot m^{-3}$) is denser but exhibits better corrosion resistance and is less prone to hydrogen embrittlement than titanium metal. Moreover, zirconium is highly corrosion resistant in strong alkaline solutions and has good inertness toward organic and inorganic acids.

Zirconium grades The zirconium grade most commonly used in electroplating is Zircadyne® 702.

Nickel Cathodes

Nickel is used extensively as a cathode in alkaline electrolytes because of its immune behavior in strongly alkaline solutions, especially concentrated solutions of NaOH and KOH, and also because it does not form hydride with hydrogen.

Mercury Cathodes

Mercury is the only liquid metal cathode used industrially in aqueous solutions because of its high overpotential for the evolution of hydrogen, which even allows it to electrodeposit alkali and alkaline earth metals from aqueous electrolytes, forming amalgams. For that reason, it was used extensively in the chlor-alkali industry despite being progressively phased out for obvious health, safety, and environmental reasons. Moreover, with an average price of US$ 2000 per UK flask (i.e., 76 lb) in 2006, which corresponds to US$ 16.8 per kilogram, it is an expensive material to use in large quantities such as those required in chlor-alkali plants.

See ◘ Tables 9.14–9.17.

9.7.3.2 Industrial Anode Materials

Although the selection of the suitable material for an anode follows the same pattern as for cathode materials, this step is still a critical issue in the final design of an industrial electrolyzer because of the particular operating conditions that anodes must withstand. Historically, the failure of the anode has often led to the abandonment of some industrial processes. For instance, in aqueous solutions, a major problem arises because the anode is the electrode where the electrochemical oxidation occurs; hence, the anode material must withstand harsh conditions due to both the elevated positive potential and the high acidity of the electrolyte. Moreover, traces of impurities in the electrolyte might be an additional source of corrosion and deactivation in some cases. Therefore, the material selection process must always be based on strong knowledge of previous methods and clear understanding of the properties of the materials involved,

18 La Conti, A.B.; Fragala, A.R.; Boyack, J.R. (1977) *ECS Meeting*, Philadelphia, May 1977.

19 Bishop, C.R.; Stern, M. (1961) Hydrogen embrittlement of tantalum in aqueous media. *Corrosion*, **17**, 379t–385t.

Table 9.14 Cathode materials for hydrogen (H_2) evolution in acidic media

Overvoltage range	Cathode material	Electrolyte composition	Molarity (C/mol · dm^{-3})	Temperature (°C)	Cathodic Tafel slope (b_c/mV· $\log_{10} j_0^{-1}$)	Exchange current density decimal logarithm ($\log_{10} j_0$/A · cm^{-2})	Absolute value of overvoltage at 200 A · m^{-2} (η/mV)
Extralow hydrogen overvoltage	Iridium (Ir)	H_2SO_4	0.5	25	30	–2.699	30
	Palladium (Pd)	HCl	1	25	30	–2.500	24
		H_2SO_4	1	25	29	–3.200	44
	Platinum (Pt)	HCl	1	25	29	–3.161	43
		H_2SO_4	2	25	25	–3.200	38
	Rhodium (Rh)	H_2SO_4	4	25	28	–3.200	42
	Ruthenium	HCl	1	25	30	–4.200	75
Low hydrogen overvoltage	Molybdenum (Mo)	HCl	0.1	25	104	–6.400	343
	Tungsten (W)	HCl	5.0	25	110	–5.000	363
	Nickel (Ni)	HCl	1.0	25	109	–5.222	384
		H_2SO_4	1.0	25	124	–5.200	434
	Silver (Ag)	HCl	5.0	25	120	–5.301	432
		H_2SO_4	1.0	25	120	–5.400	444
	Iron (Fe)	HCl	0.5	25	133	–5.180	425
		H_2SO_4	0.5	25	118	–5.650	466
	Gold (Au)	HCl	0.1	25	123	–5.500	468
		H_2SO_4	1.0	25	116	–5.400	430
			4.0	25	130	–6.500	624
	Copper (Cu)	HCl	0.1	25	120	–6.823	615
		H_2SO_4	0.5	25	120	–7.700	720

Table 9.14 (*continued*)

Overvoltage range	Cathode material	Electrolyte composition	Molarity (C/mol · dm^{-3})	Temperature (°C)	Cathodic Tafel slope (b_c/mV· $\log_{10} j_0^{-1}$)	Exchange current density decimal logarithm ($\log_{10} j_0$/A · cm^{-2})	Absolute value of overvoltage at 200 A · m^{-2} (η/mV)
High hydrogen overvoltage	Niobium (Nb)	HCl	1	25	110	–9.000	803
		H_2SO_4	2	25	120	–8.400	804
	Titanium (Ti)	HCl	1	25	130	–7.500	754
		H_2SO_4	0.5	25	135	–8.200	877
			1	25	119	–8.150	767
	Tin (Sn)	H_2SO_4	4	25	120	–9.00	877
	Zinc (Zn)	HCl	1	25	120	–10.800	1092
		H_2SO_4	2	25	120	–10.800	1092
	Cadmium (Cd)	H_2SO_4	0.25	25	135	–10.769	1225
	Lead (Pb)	HCl	1	25	117	–12.900	1311
		H_2SO_4	0.5	25	120	–12.700	1320
	Mercury (Hg)	HCl	1	25	118	–12.500	1475
		H_2SO_4	2	25	119	–12.107	1239

$\eta_c = (E_{c,j} - E_{th}) = b_c(\log_{10} j_{eq} - \log_{10} j) = (\ln 10 RT/\beta nF)\log_{10} j_{eq} - (\ln 10 RT/\beta nF)\log_{10} j$

Table 9.15 Anode materials for oxygen (O_2) evolution in acidic media

Overvoltage range	Anode material	Electrolyte composition	Molarity (C/mol · dm^{-3})	Temperature (°C)	Anodic Tafel slope (b_a/mV · $\log_{10} j_0^{-1}$)[a]	Exchange current density decimal logarithm ($\log_{10} j_0$/A · cm^{-2})[a]	Overvoltage at 200 A · m^{-2} (mV)
Low oxygen overvoltage	Ta/Ta_2O_5–IrO_2	H_2SO_4 30wt%	3.73	80	52 133	–3.630 –10.21	101
	Ti–Pd (grade 7)/ Ta_2O_5–IrO_2	H_2SO_4 30wt%	3.73	80	54 164	–4.53 –8.21	153
	Ti/TiO_2–IrO_2	H_2SO_4 30wt%	3.73	80	60	–4.886	191
	Ti (grade 2)/ Ta_2O_5–IrO_2	H_2SO_4 30wt%	3.73	80	51 158	–5.82 –7.69	210
Medium oxygen overvoltage	Ti/TiO_2–RuO_2 (DSA®-Cl_2)	H_2SO_4	1	80	66	–7.900	409
		CF_3SO_3H	1	80	65	–8.000	410
	Ruthenium-iridium	H_2SO_4	1	80	74	–7.020	400
		CF_3SO_3H	1	80	86	–6.630	419
	Iridium (Ir)	H_2SO_4	1	80	85	–6.800	433
		CF_3SO_3H	1	80	84	–6.800	428

Table 9.15 (*continued*)

Overvoltage range	Anode material	Electrolyte composition	Molarity (C/mol · dm^{-3})	Temperature (°C)	Anodic Tafel slope (b_a/mV · $\log_{10} j_0^{-1}$)[a]	Exchange current density decimal logarithm ($\log_{10} j_0$/A · cm^{-2})[a]	Overvoltage at 200 A · m^{-2} (mV)
High oxygen overvoltage	α-PbO_2	H_2SO_4	4	30	45	–15.700	630
	Platinum-ruthenium	H_2SO_4	1	80	120	–7.700	710
		CF_3SO_3H	1	80	120	–7.500	670
	Platinum-rhodium	H_2SO_4	1	25	115	–7.600	679
	Rhodium (Rh)	$HClO_4$	1	25	125	–7.520	727
	Platinum (Pt)	H_2SO_4	1	80	90	–10.900	828
		CF_3SO_3H	1	80	94	–9.800	762
		$HClO_4$	1	25	110	–9.000	803
	Pt/MnO_2	H_2SO_4	0.5	25	110	n. a.	n. a.
	β-PbO_2	H_2SO_4	4	30	120	–9.200	900
	PbO_2	H_2SO_4	4	30	120	–10.000	996
	Ti_4O_7 (Ebonex®, bare)	H_2SO_4	1	25	n. a.	n. a.	1800

$\eta_a = (E_{a,j} - E_{th}) = b_a(\log_{10} j - \log_{10} j_{eq}) = (\ln 10RT/anF)\log_{10} j - (\ln 10RT/anF)\log_{10} j_{eq}$

n. a. not available

[a] Where there are two values, they refer to the low current density region (100–500 A/m^2) and the high current density region (1000–50,000 A/m^2)

Table 9.16 Anode materials for chlorine (Cl_2) evolution

Overvoltage range	Anode material (wt%)	Electrolyte composition	Molarity (C/mol · dm^{-3})	Temperature (°C)	Anodic Tafel slope (b_a/ mV · $\log_{10} j_0^{-1}$)	Exchange current density decadic logarithm ($\log_{10} j_0$/A · cm^{-2})	Anodic overvoltage at 5 kA · m^{-2} (V)
Low chlorine overpotential	Pt30-Ir70	NaCl	Saturated	65	n. a.	n. a.	0.000
	Ti/TiO_2-RuO_2–SnO_2 (61:31:8)	NaCl	Saturated	65	n. a.	n. a.	+0.020 to +0.060
	Ti/TiO_2-RuO_2 (83:17)	NaCl	Saturated	65	n. a.	n. a.	+0.025 to +0.076
	Ti/TiO_2-RuO_2 (65:35)	HCl	1	25	30	–1.409	+0.043
		NaCl	5	20	108	–1.409	+0.152
	Ti/Ta_2O_5–RuO_2-IrO_2 (89:6:5)	NaCl	Saturated	65	n. a.	n. a.	+0.090
	Ti/MnO_2	NaCl	6	25	20–110	–4.000 to –2.273	+0.080 to +0.250
		HCl	1	20	37	–2.8861	+0.107
	Ti/Ta_2O_5–RuO_2-IrO_2 (79:11:10)	NaCl	Saturated	65	n. a.	n. a.	+0.140

Table 9.16 (*continued*)

Overvoltage range	Anode material (wt%)	Electrolyte composition	Molarity (C/mol · dm^{-3})	Temperature (°C)	Anodic Tafel slope (b_a/ mV · $\log_{10} j_0^{-1}$)	Exchange current density decadic logarithm ($\log_{10} j_0$/A · cm^{-2})	Anodic overvoltage at 5 kA · m^{-2} (V)
High chlorine overpotential	Graphite	HCl	18	80	70	–4.286	+0.440
	Ti/MnO_2-SnO_2 (56:44)	NaCl	Saturated	65	n. a.	n. a.	+0.620
	Fe_3O_4	NaCl	5.3	25	73	–7.796	+0.569
		NaCl	2	25	90	–7.796	+0.702
	PbO_2	NaCl	6	25	150–200	–4.174 to –4.097	+0.626 to +0.819
	Platinum (Pt)	NaCl	2	85	250	–4.200	+1.050
		NaCl	2	25	290	–3.700	+1.073
		NaCl	5	25	305	–3.700	+1.129

$\eta_a = (E_{a,j} - E_{th}) = b_a(\log_{10} j - \log_{10} j_{eq}) = (\ln 10 RT/anF)\log_{10} j - (\ln 10 RT/anF)\log_{10} j_{eq}$

n. a. not available

Table 9.17 Practical hydrogen overpotentials ($^{(\eta)}H_2$/V) measured in sulfuric acid for various cathode materials polarized under various current densities

Cathode materials	Hydrogen overpotential				
	10 A/m^2	100 A/m^2	1000 A/m^2	5000 A/m^2	10,000 A/m^2
Platinum (platinized)	0.015	**0.030**	0.040	0.050	0.050
Platinum (smooth)	0.024	**0.070**	0.290	0.570	0.680
Duriron	0.200	**0.290**	0.610	0.860	1.020
Palladium	0.120	**0.300**	0.700	1.000	1.000
Monel 400	0.280	**0.380**	0.620	0.860	1.070
Gold	0.240	**0.390**	0.590	0.770	0.800
Tellurium	0.400	**0.450**	0.480	0.540	0.600
Iron (electrolytic)	0.400	**0.560**	0.820	1.260	1.290
Copper (C101)	0.480	**0.580**	0.800	1.190	1.250
Brass	0.500	**0.650**	0.910	1.230	1.250
Carbon	n. a.	**0.700**	0.900	1.100	1.170
Nickel 201	0.560	**0.750**	1.050	1.210	1.240
Zinc	0.720	**0.750**	1.060	1.200	1.230
Silver	0.470	**0.760**	0.880	1.030	1.090
Graphite	0.600	**0.780**	0.980	1.170	1.220
Aluminum	0.560	**0.830**	1.000	1.240	1.290
Tin	0.860	**1.080**	1.220	1.240	1.230
Mercury	0.900	**1.040**	1.070	1.100	1.120
Bismuth	0.780	**1.050**	1.140	1.210	1.230
Lead	0.520	**1.090**	1.180	1.240	1.260
Cadmium	0.980	**1.130**	1.220	1.250	1.250

Electrode potentials measured in a 1 mol/L aqueous solution of H_2SO_4 at 25 °C

experimental results acquired from accelerated service-life tests performed in the laboratory, and field tests conducted over long periods. The following sections present the most common anode materials available industrially, with a brief historical background, key properties, the techniques for their preparation, their failure modes, and major industrial applications.

9.7.3.2.1 Precious and Noble Metal Anodes

Electrochemists early on observed that noble and precious metals were stiff materials, with good tensile properties and machinability, high electronic conductivity, and exceptional chemical and

electrochemical inertness in most corrosive media,[20] all combined with intrinsic electrocatalytic properties.[21] Consequently, the first industrial anodes used in electrochemical processes requiring an excellent dimensional stability were made of the noble and precious metals (e.g., Au and Ag), the six platinum group metals (PGMs) (i.e., Ru, Rh, Pd, Os, Ir, and Pt), or their alloys (e.g., 90Pt-10Ir and 90Pt-10Rh)[22]. Of these, the PGMs, especially platinum and iridium, occupied a particular place owing to their electrochemical inertness and intrinsic electrocatalytic activity. Platinum is the most appropriate anode material for the preparation of persulfates, perchlorates, and periodates and for the regeneration of cerium(IV). However, the extremely high price of the bulk metal, which reached US$ 1100 per ounce in early 2006, combined with its density (21,450 $kg \cdot m^{-3}$), has drastically restricted its industrial uses. However, early in the twentieth century there was an attempt to develop an inert anode for oxygen evolution in sulfuric acid based electrolytes. The anode was obtained by the coating of a cheaper base metal with a thin layer of platinum or iridium. These first composite electrodes were patented in 1913 by Stevens.[23, 24] A refractory metal such as tungsten or tantalum was electroplated with the thin platinum or iridium layers. The role of the platinum coating was to ensure the electrical conduction of the base metal, even under anodic polarization. Despite its novelty, this bright idea was not industrially developed at that time because it was impossible commercially to obtain these refractory metals, especially their mill products (e.g., plates, rods, sheet, and strips) needed for the manufacture of large industrial anodes. It was not until the 1960s that the first commercial platinized anodes appeared.

Besides the precious metal anodes, early electrochemists used anodes made of two inexpensive materials such as lead and carbon-based materials such as graphite. Lead and graphite were the only cheap anode materials that were industrially used up to the 1960s.

9.7.3.2.2 Lead and Lead-Alloy Anodes

Historically, the use of lead anodes resulted first from the widespread use of lead vessels in industrial manufacturing involving corrosive media such as the synthesis of sulfuric acid[25] and later from the original studies in the lead–acid battery invented by Gaston Planté in 1859.[26]

Properties Lead is a common and cheap metal, and the average price for lead of 99.99 wt% purity is US$ 0.980 per kilogram.[27] Pure lead exhibits several attractive features, such as good electronic conductivity (20.64 $\mu\Omega \cdot cm$) and a good chemical and electrochemical corrosion resistance in numerous corrosive and oxidizing environments (e.g., chromates, sulfates, carbonates, and phosphates).[28] This chemical and electrochemical inertness is due to the self-formation of a protective passivating layer. For instance, the corrosion rate of the pure metal in 50 wt% sulfuric acid is 130 μm per year at 25 °C. When the metal undergoes an anodic current density of 1 $kA \cdot m^{-2}$ in

20 Dreyman, E.W. (1972) Selection of anode materials. *Eng. Exp. Stn. Bull.* (West Virginia University), **106**, 76–83.
21 Cailleret, L.; Collardeau, E. (1894) *C.R. Acad. Sci*., **830**.
22 Howe, J.L. (ed.) (1949) *Bibliography of the Platinum Metals 1931–1940.* Baker, Newark, NJ.
23 Stevens, R.H. (1913) Platinum-plated tungsten electrode. US Patent 1,077,894; November 4, 1913.
24 Stevens, R.H. (1913) Iridium-plated tungsten electrode. US Patent 1,077,920; November 4, 1913.
25 Lunge, G.; Naville, J. (1878) Traité de la grande industrie chimique. Tome I: acide sulfurique et oléum. Masson & Cie, Paris.
26 Planté, G. (1859) *Compt. Rend. Acad. Sci*., **49**, 221.
27 Metal Bulletin Weekly, May 8, 2006.
28 Greenwood, N.N.; Earnshaw, N. (1984) *Chemistry of the Elements*. Pergamon, Oxford, p. 435.

60 wt% sulfuric acid, the corrosion rate reaches only 9 mm per year.[29, 30] Pavlov[31] has shown in acidic sulfate electrolytes that, with an increasing anodic polarization, first an insulating layer of ***anglesite*** ($PbSO_4$) forms between 1.52 and 1.72 V versus the standard hydrogen electrode (SHE), then a brown layer of semiconductive lead dioxide (PbO_2) appears. If anodic polarization is increased further, an insulating film of PbO forms, preventing the current from flowing. The lead anode is characterized by a high anodic overpotential for the evolution of oxygen. It is important to note that among the dimorphic forms of PbO_2 only ***plattnerite***, with a rutile structure, is electrocatalytic to oxygen evolution (see Sect. 9.7.3.2.4). Because lead is malleable and ductile, with a high density (11,350 $kg \cdot m^{-3}$), low melting point (327.5 °C), and high coefficient of linear thermal expansion ($30 \times 10^{-6}\ K^{-1}$), it exhibits a severe creep phenomenon when electrolysis is conducted well above the ambient temperature. To improve the mechanical properties of pure lead and its corrosion properties, industrial lead anodes are typically made of lead alloys instead of pure lead metal. Moreover, the use of alloying elements usually decreases the melting temperature required to cast new anode slabs. Castability determines the anode integrity, and the temperature interval between the liquidus and solidus temperatures is still an important consideration for anode manufacturers.

Grades of pure lead and lead alloys used in industrial anodes Pure lead grades are called ***corroding lead*** and ***common lead***, both containing a minimum of 99.94 wt% Pb, and ***chemical lead*** and ***acid-copper lead***, both containing a minimum of 99.90 wt% Pb. Lead of higher specified purity (99.99 wt% Pb) is also available in commercial quantities but is rarely used as anodes. International specifications include ASTM B29 in the USA for grades of pig lead, including federal specification QQ-L-171, German standard DIN 1719, British Standard BS EN 12659:1999, Canadian Standard CSA-HP2, and Australian Standard 1812. Corroding lead exhibits the outstanding corrosion resistance typical of lead and its alloys. Chemical lead is a refined lead with a residual copper content of 0.04–0.08 wt% and a residual silver content of 0.002–0.02 wt% and is particularly desirable in the chemical industries. Copper-bearing lead provides corrosion protection comparable to that of chemical lead in most applications that require high corrosion resistance. ***Common lead*** contains higher amounts of silver and bismuth than does corroding lead. In ***antimonial lead***, the antimony content ranges 0.5–25 wt%, but it is usually between 2 and 5 wt%. Antimony imparts greater hardness and strength. Lead–calcium alloys have replaced lead–antimony alloys in a number of applications. These alloys contain 0.03–0.15 wt% Ca. More recently, aluminum has been added to calcium–lead and calcium–tin–lead alloys as a stabilizer for calcium. Adding tin to lead or lead alloys increases hardness and strength, but lead–tin alloys are more commonly used for their good melting, casting, and wetting properties. Tin gives an alloy the ability to wet and bond with metals such as steel and copper; unalloyed lead has poor wetting characteristics. The most common lead alloys used to manufacture industrial anodes together with their electrochemical applications are briefly summarized in ◘ Table 9.18.

Industrial applications For those reasons, and despite the poor electrocatalytic properties of lead and problems related to its toxicity arising with anodic dissolution, today lead anodes are the most common industrial anodes used worldwide for electrowinning of metals from acidic

29 Beck, F. (1971) Lead dioxide-coated titanium anodes. German Patent 2,023,292; May 13, 1971.

30 Beck, F.; Csizi, G. (1971) Lead dioxide-titanium compound electrodes. German Patent 2,119,570; April 22, 1971.

31 Pavlov, D.; Rogachev, T. (1986) Mechanism of the action of silver and arsenic on the anodic corrosion of lead and oxygen evolution at the lead/lead oxide (PbO_{2-x})/water/oxygen/sulfuric acid electrode system. *Electrochim. Acta.*, **31**(2), 241–249.

Table 9.18 Lead and lead-alloy anode composition and electrochemical uses

Lead alloy and UNS numbers	Typical composition range	Alloying effect	Electrochemical use
Pure lead (Pb), "corroding lead" (L50000 to L50099)	> 99.94 wt% Pb	n. r.	Nickel electrowinning (200 A · m^{-2})
Lead–silver (Pb–Ag) (L50100 to L50199)	0.25–0.80 wt% Ag[a] (usually 0.5 wt%)	Increases corrosion resistance and oxygen overvoltage	Zinc electrowinning, cobalt electrowinning
Lead–tin (Pb-Sn) [L54000 to L55099]	Usual 5–10 wt% Sn (historically 4 wt% Sn)	Tin increases mechanical strength, forms corrosion-resistant intermetallics, and improves melt fluidity during anode casting	Cobalt electrowinning (500 A · m^{-2})
Antimonial lead (Pb-Sb)[b] (hard lead) [L52500 to L53799]	2–6 wt% Sb	Antimony lowers oxygen overvoltage, increases stiffness, strength, and creep resistance, extends the freezing range, and lowers the casting temperature	Cobalt electrowinning, copper electrowinning (200 A · m^{-2})
Lead–calcium–tin (Pb-Ca-Sn) ("nonantimonial" lead) (L50700 to L50899)	0.03–0.15 wt% Ca	Calcium imparts corrosion resistance and minimizes oxygen and hydrogen overpotentials, while it imparts stiffness	Copper electrowinning (500 A · m^{-2})

n. r. not relevant, *UNS* Unified Numbering System for Metals and Alloys

[a] Hoffmann, W. (1962) *Blei und Bleilegierungen*. Springer, Berlin Heidelberg New York; English translation in 1962: *Lead and Lead Alloys*. Springer, Berlin Heidelberg New York

[b] Mao, G.W.; Larson, J.G.; Rao, G.P. (1969) Effect on small additions of tin on some properties of lead 4.5 wt% antimony alloys. *J. Inst. Metal*, **97**, 343–350

sulfate electrolytes[32] (e.g., Zn, Co, Ni) and in hexavalent chromium electroplating.[33] The low price of lead anodes compared with titanium-coated electrodes and a service life in the range of 1–3 years are their major advantages. Moreover, the low melting temperature of lead and its alloys makes it possible to recycle in-house spent industrial lead anodes by simply remelting the discarded anodes and casting the recycled molten metal into new anode slabs. Zinc electrowinning uses lead–silver because cobalt addition cannot be used. The silver alloy imparts some corrosion resistance to the base lead. Lead-based anodes are used because of their low cost and robustness. The major drawbacks are sludge generation, leading to product quality issues and high oxygen overpotential (i.e., higher power costs). Copper electrowinning uses

32 De Nora, O. (1962) Anodes for use in the evolution of chlorine. British Patent 902,023; July 25, 1962.

33 Nidola, A. (1995) Technologie di cromatura galvanica a spessore. *Rivista AIFM: Galvanotecnica e nuove finiture*, **5**, 203–218.

lead–calcium–tin, which is favored to avoid the cost of silver addition. Stabilization of Pb-Ca-Sn anodes is ensured by the careful addition of cobalt(II) as a depolarizer in the electrowinning electrolyte. In the electrolytic production of manganese metal, silver–lead anodes (1 wt% Ag) are used, which results in anode sliming of 0.38–0.45 tonnes per tonne of manganese. Slime of manganese and lead compounds is a process waste that engenders a number of problems:

1. Environmental pollution by waste products
2. Unproductive raw-material consumption, resulting in an increase in the overall volume of facilities and capital investments
3. High specific energy consumption during preparation of additional quantities of manganese-containing solutions for electrolysis baths
4. Unpredictable anode destruction caused by active corrosion along waterlines
5. Frequent cleanup of anodes and baths (once every 20–24 days), replacement of diaphragms, and remelting of anodes

Recent developments Some work is still being conducted to overcome some of the drawbacks of industrial lead anodes. For instance, Permelec Co., a Japanese subsidiary of De Nora, developed a reinforced lead anode for the electrowinning of zinc from sulfate baths. This anode is made of a skin portion formed by a conventional silver–lead alloy and a stiffening reinforcing component made of titanium or zirconium mesh. The reduction in the thickness of the anodes, which is made possible by the provision of the reinforcing member, results in substantial savings in the amount of silver-bearing lead that is immobilized and a substantial reduction in the mass of the bulk anode. Later, Eltech Systems Corporation introduced its new patented technology,[34] known by the brand name Mesh-on-Lead™ (MOL) anode. The MOL anode is a composite structure obtained by attachment of disposable electrocatalytically active titanium mesh to existing lead anodes. Hence, it combines the benefits of a standard lead anode with the power savings of a precious metal oxide coated titanium found typically in dimensionally stable anodes (see Sect. 9.7.3.2.10). The MOL product is still being developed to overcome its major drawback, cost. This new anode is specifically designated for replacement of Pb-Ca-Sn anodes for primary copper electrowinning operations (e.g., solvent extraction and electrowinning process). The MOL concept was demonstrated with full-scale anodes at several premier commercial tankhouses. During these demonstrations MOL anodes exhibited numerous performance advantages relative to standard Pb-Ca-Sn anodes: they reduced the specific energy consumption because of a lower oxygen evolution overpotential, improved cathode quality, minimized lead-sludge generation, eliminated cobalt addition as a result of a stabilized lead substrate, and increased current efficiency because of reduced short-circuiting.[35]

Failure modes In acidic sulfate baths, the most common failure mode of lead anodes consists of the formation of a thick solid and intermediate passivating layer of $PbSO_4$ and PbO_2 that can grow up to 5 mm thick and that eventually flakes off, leaving patches of freshly exposed surface. This deactivation of the lead anode is accompanied by two major drawbacks of industrial electrolysis: loss of faradic efficiency, usually below 90% for zinc and below 95% for cobalt, and an uneven and dendritic aspect of the electrodeposited metal usually contaminated by traces of lead. Another important failure mode occurs because of the deleterious effect of

34 Brown, C.W.; Bishara, J.I.; Ernes, L.M.; Getsy, A.W.; Hardee, K.L.; Martin, B.L.; Pohto, G.R. (2002) Lead electrode structure having mesh surface. US Patent 6,352,622; March 5, 2002.

35 Moats, M.; Hardee, K.; Brown, Jr., C. (2003) Mesh-on-Lead anodes for copper electrowinning. *JOM*, **55**(7), 46–48

manganese(II) cations. The presence of manganous cations as impurities in many electrolyte streams may cause important secondary anodic reactions to occur. During the anodic process, manganous cations (Mn^{2+}) may react at the anode surface to form either soluble permanganate species (MnO_4^-) or insoluble manganese dioxide (MnO_2) that passivates the anode surface and then impedes the proper evolution of oxygen. Eventually, flakes on the anode can detach as slime that contains oxides and/or sulfates, which are the major source of lead contamination in electrowon cathodes. In copper electrowinning, cobalt(II) is often used as a depolarizer for the oxygen evolution reaction. However, cobalt cannot be used during zinc electrowinning because it affects the overall current efficiency.

9.7.3.2.3 Carbon Anodes

History Carbon-based electrode materials (e.g., carbon, semigraphite, and graphite) have been used in various electrochemical technologies since the beginning of electrochemistry, including electroanalysis, energy storage devices, and electrosynthesis. For instance, because of its chemical inertness toward hydrochloric acid and hydrogen chloride, graphite was the early anode material selected for HCl electrolysis for production of chlorine gas.[36] This process, initially developed in Germany during World War II[37] by Holemann and Messner at IG Farben Industrie,[38, 39] continued to be used in the 1950s by De Nora in a joint venture with Monsanto in the USA[40, 41] and by Hoechst in a joint venture with Uhde in Germany.[42, 43]

Structure As a general rule, carbon-based materials have similar microstructures consisting of a planar network of a six-membered aromatic-forming layered structure with sp^2-hybridized carbon atoms trigonally bonded to one another. The crystallite size and extent of microstructural order can differ from material to material (i.e., edge to basal plane ratio), which has important implications for electron transfer kinetics.

Properties Carbon-based electrodes are attractive because carbon is a cheap material with excellent chemical inertness, and it is easy to machine and has a low bulk density (2260 $kg \cdot m^{-3}$). Furthermore, there is a great diversity of commercially available products (e.g., graphite, pyrolytic, impervious, or glassy) and in several forms (e.g., fibers, cloths, blacks, powders, or reticulated). The graphite variety, despite its anisotropy, high electrical resistivity (1375 $\mu\Omega \cdot cm$), and extreme brittleness, was once widely used for the electrolysis of brines. Graphite is highly corrosion resistant to concentrated hydrochloric acid even at the high anodic potential required for production of chlorine. Corrosion is not detectable if the concentration of hydrochloric acid is always maintained above 20 wt% during electrolysis. Carbon anodes are also the only appropriate anode material in certain processes where no other materials exhibit both low cost and satisfactory corrosion

36 Isfort, H. (1985) State of the art after 20 years experience with industrial hydrochloric acid electrolysis. *DECHEMA Monographien,* **98**, 141–155.

37 Gardiner, W.C. (1946) *Hydrochloric Acid Electrolysis at Wolfen*. Field Information Agency, Technical (FIAT) Report No. 832, US Office of Military Government for Germany.

38 Gardiner, W.C. (1947) Hydrochloric acid electrolysis. *Chem. Eng.*, **54**(1), 100–101.

39 Holemann, H. (1962) The hydrochloric acid electrolysis. *Chem. Ing. Techn.*, **34**, 371–376.

40 Gallone, P.; Messner, G. (1965) Direct electrolysis of hydrochloric acid. *Electrochem. Technol.*, **3**(11–12), 321–326.

41 Messner, G. (1966) Cells for the production of chlorine from hydrochloric acid. US Patent 3,236,760; February 22, 1966.

42 Grosselfinger, F.B. (1964) New chlorine source: by-product hydrochloric acid. *Chem. Eng.*, **71**(19), 172–174.

43 Donges, E.; Janson, H.G. (1966) *Chem. Ing. Techn.*, **38**, 443.

resistance. Several industrial electrolytic processes performed in molten-salt electrolytes continue to use carbon anodes; these processes are the electrowinning of aluminum by the Hall–Héroult process, the electrolytic production of alkali metals (e.g., Na, Li) and alkaline earth metals (e.g., Be, Mg), and the electrolytic production of elemental fluorine. However, the use of carbon anodes in the chlor-alkali process for the production of chlorine gas has now been discontinued because of the replacement by modern and more efficient anodes. In fact, in the 1960s, the improvement of the chlor-alkali processes (e.g., mercury cathode cell and diaphragm cell) required great efforts in research and development. The research was essentially focused on improving graphite anodes, which had some serious drawbacks: first, the nondimensional stability of the carbon anodes during electrolysis led to continuous increases in the interelectrode gap, which caused an ohmic drop; second, they had a high chlorine evolution overpotential; and third, they had a very short service life (i.e., 6–24 months) due to corrosion by the chlorine and the inescapable traces of oxygen, which formed chlorinated hydrocarbons and carbon dioxide. These efforts led to the birth of the third generation of industrial dimensionally stable anodes (see Sect. 9.7.3.2.10).

Failure modes Because of its lamellar structure, graphite severely corrodes because of the intercalation of anions between graphene planes such as sulfate or perchlorate during anodic discharge, while alkali metal cations and ammonium intercalate when cathodically polarized lead to severe exfoliation of the electrode materials. The degradation of carbon-based materials depends on the electrolyte, the nature of the carbon materials, and the concentration of the intercalating species. Once the graphite particles float on the electrolyte surface, they can lead to serious electrical continuity issues (i.e., short circuit), especially in molten-salt electrolytes that are denser than graphite.

9.7.3.2.4 Lead Dioxide (PbO_2)

Structure Lead dioxide exhibits two polymorphic forms: ***scrutinyite*** (α-PbO_2), with orthorhombic crystals ($a = 497.1$ pm, $b = 595.6$ pm, and $c = 543.8$ pm) with a density of 9867 $kg \cdot m^{-3}$, and ***plattnerite*** (β-PbO_2), with tetragonal crystals ($a = 495.25$ pm and $c = 338.63$ pm) having a rutile-type structure and a density of 9564 $kg \cdot m^{-3}$.

Properties Only plattnerite has attractive features for electrochemical applications, such as low electrical resistivity (40–50 $\mu\Omega \cdot cm$), good chemical and electrochemical corrosion resistance in sulfate media even at low pH, and a high overvoltage for the evolution of oxygen in sulfuric and nitric acid containing electrolytes, while it withstands chlorine evolution in hydrochloric acid. The more electrochemically active phase consists of a nonstoichiometric lead dioxide with the empirical chemical formula PbO_n (with $1.4 < n < 2$). A review of its preparation is presented by Thangappan et al.[44]

Preparation Lead dioxide forms on pure lead, in dilute sulfuric acid, when polarized anodically at electrode potentials ranging from +1.5 to +1.8 V versus SHE. Hence, industrially, lead dioxide anodes are prepared by in situ anodization of a pure lead anode conducted at 20 °C. The lead anode and a copper cathode are immersed in an undivided cell containing dilute sulfuric acid (98 $g \cdot dm^{-3}$) flowing with a rate ranging 5–10 $dm^3 \cdot min^{-1}$, and the electrodeposition is conducted galvanostatically by application of an anodic current density of 100 $A \cdot m^{-2}$ for 30 min. The inherent brittleness of the PbO_2 ceramic coating on soft lead can be overcome by anodic

44 Thangappan, R.; Nachippan, S.; Sampath, S. (1970) Lead dioxide-graphite electrode. *Ind. Eng. Chem. Prod. Res. Dev.*, **9**(4), 563–567.

electrodeposition of lead dioxide onto inert and stiff substrates such as titanium, niobium, tantalum, graphite, and Ebonex®. These supported anodes (i.e., Ti/PbO_2 and Ta/PbO_2[45]) are now commercially available.[46, 47] The anodic electrodeposition of a layer of PbO_2 is usually conducted in an undivided cell with a copper cathode and a stationary or flowing electrolyte consisting of dilute sulfuric acid ($98\ g \cdot dm^{-3}$) containing lead(II) nitrate ($1\ mol \cdot dm^{-3}$) and minute amounts of copper(II) nitrate or nickel(II) nitrate. Copper and nickel cations are used as cathodic depolarizers to impede the deleterious electrodeposition of lead on the cathode. Before coating, the metal substrate is sandblasted to increase the roughness and enhance the coating adhesion; this is followed by chemical etching. Etching is conducted, for instance, in boiling concentrated hydrochloric acid for titanium and its alloys or in cold concentrated hydrofluoric acid for niobium and tantalum. Etching removes the passivating layer that is always present on refractory metals. Then lead dioxide is electrodeposited galvanostatically at $200\ A \cdot m^{-2}$ for several hours to reach anode loadings of several grams per square meter. The PbO_2 coating obtained is smooth, dense, hard, uniform, and free of pinholes and adheres to the surface of the substrate material. Sometimes a thin intermediate platinum layer is inserted between the base metal and the PbO_2 coating to enhance the service life by preventing the undermining process. Finally, for particular applications requiring bulk ceramic anodes, the electrodeposited lead dioxide can also be crushed, melted, and cast into intricate shapes.

Applications PbO_2-based anodes are used for their inertness and low cost and when the oxidation should be performed without the competitive evolution of oxygen. PbO_2 anodes were once used as a substitute for the conventional graphite and platinum electrodes for regeneration of potassium dichromate and in the production of chlorates and perchlorates.[48] These anodes were also extensively used in hydrometallurgy as oxygen anodes for the electroplating of copper and zinc in sulfate baths[49, 50, 51] and in organic electrosynthesis for the production of glyoxylic acid from oxalic acid with use of sulfuric acid as a supporting electrolyte.[52]

Failure modes For lead dioxide supported on lead, the mismatch of strength and thermal expansion between the lead metal substrate and its lead dioxide ceramic coating leads to flaking and spalling with loss of the coating. As mentioned previously, a thin platinum underlayer can delay the catastrophic undermining process induced by the loss of the coating, but usually the use of lead dioxide coated titanium anodes solves this issue but increases capital costs. Another failure mode occurs when manganese(II) cations are present that form insoluble manganese dioxide (MnO_2). Eventually, flakes on the anode can detach, entraining the coating and forming slimes at the bottom of the electrolyzer.

---

45 Pohl, J.P.; Richert, H. (1980) In: Trasatti, S. (ed.) *Electrodes of Conductive Metallic Oxides*, Part A. Elsevier, Amsterdam, Chap. 4, pp. 183–220.

46 De Nora, O. (1962) Anodes for use in the evolution of chlorine. British Patent 902,023; July 25, 1962.

47 Kuhn, A.T. (1976) The electrochemical evolution of oxygen on lead dioxide anodes. *Chemistry & Industry,* **20**, 867–871.

48 Grigger, J.C.; Miller, H.C.; Loomis, F.D. (1958) Lead dioxide anode for commercial use. *J. Electrochem. Soc.*, **105**, 100–102.

49 Engelhardt, V.; Huth, M. (1909) Electrolytic recovery of zinc. US Patent 935,250; September 28, 1909.

50 Gaunce, F.S. (1964) Treatment of lead or lead alloy electrodes. French Patent 1,419,356; November 26, 1964.

51 Higley, L.W.; Dressel, W.M.; Cole, E.R. (1976) U.S. Bureau of Mines, Report No. R8111.

52 Goodridge, F.; Lister, K.; Plimley, R.; Scott, K. (1980) Scale-up studies of the electrolytic reduction of oxalic to glyoxylic acid. *J. Appl. Electrochem.*, **10**(1), 55–60.

9.7.3.2.5 Manganese Dioxide (MnO_2)

Manganese dioxide was used for a long time following the work of Huth,[53] where hard and dense anodes of MnO_2 were obtained by forming a main body of the MnO_2 anode and then repeatedly treating this body with $Mn(NO_3)_2$ and heating it to decompose the nitrate and form additional MnO_2. These anodes were once used extensively in hydrometallurgy for the electrowinning or electroplating of zinc,[54] copper, and nickel in sulfate baths. They are prepared by solution impregnation–calcination[55] or by anodization in a sulfuric solution containing manganous cations. However, they never been used as widely as lead dioxide anodes owing to their high corrosion rate under extreme conditions (i.e., at high temperature, high pH, and elevated anodic current density). Nevertheless, some improvements have been made to increase their stability. Feige prepared a supported Ti/MnO_2 anode made by sintering titanium and lead particles with MnO_2.[56] De Nora et al. obtained a Ti/MnO_2-type anode by the application of the classic painting–thermal decomposition procedure used for the preparation of DSA®.[57]

9.7.3.2.6 Spinel (AB_2O_4)- and Perovskite (ABO_3)-Type Oxides

Structure It is well known that some ceramic oxides of the inner transition metals (e.g., Mn, Fe, Co, and Ni) with a spinel-type structure ($A^{II}B_2^{III}O_4$) or, to a lesser extent, a perovskite-type structure ($A^{II}B^{IV}O_3$) are electrical conductors with electrocatalytic activities when doped with lithium, nickel, and cobalt. Moreover, being sufficiently stable in corrosive electrolytes, they were developed as good candidates for the development of oxygen-evolving electrodes. Spinels are oxides with the general formula $^{IV}(A_{1-x}B_x)^{VI}(A_xB_{2-x})O_4$, where the divalent cations are denoted A (Mg^{2+}, Fe^{2+}, Ni^{2+}, Co^{2+}, and Zn^{2+}) and the trivalent cations are denoted B (Al^{3+}, Fe^{3+}, Cr^{3+}, and V^{3+}). Hence, two types of spinel structure must be distinguished: normal spinels, with $x = 0$, meaning that all the divalent cations occupy tetrahedral sites; and inverse spinels, with $x = 1$. Of these, rods of pure magnetite (Fe_3O_4) or its doped form[58] obtained by the casting of molten iron oxides have been used as industrial anodes since 1870. Apart from magnetite and ferrites, today other classes of spinels have been investigated, such as cobaltites and chromites. Because of their better electrocatalytic properties and fewer health and safety issues, cobaltites (e.g., MCo_2O_4 with M is Mg, Cu, and Zn) are now preferred and are the only ones being developed.

Properties These anodes, despite their good chemical inertness and electrochemical stability under a high positive potential,[59, 60] have two main drawbacks: they are brittle, which means a ceramic must be supported on a stiff metal substrate, and they exhibit very high electrical resistivities (27,000 $\mu\Omega \cdot cm$) with respect to other electrode materials.

53 Huth, M. (1919) Anodes of solid manganese peroxide. US Patent 1,296,188; March 4, 1919.
54 Bennett, J.E.; O'Leary, K.J. (1973) Oxygen anodes. US Patent 3,775,284; November 27, 1973.
55 Ohzawa, K.; Shimizu, K.; Takasue, T. (1967) Insoluble electrode for electrolysis. US Patent 3,616,302; February 27, 1967.
56 Feige, N.G. (1974) Method for producing a coated anode. US Patent 3,855,084; December 17, 1974.
57 De Nora, O.; Nidola, O.; Spaziante, P.M. (1978) Manganese dioxide electrodes. US Patent 4,072,586; February 7, 1978.
58 Kuhn, A.T.; Wright, P.M. In: Kuhn, A.T. (ed.) (1971) *Industrial Electrochemical Processes*, Chap. 14. Elsevier, New York.
59 Matsumura, Takashi; Itai, R.; Shibuya, M.; Ishi, G. (1968) Electrolytic manufacture of sodium chlorate with magnetite anodes. *Electrochem. Technol.,* **6**(11–12), 402–404.
60 Itai, R.; Shibuya, M.; Matsumura, T.; Ishi, G. (1971) Electrical resistivity of magnetite anodes. *J. Electrochem. Soc.*, **118**(10), 1709–1711.

Preparation These oxides are usually produced by the firing of metallic precursors (e.g., nitrates, oxalates) in a moderately oxidizing atmosphere (e.g., steam, or argon–carbon dioxide mixture) at moderate temperatures (700–900 °C). For reinforcement of a brittle ceramic, these oxides can be used supported on a stiff base metal such as titanium.[61] Sometimes, such as for PbO_2 anodes, a thin intermediate layer of platinum is deposited between the base metal and the magnetite to enhance the service life and delay the undermining process.

9.7.3.2.7 Ebonex® (Ti_4O_7 and Ti_5O_9)

Since 1983, the date of the original patent of Hayfield[62] from IMI Marston describing a novel semiconductive electrode material that was prepared from substoichiometric oxides of titanium, these ceramics have attracted particular attention in the electrochemical community.[63, 64] Soon afterward, the intellectual property related to the suboxides of titanium was purchased by the company Ebonex Technologies Incorporated, which was itself a subsidiary of ICI Americas and commercialized under the name Ebonex®.[65] Later, in 1992, the company was renamed Atraverda Ltd. Bulk ceramic electrodes are manufactured in various forms (e.g., plates, tubes, rods, honeycombs, fibers, powders, and pellets) and grades (e.g., vitreous and porous). From a crystallochemical point of view, these ceramics consist of substoichiometric oxides of titanium with the Andersson–Magnéli crystal lattice structure[66] and the general chemical formula Ti_nO_{2n-1}, where n is an integer equal to or greater than 4 (e.g., Ti_4O_7, Ti_5O_9, Ti_6O_{11}, Ti_7O_{13}, Ti_8O_{15}, Ti_9O_{17}, and $Ti_{10}O_{19}$). They are usually prepared by thermal reduction at 1300 °C of pure TiO_2 by hydrogen, methane, or carbon monoxide, or a blend of titanium dioxide and titanium metal powder. These oxides all have comparably elevated electronic conductivity similar to, and in some cases greater than, that of graphite (e.g., 630 μΩ · cm for Ti_4O_7 compared with 1375 μΩ · cm for graphite). From a corrosion point of view, Ebonex® exhibits an unusual chemical inertness in several corrosive media, such as strong, oxidizing, or reducing mineral acids (e.g., HCl, H_2SO_4, HNO_3, and even HF). The anomalous high resistance to HF, and fluoride anions, which usually readily attack titania even in dilute solutions, seems to be due to the difference in the lattice structure and the absence of hydrates. Ebonex® has also served as a substrate for electrodeposition with a platinum coating[67] and has been used as a platinized anode.[68] Such anodes show no major differences from bulk platinum anodes.

Moreover, Pletcher and coworkers succeeded in electroplating coatings of metals such as copper, gold, nickel, palladium, and platinum without any pretreatment of the substrate. In addition, by contrast with titanium, which is highly sensitive to hydrogen embrittlement,

61 Hayes, M.; Kuhn, A.T. (1978) The preparation and behavior of magnetite anodes. *J. Appl. Electrochem.*, **8**(4), 327–332.

62 Hayfield, P.C.S. (1983) Electrode material, electrode and electrochemical cell. US Patent 4,422,917; December 27, 1983.

63 Baez, V.B.; Graves, J.E.; Pletcher, D. (1992) The reduction of oxygen on titanium oxide electrodes. *J. Electroanal. Chem.*, **340**(1–2), 273–86.

64 Graves, J.E.; Pletcher, D.; Clarke, R.L.; Walsch, F.C. (1991) The electrochemistry of Magneli phase titanium oxide ceramic electrodes. I. The deposition and properties of metal coatings. *J. Appl. Electrochem.*, **21**(10), 848–857.

65 Clarke, R.; Pardoe, R. (1992) Applications of ebonex conductive ceramics in effluent treatment. In: Genders, D.; Weinberg, N. (eds.) *Electrochemistry for a Cleaner Environment*. Electrosynthesis Company, Amherst, NY, pp. 349–363.

66 Andersson, S.; Collén, B.; Kuylienstierna, U.; Magnéli, A. (1957) *Acta Chem. Scand.*, **11**, 1641.

67 Farndon, E.E.; Pletcher, D.; Saraby-Reintjes, A. (1997) The electrodeposition of platinum onto a conducting ceramic, Ebonex. *Electrochimica Acta*, **42**(8), 1269–1279.

68 Farndon, E.E.; Pletcher, D. (1997) Studies of platinized Ebonex electrodes. *Electrochimica Acta*, **42**(8), 1281–1285.

Ebonex® has no tendency to form brittle titanium hydride in contact with nascent hydrogen evolved during cathodic polarization. From an electrochemical point of view, Ebonex® exhibits poor intrinsic electrocatalytic properties[69] and hence has high overpotentials for both hydrogen and oxygen evolution reactions[70] (e.g., oxygen starts to evolve at +2.2 V vs SHE in 0.1 M $HClO_4$).[71] This dual behavior allows Ebonex® to be used without restriction either as a cathode or as an anode. Nevertheless, the use of the bare materials is limited under severe conditions such as high anodic current density because of the irreversible oxidation of Ti_4O_7 to insulating TiO_2. However, the overpotential of the Ebonex® material can be modified by the application of electrocatalysts (e.g., RuO_2, IrO_2) by the painting–thermal decomposition procedure use for the preparation of DSA®. By contrast, coated Ebonex® is capable of operating with traces of fluoride anions up to anodic current densities of 4 kA · m^{-2} in baths where DSA® failed rapidly because of the undermining mechanism (e.g., concentrated HCl, HF–HNO_3 mixtures, elevated fluoride content). Industrially, Ebonex® is recommended for several applications, including the replacement of lead anodes in zinc electrowinning, for cathodic protection of steel reinforcing bars (i.e., rebars) in concrete, for in situ electrochemical remediation of contaminated soils, in the purification of drinking water, in the treatment of waste effluents, and as bipolar electrodes in rechargeable batteries and even coated with PbO_2 for ozone generation.[72] The high cost of Ebonex®, combined with its brittleness, still limits its widespread use. Selected properties of Ebonex® are listed in ◘ Table 9.19.

9.7.3.2.8 Noble-Metal-Coated Titanium Anodes

During the 1950s and 1960s, at the peak of expansion of the American and Russian aircraft and space programs and with the development of nuclear power plants, industrial processes for the production of refractory metals (e.g., Ti, Zr, Hf, Nb, and Ta) reached commercial scale. These processes, such as the Kroll process,[73] made reactive metals with a wide range of alloy compositions available for the first time. This development brought several advantages: a reduction in production costs, the standardization of alloy grades, and a great effort in research and development for the use of these metals beyond their original aircraft and nuclear applications. At this stage, all the difficulties associated with preparing anodes of refractory metals coated with precious metals vanished, and the idea invented 40 years before by Stevens reappeared. Hence, niobium- and tantalum-platinized anodes were prepared following the work of Rhoda[74] and Rosenblatt[75] in 1955. In the latter patent, a layer of platinum was obtained on tantalum by the thermal decomposition of H_2PtCl_6 in an inert atmosphere. This thermal treatment, which was conducted between 800 and 1000 °C, gave a thin interdiffusion layer of a few micrometers, consisting of an alloy of tantalum and platinum. Furthermore, titanium, now commercially available because of the strong demand for turbine blades in aircraft engines, was studied both

69 Miller-Folk, R.R.; Noftle, R.E.; Pletcher, D. (1989) Electron transfer reactions at Ebonex ceramic electrodes. *J. Electroanal. Chem.*, **274**(1–2), 257–261.

70 Pollock, R.J.; Houlihan, J.F.; Bain, A.N.; Coryea, B.S. (1984) Electrochemical properties of a new electrode material, titanium oxide (Ti_4O_7). *Mater. Res. Bull.*, **19**(1), 17–24.

71 Park, S.-Y.; Mho, S.-I.; Chi, E.-O.; Kwon, Y.-U.; Yeo, I.-H. (1995) Characteristics of Ru and RuO_2 thin films on the conductive ceramics TiO and Ebonex (Ti_4O_7). *Bull. Kor. Chem. Soc.*, **16**(2), 82–84.

72 Graves, J.E.; Pletcher, D.; Clarke, R.L.; Walsh, F.C. (1992) The electrochemistry of Magneli phase titanium oxide ceramic electrodes. II. Ozone generation at Ebonex and Ebonex/lead dioxide anodes. *J. Appl. Electrochem.*, **22**(3), 200–203.

73 Kroll, W.J. (1940) The production of ductile titanium. *Trans. Electrochem. Soc.*, **112**, 35–47.

74 Rhoda, R.N. (1952) Electroless palladium plating. *Trans. Inst. Met. Finish.*, **36**(3), 82–85.

75 Rosenblatt, E.F.; Cohn, J.G. (1955) Platinum-metal-coated tantalum anodes. US Patent 2,719,797; October 4, 1955.

Table 9.19 Miscellaneous properties of Ebonex®. (Data from Atraverda)

Properties (at room temperature unless otherwise specified)	Bulk ceramic	Composite with polymer
Density (ρ/kg · m^{-3})	3600–4300	2300–2700
Specific heat capacity (c_p/J · kg^{-1} · K^{-1})	750	n. a.
Thermal conductivity (k/W · m^{-1} · K^{-1})	10–20	n. a.
Coefficient of linear thermal expansion (α/10^{-6} K^{-1})	6	n. a.
Flexural strength (MPa)	60–180	n. a.
Vickers microhardness (H_v)	230	n. a.
Electrical conductivity (κ/S · m^{-1})	3000–30,000	100–1000
Temperature range (°C)	Up to 250 °C in air or 800 °C (reducing atmosphere)	Up to 250 °C
Oxygen overpotential (V vs SHE)		
In H_2SO_4 (1 mol · dm^{-3})	+1.75	
In NaOH (1 mol · dm^{-3})	+1.65	
Hydrogen overpotential (V vs SHE)		
In H_2SO_4 (1 mol · dm^{-3})	−0.75	
In NaOH (1 mol · dm^{-3})	−0.60	

n. a. not available, *SHE* standard hydrogen electrode

from a corrosion and an electrochemical point of view at ICI by Cotton.[76, 77] The studies showed that the exceptional resistance of titanium to corrosion in seawater was due to the valve action property of its oxide, which allowed the metal to be protected under anodic polarization by an insulating layer of rutile (TiO_2). It was only in 1957 that Beer[78] at Magneto Special Anodes BV (Netherlands) and Cotton[79, 80] with the help of Angell at ICI (UK) showed independently but concurrently that attaching rhodium or platinum at the surface of titanium, either by electroplating or by spot welding, provided sufficient electrical conductivity to the base metal that it could be polarized anodically despite its passivation. It was assumed that anodic current passed through platinum or rhodium metal. These rhodized or platinized titanium bielectrodes were named ***noble-metal-coated titanium*** electrodes. During the following decade, noble-metal-coated titanium electrodes were actively developed through a partnership between ICI and Magneto

76 Cotton, J.B. (1958) Anodic polarization of titanium. *Chem. & Ind.*, **3**, 492–493.

77 Cotton, J.B. (1958) The corrosion resistance of titanium. *Chem. Ind.*, **3**, 640–646.

78 Beer, H.B. (1960) Precious-metal anode with a titanium core. British Patent 855,107; November 11, 1960.

79 Cotton, J.B.; Williams, E.C.; Barber, A.H. (1957) Titanium electrodes plated with platinum-group metals for electrolytic processes and cathodic protection. Electrodes. British Patent 877,901; July 17, 1957.

80 Cotton, J.B. (1958) Platinum-faced titanium for electrochemical anodes. A new electrode material for impressed current cathodic protection. *Platinum Metals Rev.*, **2**, 45–47.

Chemie, with the close contribution of other companies, such as Inco, Engelhard,[81, 82] and IMI Kynock.[83] Other firms such as W.C. Heraeus,[84] Metallgeselschaft,[85] and Texas Instruments[86] have also worked independently on the subject. The best preparation procedure involves electroplating with platinum or rhodium because the electrodeposition allows smooth and nonporous deposits with a good throwing power without requiring a large amount of platinum.[87] The electroplating baths contain a platinum salt such as the so-called P-salt, hexachloroplatinic acid, or sodium hexachloroplatinate(IV).[88] The electrocatalytic coating consists of platinum and rhodium present in their metallic forms. However, both rhodium and platinum have high chlorine overvoltage (e.g. 300 mV for Rh and 486 mV for Pt at 10 $kA \cdot m^{-2}$) and exhibit slight corrosion, with the rate depending on the electrolyte and the nature of the bath impurities (e.g., Cl^-, F^-, organics).

9.7.3.2.9 Platinized Titanium and Niobium Anodes (70/30 Pt/Ir)

The improvement of the noble-metal-coated-titanium anodes was the starting point of the study and preparation of ***platinized titanium anodes*** by the thermal decomposition of a precursor with the pioneering work of, for example, Angell and Deriaz, both from ICI.[89, 90] The precursor consisted of a given mixture of hexachloroplatinic acid (H_2PtCl_6) and hexachloroiridic acid (H_2IrCl_6) dissolved in an appropriate organic solvent (e.g., linalool, 2-propanol, or ethyl acetoacetate). Before application of the painting solution, the titanium substrate was thoroughly sandblasted to increase its roughness and chemically etched to remove the passivating layer. The etchants included various chemicals, such as hot concentrated hydrochloric acid, hot 10 wt% oxalic acid, and hot 30 wt% sulfuric acid. After each application the treated piece underwent a long thermal treatment at high temperature in air between 400 and 500 °C. At such temperatures thermal oxidation of the underlying titanium substrate is negligible. This original protocol was inspired by Taylor's work[91] used in the 1930s to obtain reflective coatings of platinum on glass for the manufacture of optical mirrors. The thermal decomposition of these particular painting solutions was studied by Hopper[92] in 1923 and later by Kuo[93] in 1974. Other companies interested in platinized titanium anodes prepared by thermal decomposition were Engelhard[94]

81 Haley, A.J.; Keith, C.D.; May, J.E. (1969) Two-layer metallic electrodes. US Patent 3,461,058.
82 May, J.E.; Haley, A.J. (1970) Electroplating with auxiliary platinum-coated tungsten anodes. US Patent 3,505,178; April 7, 1970.
83 Cotton, J.B.; Hayfield, P.C.S. (1965) Electrodes and methods of making same. British Patent 1,113,421; May 15, 1965.
84 Muller, P.; Speidel, H. (1960) New forms of platinum-tantalum electrodes. *Metall.* **14**, 695–696.
85 Schleicher, H.W. (1963) Electrodes for electrolytic processes. British Patent 941,177; November 6, 1963.
86 Whiting, K.A. (1964) Cladding copper articles with niobium or tantalum and platinum outside. US Patent 3,156,976; November 17, 1964.
87 Balko, E.N. (1991) *Electrochemical Applications of the Platinum Group: Metal Coated Anodes.* In: Hartley, F.R. (ed.) *Chemistry of the Platinum Group Metals: Recent Developments.* Elsevier, New York.
88 Lowenheim, F.A. (1974) *Modern Electroplating*, 3rd ed. Wiley, New York.
89 Angell, C.H.; Deriaz, M.G. (1961) Improvements in or relating to a method for the production of assemblies comprising titanium. British Patent 885,819; December 28, 1961.
90 Angell, C.H.; Deriaz, M.G. (1965) Improvements in or relating to a method for the production of assemblies comprising titanium. British Patent 984,973; March 3, 1965.
91 Taylor, J.F. (1929) *J. Opt. Soc. Am.*, **18**, 138.
92 Hopper, R.T. (1923) *Ceram. Ind.* (June).
93 Kuo, C.Y. (1974) Electrical applications of thin-films produced by metallo-organic deposition. *Solid State Technol.* **17**(2), 49–55.
94 Anderson, E.P. (1961) Method for preparing anodes for cathodic protection systems. US Patent 2,998,359; August 29, 1961.

and Ionics.[95] After long-term trials, the formulation and procedure were finally optimized. These anodes were initially commercialized in 1968 by IMI Marston under the trade name **K-type®** or **70/30 Pt/Ir**.[96] For optimum performance, the commercially pure titanium must be of ASTM grade 1 or grade 2 with equiaxed grain sizes ranging between 30 and 50 μm. The electrocatalytic coating consists of platinum and rhodium present in their metallic forms either as separate phases or as platinum–iridium intermetallic. After thermal decomposition, titanium is coated with a highly divided mixture of metal oxides consisting essentially of 70 wt% PtO_x and 30 wt% IrO_x. The common anode loading is 10 $g \cdot m^{-2}$. Later, Millington[97] observed that niobium, tantalum, and even tungsten[98] could also be used as substrates, but they were only considered by certain suppliers[99] when titanium showed deficiencies owing to their greater cost. These anodes were rapidly used in numerous processes requiring a long service life under severe conditions. For example, they were used for the cathodic protection of immersed plants such as oil rigs, storage tanks, and subterranean pipelines,[100, 101] in the electrolytic processes for the production of sodium hypochlorite,[102] electrodialysis, for regeneration of Ce(IV) in perchloric or nitric acid,[103] and for oxidation of sulfuric acid in peroxodisulfuric acid.[104] It is interesting to note that De Nora registered a patent on a platinum-coated anode in which the base metal was a ferrosilicon with some amounts of chromium.[105] Other formulations consisted of clad platinum metal on a copper-clad titanium or niobium core by roll bonding or a sandwich of platinum–titanium (or niobium)–copper. This technique, which provides a thick, dense, and impervious platinum coating, is now commercialized by Anomet in the USA for the cathodic protection of oil rigs. This continuous research effort, always developed under pressure from industry, resulted in the 1960s in a new generation of anodes that are still widely used in all electrochemical fields and are discussed in the following sections. Nevertheless, although platinized titanium electrodes were found to be active, they were still found to be unsatisfactory for chlorine production. It was for this reason that Beer patented a new type of anode, discussed in the next section.

9.7.3.2.10 Dimensionally Stable Anodes (DSA®) for Chlorine Evolution

In the 1960s, Henri Bernard Beer, who worked at Permelec,[106] and the Italian team of Giuseppe Bianchi, Vittorio De Nora, Patrizio Gallone, and Antonio Nidola started studying the electrocatalytic behavior of mixed metal oxides and nitride coatings for the evolution of chlorine and

95 Tirrel, C.E. (1964) Method for making non corroding electrode. US Patent 3,117,023; January 7, 1964.

96 Hayfield, P.C.S.; Jacob, W.R. (1980) In: Coulter, M.O. (ed.) *Modern Chlor-Alkali Technology*. Ellis Horwood, London, Chap. 9, pp. 103–120.

97 Millington, J.P. (1974) Lead dioxide electrode. British Patent 1,373,611; November 13, 1974.

98 May, J.E.; Haley, Jr., A.J. (1970) Electroplating with auxiliary platinum-coated tungsten anodes. US Patent 3,505,178; April 7, 1970.

99 Haley, Jr., A.J. (1967) *Engelhard Ind. Tech. Bull.*, **7**, 157.

100 Cotton, J.B.; Williams, E.C.; Barber, A.H. (1961) Improvements relating to electrodes and uses thereof. British Patent 877,901; September 20, 1961.

101 Anderson, E.P. (1961) Method for preparing anodes for cathodic protection systems. US Patent 2,998,359; August 29, 1961.

102 Adamson, A.F.; Lever, B.G.; Stones, W.F. (1963) *J. Appl. Chem.*, **13**, 483.

103 Ibl, N.; Kramer, R.; Ponto, L.; Robertson, P.M. (1979) *Electroorganic Synthesis Technology*. *AIChE Symposium Series* No. 185 75, 45.

104 Rakov, A.A.; Veselovskii, V.I.; Kasatkin, E.V.; Potapova, G.F.; Sviridon, V.V. (1977) *Zh. Prikl. Khim.* **50**, 334.

105 Bianchi, G.; Gallone, P.; Nidola, A.E. (1970) Composite anodes. US Patent 3,491,014; January 20, 1970.

106 Beer, H.B. (1963) Noble metal coated titanium electrode and method for making and using it. US Patent 3,096,272; July 2, 1963.

oxygen.[107, 108] These oxides were obtained by the calcination of precursors but in an oxidizing atmosphere (i.e., air or pure oxygen). These RuO_2-based anodes or so-called ruthenized titanium anodes, composed of titanium metal coated with mixed metal oxides (TiO_2-RuO_2), have been developed with great success since 1965, the year of Beer's famous patent.[109] At this stage, the selection of ruthenium was based only on the low cost of the metal and its commercial availability. These electrodes were later protected by several patents.[110, 111, 112, 113] It was the birth of the ***activated titanium anode***, also called an ***oxide-coated titanium anode***, a designation that is now obsolete and that was modernized in the 1990 to ***mixed metal oxide anode***. These anodes are characterized by a geometrical stability and a constant potential over a long time (more than 2–3 years). It is this dimensional stability in comparison with the graphite anodes that gives them their trade name: ***dimensionally stable anodes*** (the acronym DSA® is a trademark of De Nora Permelec Ltd). The classic composition of the composite anodes is defined in ◘ Table 9.20.[114]

As a general rule, these anodes are made from a titanium base metal covered by a rutile layer of TiO_2 doped with RuO_2 (30 mol%).[115, 116] They were used extensively in the industry (e.g., De Nora, Magnetochemie, Permelec, Eltech Systems Corporation, US Filter, and Heraeus), and today they are used in all chlor-alkali processes and in chlorate production.[117] The dimensionally stable anodes for chlorine evolution are described in the technical literature by the brand names DSA®(RuO_2) and DSA®-Cl_2, and they enjoyed great success in industry for two reasons: first, ruthenium has the lowest price of all the PGMs and, second, its density is half that of its neighbors. Moreover, its electrocatalytic characteristics for the evolution of chlorine are satisfactory. In industrial conditions (2–4 $kA \cdot m^{-2}$) the service life of these electrodes is more than 5 years. Therefore, today, titanium is the only base metal used for the manufacture of dimensionally stable anodes for chlorine evolution. The contribution of Beer's discovery to the development of industrial electrochemistry is very important. The reader can also find a complete story of the invention of DSA® as told by the inventor himself and written on the occasion of his receiving the *Electrochemical Society Medal*.[118]

107 Bianchi, G.; De Nora, V.; Gallone, P.; Nidola, A. (1971) Titanium or tantalum base electrodes with applied titanium or tantalum oxide face activated with noble metals or noble metal oxides. US Patent 3,616,445; October 26, 1971.
108 Bianchi, G.; De Nora, V.; Gallone, P.; Nidola, A. (1976) Valve metal electrode with valve metal oxide semi-conductive face. US Patent 3,948,751; April 6, 1976.
109 Beer, H.B. (1966) Electrode and method for making the same. US Patent 3,234,110; February 8, 1966.
110 Beer, H.B. (1966) Method of chemically plating base layers with precious metals of the platinum group. US Patent 3,265,526; August 9, 1966.
111 Beer, H.B. (1972) Electrode and coating therefor. US Patent 3,632,498; January 4, 1972.
112 Beer, H.B. (1973) Electrode having a platinum metal oxide. US Patent 3,711,385; January 13, 1973.
113 Beer, H.B. (1973) Electrode and coating therefor. US Patent 3,751,291; August 7, 1973.
114 Nidola, A. In: Trasatti, S. (ed.) (1981) *Electrodes of Conductive Metallic Oxides*. *Part B*. Elsevier, Amsterdam, Chap. 11, pp. 627–659.
115 Vercesi, G.P.; Rolewicz, J.; Comninellis, C.; Hinden, J. (1991) Characterization of dimensionally stable anodes DSA-type oxygen evolving electrodes. Choice of base metal. *Thermochimica Acta*, **176**, 31–47.
116 Comninellis, Ch.; Vercesi, G.P. (1991) Characterization of DSA-type oxygen evolving electrodes: choice of a coating. *J. Appl. Electrochem.*, **21**(4), 335–345.
117 Gorodtskii, V.V.; Tomashpol'skii, Yu.Ya.; Gorbacheva, L.B.; Sadovskaya, N.V.; Percherkii, M.M.; Erdokimov, S.V.; Busse-Machukas, V.B.; Kubasov, V.L.; Losev, V.V. (1984) *Elektrokhimiya*, **20**, 1045.
118 Beer, H.B. (1980) The invention and industrial development of metal anodes. *J. Electrochem. Soc.*, **127**, 303C–307C.

Table 9.20 Definition of dimensionally stable anodes

	Component	Description
A dimensionally stable anode is a composite electrode made of	A base metal or substrate	A base metal with a valve action property, such as the refractory metals (e.g., Ti, Zr, Hf, Nb, Ta, Mo, W) or their alloys (e.g., Ti-0.2Pd, Ti–Ru). This base metal acts as a current collector.[a] Sometimes it is possible to find in the claims of some particular patents unusual base materials (e.g., Al, Si-cast iron, Bi, C, Ti_4O_7, Fe_3O_4)
	A protective passivating layer	A thin and impervious layer (a few micrometers thick) of a protective valve metal oxide (e.g., TiO_2, ZrO_2, HfO_2, Nb_2O_5, Ta_2O_5, NbO_2, and TaO_2)
	An electrocatalyst	An electrocatalytic oxide of a noble metal or, more often, an oxide of the PGMs. This PGM oxide (e.g., RuO_2, PtO_x, IrO_2) increases the electrical conductivity of the passivating film. Sometimes other oxides are added (e.g., SnO_2, Sb_2O_5, Bi_2O_3) and also carbides (e.g., B_4C) or nitrides

PGM platinum group metal

[a] De Nora, O.; Nidola, A.; Trisoglio, G.; Bianchi, G. (1973) British Patent 1,399,576

9.7.3.2.11 Dimensionally Stable Anodes (DSA®) for Oxygen

Several industrial processes require long-lasting anodes for evolution of oxygen in an acidic medium. In comparison with the chlorine-evolution reaction, the evolution of oxygen leads to higher positive potentials, combined with an increase in the acidity, leading to severer conditions for the anode material. Hence, most materials are put in their anodic dissolution or transpassive region. These conditions greatly restrict the selection of suitable materials. The only materials that can withstand these conditions are gold and the PGMs, but their use is prohibited by their high densities and high cost when they are required in bulk. Today, when highly valuated chemicals are produced, common base metals can be clad with these metals and these metals can be polarized under low anodic current densities ($1\ kA \cdot m^{-2}$), while for more demanding conditions a hydrogen-diffusion anode must be used. Nevertheless, their high electrocatalytic activity dictates their use as electrocatalysts. As a general rule, the increasing electrochemical activity can be classified as follows: Ir > Ru > Pd > Rh > Pt > Au.[119] Carbon anodes, sometimes impregnated with a dispersion of PGMs, are now totally obsolete owing to their high oxygen overvoltage and rapid failure during electrolysis. Owing to their high porosity,

119 Miles, M.H.; Thomason, J. (1976) Periodic variations of overvoltages for water electrolysis in acid solutions from cyclic voltammetric studies. *J. Electrochem. Soc.*, **123**(10), 1459–1461.

Table 9.21 Standard potentials for several oxide couples. (Tseung, A.C.C.; Jasem, S. (1977) Oxygen evolution on semiconducting oxides. *Electrochim. Acta,* **22**, 31)

Higher/lower oxide couple	Standard electrode potential at 298.15 K (*E*/V vs SHE)
IrO_2/Ir_2O_3	0.930
RuO_2/Ru_2O_3	0.940
OsO_2/OsO_4	1.00
NiO_2/Ni_2O_3	1.43
CoO_2/Co_2O_3	1.45
RhO_2/Rh_2O_3	1.73
PtO_3/PtO_2	2.00
PdO_3/PdO_2	2.03

SHE standard hydrogen electrode

an intercalation phenomenon occurs: the anions penetrate the lattice and expand the structure, leading rapidly to spalling of the electrode.[120]

Therefore, most of the electrode materials described previously fail rapidly when operating at the high anodic current densities (e.g., 2–15 $kA \cdot m^{-2}$) imposed by demanding electrochemical processes such as high-speed gold plating,[121] high-speed electrogalvanizing of steel (e.g., Andritz Ruthner AG technology),[122] and zinc electrowinning. On the basis of good results obtained with mixed metallic oxides such as TiO_2-RuO_2 and Ta_2O_5-RuO_2 for the chlorine reaction and the huge success of DSA® in the chlor-alkali industry, these anodes were optimized for the oxygen-evolution reaction. Several compositions of electrocatalysts and base metals were then actively studied. Many metal oxides exhibiting good electronic conductivity, multivalence states, and a low redox potential for the higher oxide versus the lower oxide couple have been reported as promising electrocatalysts. Experimental values for the standard redox potentials of oxide couples are presented in Table 9.21.

These data show clearly that of the candidate electrocatalysts, iridium, ruthenium, osmium, nickel, and cobalt have lower redox potentials than rhodium, palladium, and platinum. Despite its excellent electrocatalytic activity, ruthenium dioxide (RuO_2) is readily oxidized at 1.39 V versus SHE to give off the volatile ruthenium tetroxide (RuO_4),[123] and it is too sensitive to electrochemical dissolution.[124, 125] Osmium was excluded owing to the formation of volatile

120 Jasinski, R.; Brilmyer, G.; Helland, L. (1983) Stabilization of glassy carbon electrodes. *J. Electrochem. Soc.*, **130**(7), 1634.

121 Smith, C.G.; Okinaka, Y. (1983) High speed gold plating: anodic bath degradation and search for stable low polarization anodes. *J. Electrochem. Soc.*, **130**, 2149–2157.

122 Hampel, J. (1984) Process and apparatus for the continuous electroplating of one or both sides of a metal strip. US Patent 4,469,565; February 22, 1984.

123 Hine, F.; Yasuda, M.; Noda, T.; Yoshida, T.; Okuda, J. (1979) Electrochemical behavior of the oxide-coated metal anodes. *J. Electrochem. Soc.*, **126**(9), 1439–1445.

124 Manoharan, R.; Goodenough, J.B. (1991) *Electrochim. Acta,* **36**, 19.

125 Yeo, R.S.; Orehotsky, J.; Visscher, W.; Srinivasan, S. (1981) Ruthenium-based mixed oxides as electrocatalysts for oxygen evolution in acid electrolytes. *J. Electrochem. Soc.,* **128**(9), 1900–1904.

(boiling point 130 °C) and hazardous osmium tetroxide (OsO_4), while nickel and cobalt oxides exhibit poor conductivity. Therefore, iridium dioxide (IrO_2) is the stablest and most active electrocatalyst coating, especially when prepared by the thermal decomposition of iridium chloride precursors (e.g., H_2IrCl_6, $IrCl_4$). Other studies demonstrated the important selection of the valve metal oxide (e.g., TiO_2, Nb_2O_5, and Ta_2O_5). De Nora showed that the best formulation was Ta_2O_5-IrO_2.[126] Later, Comninellis and coworkers optimized the composition by preparing a coating containing 70 mol% IrO_2.[127] This product was later developed commercially by Eltech Systems Corporation under the trade name TIR-2000®. These anodes have achieved operation in high-speed electrogalvanizing at current densities as high as 15 $kA \cdot m^{-2}$ and with service lives exceeding 4300 h.[128] In contrast to the coating wear limiting anode life in chlorine, the complex corrosion-passivation mechanism of the substrate beneath the coating is typically the limiting factor for oxygen-evolving anodes. Indeed, during coating preparation the thermal stresses transform the electrocatalyst layer into a typical microcracked structure.[129] The gaps between grains facilitate the penetration of the corrosive electrolyte down to the base metal (i.e., undermining process).[130, 131, 132] According to Hine et al.,[133] by analogy with the anodic deactivation mechanism of PbO_2- and MnO_2-coated anodes, the failure mode involves the damage of the interface between the electrocatalyst and the base metal, forming a thin layer of insulating rutile. This insulating film decreases the anode active surface area, increasing the local anodic current density. This behavior results in the spalling of the coating. The deactivation can be easily monitored industrially because the operating cell voltage increases continuously up to the limiting potential delivered by the rectifier. At this stage the anode is considered to be deactivated and is returned to the supplier to be refurbished. The costly electrocatalyst coating is then removed from the substrate by chemical stripping. The etching operation is usually performed in a molten mixture of alkali metal hydroxides (e.g., NaOH) containing small amounts of an oxidizing salt.[134] The precious catalyst is then recovered in the slimes at the bottom of the vessel, while the clean substrate is treated and reactivated by the classic procedure. Usually, the critical parameters that influence the service life of the anode are the anodic current density, the coating preparation, and impurities. Several inorganic and organic pollutants can lead to the dissolution of titanium (e.g., fluoride anions[135]), scaling (e.g., manganous cations), and the loss of the coating (e.g. organic acids, nitroalcohols). For example, in organic electrosynthesis, the service life of these electrodes ranges 500–1000 h in 1 M sulfuric acid at 60 °C.[136] Hence

126 De Nora, O.; Bianchi, G.; Nidola, A.; Trisoglio, G. (1975) Anode for evolution of oxygen. US Patent 3,878,083.

127 Comninellis, Ch.; Vercesi, G.P. (1991) Characterization of DSA-type oxygen evolving electrodes: choice of a coating. *J. Appl. Electrochem.*, **21**(4), 335–345.

128 Hardee, K.L.; Mitchell, L.K. (1989) The influence of electrolyte parameters on the percent oxygen evolved from a chlorate cell. *J. Electrochem. Soc.*, **136**(11), 3314–3318.

129 Kuznetzova, E.G.; Borisova, T.I.; Veselovskii, V.I. (1968) *Elektrokhimiya* **10**, 167.

130 Warren, H.I., Wemsley, D., Seto, K. (1975) *Inst. Min. Met. Branch Meeting*, February 11, 1975, **53**.

131 Seko, K. (1976) *Am. Chem. Soc. Centennial Meeting*, New York.

132 Antler, M.; Butler, C.A. (1967) *J. Electrochem. Technol.*, **5**, 126.

133 Hine, F.; Yasuda, M.; Yoshida, T.; Okuda, J. (1978) *ECS Meeting*, Seattle, May 15, Abstract 447.

134 Colo, Z.J.; Hardee, K.L.; Carlson, R.C. (1992) Molten salt stripping of electrode coatings. US Patent 5,141,563; August 25, 1992.

135 Fukuda, K.; Iwakura, C.; Tamura, H. (1980) Effect of heat treatment of titanium substrate on service life of titanium-supported iridia electrode in mixed aqueous solutions of sulfuric acid, ammonium sulfate, and ammonium fluoride. *Electrochim. Acta*, **25**(11), 1523–1525.

136 Savall, A. (1992) Electrosynthèse organique. In: Électrochimie 92, *L'Actualité Chimique*, Special issue, January 1992.

the high cost (US$ 10,000 to US$ 30,000 per square meter) prevents their industrial use in those conditions. In the late 1970s, as a consequence of work done on cathodically modified alloys initially conducted in the 1940s in the former Soviet Union by the Tomashov group, followed in the 1960s by Stern and Cotton[137] at ICI, there appeared a titanium–palladium alloy (i.e., ASTM grade 7) in which a small amount of palladium (0.12–0.25 wt% Pd) greatly increased the corrosion resistance in reducing acids. Hence, several patents claimed a substrate made of titanium–palladium for preparing DSA® for oxygen. Nevertheless, despite a certain improvement, their limited service life led to the abandonment of several industrial projects. Moreover, Cardarelli and coworkers demonstrated that the service life of Ti/Ta_2O_5-IrO_2 anodes was affected by impurities in commercially pure titanium and by alloying elements in titanium alloys.[138] In addition, the influence of other reactive and refractory metals (i.e., Nb, Ta, Zr) as a substrate on the service life has been studied, and Vercesi et al.[139] found that the performance of tantalum-based anodes was better than that of titanium-based electrodes. This good behavior was due to the remarkable corrosion resistance of tantalum owing to the valve action property of its passivating and impervious film of anodically formed tantalum pentoxide. However, the development of a bulk tantalum-based electrode is not practical from the viewpoint of economics. The high price of tantalum (US$ 461 per kilogram) combined with its high density (16,654 $kg \cdot m^{-3}$), in comparison with titanium metal (4540 $kg \cdot m^{-3}$), which has a medium-range price (US$ 50 per kilogram), precludes any industrial applications. As a consequence, an anode of tantalum is 35 times more expensive than a titanium anode. Furthermore, owing to the high reactivity of titanium versus oxygen above 350 °C, the preparation of tantalum anodes involves great difficulties during the thermal treatment required for the manufacture of electrodes. For these reasons, the tantalum anode does not enjoy widespread industrial use. To decrease the cost, a thin tantalum layer deposited onto a common base metal is a very attractive alternative. This idea appeared for the first time in 1968 in a patent[140] registered by the German company Farbenfabriken Bayer and also in 1974 in a proposition by Jeffes in a patent of Allbright & Wilson.[141] In this last patent a composite DSA®-Cl_2 material was made from a steel plate coated with 500 μm of tantalum prepared by chemical vapor deposition. Then the tantalum was coated with RuO_2 (steel/Ta/RuO_2). Twenty years later, the anodes made according to this process were not industrially developed. However, in 1990, in a European patent[142] registered by ICI, Denton and Hayfield described the preparation of oxygen anodes made of a thin tantalum coating deposited onto a common base metal using several techniques. Finally, in 1993, Kumagai et al.[143] from DAIKI Engineering in Japan prepared an anode made of a thin intermediate layer of tantalum deposited onto a titanium base metal by sputtering (Ti/Ta/

137 Potgieter, J.H.; Heyns, A.M.; Skinner, W. (1990) Cathodic modification as a means of improving the corrosion resistance of alloys. *J. Appl. Electrochem.*, **20**(5), 711–15.

138 Cardarelli, F.; Comninellis, Ch.; Savall, A.; Taxil, P.; Manoli, G.; Leclerc, O. (1998) Preparation of oxygen evolving electrodes with long service life under extreme conditions. *J. Appl. Electrochem.*, **28**, 245.

139 Vercesi, G.P.; Rolewicz, J.; Comninellis, C.; Hinden, J. (1991) Characterization of dimensionally stable anodes DSA-type oxygen evolving electrodes. Choice of base metal. *Thermochimica Acta*, **176**, 31–47.

140 Farbenfabriken Bayer Aktiengesellschaft (1968) French Patent 1,516,524.

141 Jeffes, J.H.E. (1974) Electrolysis of brine. British Patent 1,355,797; July 30, 1974.

142 Denton, D.A.; Hayfield, P.C.S. (1990) Coated anode for an electrolytic process. European Patent 383,412; August 22, 1990.

143 Kumagai, N.; Jikihara, S.; Samata, Y.; Asami, K.; Hashimoto, A.M. (1993) The effect of sputter-deposited Ta intermediate layer on durability of IrO_2-coated Ti electrodes for oxygen evolution. In: *Proceeding of the 183rd Joint International Meeting of the Electrochemical Society,* 93–30 (Corrosion, Electrochemistry, and Catalysis of Metastable Metals and Intermetallics), Abstract 324–33, Honolulu, HI, May 16–21, 1993.

Ta_2O_5-IrO_2). To select the most optimized method for deposition of tantalum onto a common substrate, Cardarelli et al.[144] comprehensively compared tantalum coating techniques used in the chemical-process industry. Moreover, the same authors developed anodes made from a thin tantalum layer deposited onto a common base metal (e.g. copper, nickel, or stainless steel) coated with an electrocatalytic mixture of Ta_2O_5 and IrO_2 produced by calcination. The performances of these anodes (stainless steel/Ta/IrO_2) are identical to the performance obtained with solid tantalum base metal (Ta/IrO_2).[145]

9.7.3.2.12 Synthetic Diamond Electrodes

Structure The use of synthetic semiconductive diamond thin films in electrochemistry was reported in 1993.[146] Designations such as diamond-like carbon are now obsolete and so are not used in this book. By contrast with the other carbon allotropes, in diamond each carbon atom is tetrahedrally bonded to four other carbons using sp^3-hybridized orbitals.

Properties Diamond has several attractive properties, including the highest Young's modulus, thermal conductivity, and hardness of all solid materials, high electrical resistance, excellent chemical inertness, high electron and hole mobilities, and a wide optical transparency range (see Sect. 12.5.1). The pure material is a wide bandgap insulator (E_g = 5.5 eV) and offers advantages for electronic applications under extreme environmental conditions. Nevertheless, when doped with boron, the material exhibits p-type semiconductive properties (i.e., IIb-type diamond). Doped diamond thin films can possess electronic conductivity ranging from that of an insulator at low doping levels to that of a good semiconductor for highly doped films (i.e., impurity level more than 10^{19} atoms per cubic centimeter). For instance, synthetic diamond thin films grown with use of hot-filament or microwave-assisted chemical vapor deposition can be doped to as high as one boron atom per 100 carbon atoms, resulting in films with resistivities of less than 10^5 μΩ · cm. Boron atoms that are electron acceptors form a band located roughly 0.35 eV above the valence-band edge. At room temperature, some of the valence-band electrons are thermally promoted to this intermediate level, leaving free electrons in the dopant band and holes, or vacancies, in the valence band to support the flow of current. In addition, boron-doped diamond thin films commonly possess a rough, polycrystalline morphology with grain boundaries at the surface and a small-volume fraction of nondiamond carbon impurity. Hence, the electrical conductivity of the film surface and the bulk is influenced by the boron-doping level, the grain boundaries, and the impurities. Several interesting electrochemical properties distinguish boron-doped diamond thin films from conventional carbon-based electrodes. As a general rule, boron-doped diamond films exhibit voltammetric background currents and double-layer capacitances up to an order of magnitude lower than for glassy carbon. The residual or background current density in 0.1 M KCl measured by linear sweep voltammetry is less than 50 μA · cm^{-2} between −1.0 and +1.0 V versus SHE. This indicates that the diamond–electrolyte interface is almost ideally polarizable. The evolution of hydrogen starts at roughly −1.75 V versus SHE. The electrochemical span or working potential window, defined as the potentials at which the anodic and cathodic currents reach 250 μA · cm^{-2}, is 3.5 V for diamond and 2.5 V for glassy

144 Cardarelli, F.; Taxil, P.; Savall, A. (1996) Tantalum protective thin coating techniques for the chemical process industry: molten salts electrocoating as a new alternative. *Int. J. Refract. Metals Hard Mater.*, **14**, 365.

145 Cardarelli, F.; Comninellis, C.; Leclerc, O.; Saval, A.; Taxil, P.; Manoli, G. (1997) Fabrication of an anode with enhanced durability and method for making the same. PCT International Patent Application WO 97/43465A1.

146 Swain, G.; Ramesham, R. (1993) The electrochemical activity of boron-doped polycrystalline diamond thin film electrodes. Anal. Chem., 65(4), 345–351.

carbon. The overpotentials for hydrogen and oxygen evolution reactions are directly related to the nondiamond carbon impurity content. The higher the fraction of nondiamond carbon present, the lower the overpotentials for both these reactions. The double-layer capacitance for boron-doped diamond in 1 M KCl ranges 4–8 $\mu F \cdot cm^{-2}$ over a 2-V potential window. There is a general trend toward increasing capacitance with more positive potentials, which is characteristic of p-type semiconductor electrode–electrolyte interfaces.[147] These capacitance values are comparable in magnitude to those observed for the basal plane of highly oriented pyrolytic graphite and significantly lower than those for glassy carbon (25–35 $\mu F \cdot cm^{-2}$). The capacitance versus potential profile shape and magnitude for diamond are largely independent of the electrolyte composition and solution pH. On the other hand, boron-doped diamond electrodes have good electrochemical activity without any pretreatment.

Preparation Diamond thin films can be prepared on a substrate from thermal decomposition of dilute mixtures of a hydrocarbon gas (e.g., methane) in hydrogen with use of one of several energy-assisted chemical vapor deposition methods, the most popular being hot-filament and microwave discharge.[148, 149] The growth methods mainly differ in the manner in which the gas thermal activation is accomplished. Typical growth conditions are C/H ratios of 0.5–2 vol%, reduced pressure ranging 1.33–13.3 kPa, a substrate temperature between 800 and 1000 °C, and microwave powers of 1–1.3 kW, or filament temperatures of approximately 2100 °C, depending on the method used. The film grows by nucleation at rates in the 0.1 to 1 μm/h range. For the substrates to be continuously coated with diamond, the nominal film thickness must be 1 μm. Wafer diameters of several centimeters can easily be coated in most modern reactors. Boron doping is accomplished from the gas phase by the mixing of a boron-containing gas such as diborane (B_2H_6) with the source gases, or from the solid state by gasification of a piece of hexagonal boron nitride.[150] Before deposition, the substrate must be pretreated by it being cleaning with a series of solvents, and nucleation sites are provided by the embedding of tiny diamond particles that are polished with a diamond paste. Hydrogen plays an important role in all of the growth methods as it prevents surface reconstruction from a saturated sp^3-hybridized diamond microstructure to an unsaturated sp^2-hybridized graphite microstructure; it also suppresses the formation of nondiamond carbon impurities, and it prevents several species from forming reactive radicals.

9.7.4 Electrodes for Corrosion Protection and Control

Apart from batteries, fuel cells, and industrial electrolyzers, corrosion protection and control is another field in which electrode materials occupy an important place.

147 Alehashem, S.; Chambers, F.; Strojek, J.W.; Swain, G.M.; Ramesham, R. (1995) New applications of diamond thin film technology in electro chemical systems. *Anal. Chem.*, **67**, 2812.

148 Angus, J.C.; Hayman, C.C. (1988) Low-pressure, metastable growth of diamond and "diamondlike" phases. *Science* **241**, 913–921.

149 Argoitia, A.; Angus, J.C.; Ma, J.S.; Wang, L.; Pirouz, P.; Lambrecht, W.R.L. (1994) Pseudomorphic stabilization of diamond on non-diamond substrates. *J. Mater. Res.*, **9**, 1849.

150 Vinokur, N.; Miller, B.; Avyigal, Y.; Kalish, R. (1996) Electrochemical behavior of boron-doped diamond electrodes. *J. Electrochem. Soc.*, **143**(10), L238–L240.

Table 9.22 Cathode materials for anodic protection. (From Locke, C.E. (1992) *Anodic Protection*. In: *ASM Metals Handbook*, 10th ed. *Vol. 9. Corrosion,* ASM, Materials Park, OH, pp. 463–465)

Cathode	Corrosive chemicals
Hastelloy® C	Nitrate aqueous solutions, sulfuric acid
Illium® G	Sulfuric acid (78–100 wt%), oleum
Nickel-plated steel	Electroless nickel plating solutions
Platinized copper or brass	Acids
Silicon-cast iron (Duriron®) ASTM A518 grade 3	Sulfuric acid (89–100 wt%), oleum
Stainless steels (AISI 304, 316L)	Nitrate aqueous solutions
Steel	Kraft digester liquid

9.7.4.1 Cathodes for Anodic Protection

Anodic protection[151] is a modern electrochemical technique for protecting metallic equipment used in the chemical-process industry against corrosion and handling highly corrosive chemicals (e.g., concentrated sulfuric and orthophosphoric acids). The technique consists in impressing a very low anodic current (i.e., usually 10 $\mu A \cdot m^{-2}$) on a piece of metallic equipment (e.g., tanks, thermowells, columns) to protect them against corrosion. This anodic polarization puts the electrochemical potential of the metal in the passivity region of its Pourbaix diagram (i.e., where the dissolution reaction does not occur), and hence this leads to a negligible corrosion rate (i.e., less than 25 μm/year). The anodic protection method can be used to protect only metals and alloys exhibiting a passive state (e.g., reactive and refractory metals, stainless steels) against corrosion. Usually, the equipment required is a cathode, a reference electrode, or a power supply. The various cathode materials used in anodic protection are listed in Table 9.22.

9.7.4.2 Anodes for Cathodic Protection

Cathodic protection is the cathodic polarization of a metal to maintain its immunity in a corrosive environment. There are two ways to achieve an efficient cathodic polarization. The first is a passive protection that consists in connecting electrically the metal to a less noble material that will result in a galvanic coupling of the two materials, which leads to the anodic dissolution of the ***sacrificial anode*** (see Table 9.23). The second method is an active protection that consists in using an impressed current power supply to polarize cathodically the workpiece versus a nonconsumable or inert anode (see Table 9.24).

9.7.5 Electrode Suppliers and Manufacturers

See Table 9.25.

151 Riggs, Jr., O.L.; Locke, C.E. (1981) Anodic Protection: Theory and Practice in the Prevention of Corrosion. Plenum, New York.

Table 9.23 Sacrificial anode materials. (Dreyman, E.W. (1973) Selection of anode materials. *Eng. Exp. Stn. Bull.* (West Virginia University), **110**, 83–89)

Sacrificial anode material	Oxidation reaction	Electrode potential at 298.15 K (E_0/mV vs SHE)	Capacity (Ah · kg^{-1})	Consumption rate (kg · A^{-1} · year^{-1})	Notes
Magnesium	Mg^0/Mg^{2+}	−2360	1100	7.9	Buried soils, suitable for high-resistivity environments. Unsuitable for marine applications because of high corrosion rate of magnesium in seawater
Zinc	Zn^0/Zn^{2+}	−760	810	10.7	Used in freshwater, brackish water, and marine water
Aluminum–zinc–mercury	Al^0/Al^{3+}	−1660	920–2600	3.0–3.2	Seawater, brines. Offshore and oil rigs, marine. Addition of In, Hg, and Sn prevents passivation
Aluminum–zinc–indium			1670–2400	3.6–5.2	
Aluminum–zinc–tin			2750–2840	3.4–9.4	

SHE standard hydrogen electrode

Table 9.24 Impressed-current anode materials. (Dreyman, E.W. (1973) Selection of anode materials. *Eng. Exp. Stn. Bull.* (West Virginia University), **110**, 83–89)

Anode material	Composition	Typical anodic current density ($A \cdot m^{-2}$)	Consumption rate ($g \cdot A^{-1} \cdot year^{-1}$)	Cost per unit surface area of 1-mm-thick anode (US$/$m^2$)	Notes
Dimensionally stable anodes (DSA®)	Ti/IrO_2 $Ti–Pd/IrO_2$ Nb/IrO_2 Ta/IrO_2	700–2000	< 1	9000 15,000 13,000 54,000	Cathodic protection of water tank and buried steel structures
Silicon–cast iron (Duriron®)	Fe-14.5Si-4.0Cr-0.8C-1.50Mn-0.5Cu-0.2Mo	10–40	200–500	500–1000	Both good corrosion and abrasion/wear resistance. Used extensively offshore, on oil rigs, and in other marine technology applications
Ebonex®	Ti_4O_7, Ti_5O_9	50 (naked) 2000 (IrO_2 coated)	n. a.	2000–3000	Corrosion resistant to both alkaline and acid media. Brittle and shock-sensitive material. Density 3600–4300 $kg \cdot m^{-3}$. Conductivity 30–300 S/cm
Graphite and carbon	Carbon	10–40	225–450		Brittle and shock-sensitive materials. Used extensively buried for cathodic protection of ground pipelines
Lead-alloy anodes	Pb-6Sb-1Ag/PbO_2	160–220	45–90	15–20	Cathodic protection for equipment immersed in seawater

Table 9.24 (*continued*)

Anode material	Composition	Typical anodic current density ($A \cdot m^{-2}$)	Consumption rate ($g \cdot A^{-1} \cdot year^{-1}$)	Cost per unit surface area of 1-mm-thick anode (US$/$m^2$)	Notes
Platinized titanium (K-type 70/30)	$Ti/70PtO_x\text{-}30IrO_2$	500–1000	18	15,000	Low consumption rate, high anodic current, but expensive
Platinized niobium and tantalum anodes	Nb/Pt–Ir, Ta/Pt–Ir	500–1000	1–6	40,000–60,000	Low consumption rate, high anodic current, but expensive
Ebonex®/polymer composite	Ti_4O_7 with conductive polymer binder	n. a.	n. a.	1000	Cathodic protection of reinforced steel bars in salt-contaminated concrete. Density 2300–2700 $kg \cdot m^{-3}$. Conductivity 1–10 S/cm

n. a. not available

Table 9.25 Industrial electrode manufacturers

Electrode supplier	Typical products and brand names	Contact address
Anomet Products	Pt/Nb/Cu, Pt/Ti/Cu	830 Boston Turnpike Road, Shrewsbury, MA 01545, USA Tel.: +1-508-8423069 Fax: +1-508-8420847 E-mail: info@anometproducts.com URL: ► http://www.anometproducts.com/
Anotec Industries	High-silicon cast iron anodes for impressed current	5701 Production Way, Langley, BC V3N 4N5, Canada Tel.: +1-604-5141544 Fax: +1-604-5141546 URL: ► http://anotec.com/
Ebonex Technologies Ltd (formerly Atraverda Ltd, Ebonex Technology Inc.)	Andersson–Magnéli phases, Ti_4O_7, Ebonex®	Units A & B, Roseheyworth Business Park, Abertillery NP13 1SX, UK Tel.:+44-1495-294026 Fax:+44-1495-294179 E-mail: info@atranova.com URL: ► http://www.ebonex.co.uk/
Chemapol Industries	Ti/RuO_2, Ti/IrO_2	55/A Alli Chamber, Tamarind Lane, Mumbai 400023, India Tel.: +91-22-641010 Fax: +91-22-653636 E-mail: chemapol@rediffmail.com
De Nora Elettrodi SpA	Ti/RuO_2, Ti/IrO_2, Nb/RuO_2, Ta/IrO_2	Via Bistolfi 35, 20134 Milan, Italy Tel.: +39-02-21291 Fax: +39-02-2154873 E-mail: info@uhdenora.com URL: ► http://www.denora.it/
De Nora Tech (formerly Eltech Systems Inc.)	DSA-Cl_2 and DSA-O_2, TIR® 2000, MOL™	100 Seventh Avenue, Suite 300, Chardon, OH 44024, USA Tel.: +1-440-2850300 Fax: 1-440-285-0302 URL: ► http://www.eltechsystems.com
DISA Anodes	Ti/RuO_2, Ti/IrO_2, Nb/RuO_2, Ta/IrO_2	7 Berg Street, Jeppestown, Johannesburg, South Africa Tel.: +27-11-6145238/+27-11-6145533 Fax: +27-11-6140093 E-mail: lorenzo@disaanodes.co.za URL: ► http://www.disaanodes.co.za
Electrochem Technologies & Materials Inc.	MMO, Ti/RuO_2, Ti/IrO_2, Nb/RuO_2, Ta/IrO2, Ti/PbO_2, Ti/MnO_2, Ti/SnO_2	Head office: 2037 Aird Avenue, Suite 201, Montreal, QC H1V 2V9, Canada Facilities: 75 Blvd de Mortagne CP 112, Boucherville QC J4B 6Y4, Canada E-mail: sales@electrochem-technologies.com URL: ► http://www.electrochem-technologies.com

Table 9.25 (*continued*)

Electrode supplier	Typical products and brand names	Contact address
Farwest Corrosion	Anodic, cathodic protection	1480 West Artesia Blvd, Gardena, CA 90248-3215, USA Tel.: +1-310-5329524 Fax: +1-310-5323934 E-mail: sales@farwestcorrosion.com
Magneto Special Anodes BV (formerly Magneto-Chemie) (acquired by Evoqua in 2016)	MMO, Ti/RuO_2, Ti/IrO_2, Nb/RuO_2, Ta/IrO2	Calandstraat 109, 3125 BA Schiedam, Netherlands Tel.: +31-10-2620788 Fax: +31-10-2620201 E-mail: info@magneto.nl URL: ► http://www.magneto.nl
NMT Electrodes South Africa	MMO, Ti/RuO_2, Ti/IrO_2	28 Hillclimb Road, Westmead, Pinetown 3610, South Africa Tel.: +27-31-7006110 Fax: +27-31-7006828 E-mail: stephen@nmtanodes.co.za URL: ► http://www.nmtelectrodes.com
NMT Electrodes Australia	MMO, Ti/RuO_2, Ti/IrO_2	Unit 2, 26 Baile Road, Canning Vale, WA 6155, Australia Tel.: +61-8-92564499 Fax: +61-8-92564599 E-mail: gareth@nmtelectrodes.com URL: ► http://www.nmtelectrodes.com
Optimum Anode Technologies	MMO, Ti/RuO_2, Ti/IrO_2, Nb/RuO_2, Ta/IrO2	Headquarters: Warren, NJ 07059, USA Facilities: 847 Flynn Road, Camarillo, CA 93012, USA Tel.: +1-805-4377435 Fax: +1-805-4845880 URL: ► http://www.optimumanodes.com
Republic Anode Fabricators	MMO, Ti/RuO_2, Ti/IrO_2	5478 Grafton road, Valley City, OH 44280, USA Tel.: +1-440-5725999 Fax: +1-440-5724499 URL: ► http://www.republicanodes.com
Permascand AB	MMO, Ti/RuO_2, Ti/IrO_2	P.O. Box 42, Ljungaverk, 840 10, Sweden Tel.: +46-691-35500 Fax: +46-691-33130 E-mail: info@permascand.se URL: ► http://www.permascand.com
EVOQUA Water Technologies (formerly US Filter Corporation and previously Electrode Products Inc.)	MMO, Ti/RuO_2, Ti/IrO_2	2 Milltown Court, Union, NJ 07083, USA Tel.: +1-908-8516924 Fax: +1-908-8516906 URL: ► www.evoqua.com

Table 9.25 (*continued*)

Electrode supplier	Typical products and brand names	Contact address
Ti Anode Fabricators (TAF)	MMO, Ti/RuO_2, Ti/IrO_2	# 48, Noothanchery, Madambakkam, Chennai 600073, India Tel.: +91-44-22781149 Fax: +91-44-22781362 E-mail: info@tianode.com URL: ► http://www.tianode.com
Titanium Equipment & Anode Manufacturing Company (TEAM)	MMO, Ti/RuO_2, Ti/IrO_2	TEAM House, Grand Southern Trunk Road, Vandalur, Chennai 600048, India Tel.: +91-44-22750323/+91-44-22750324 Fax: + 91-44-22750860 E-mail: team@drraoholdings.com URL: ► http://www.team.co.in/
Titaninum Tantalum Products (TiTaN)	MMO, Ti/RuO_2, Ti/IrO_2, Nb/RuO_2, Ta/IrO_2	86/1, Vengaivasal Main Road, Gowrivakkam, Chennai 601302, India Tel.: +91-44-22781210 Fax: +91-44-22780209 URL: ► http://www.titanindia.com/
Uyemura (Umicore)	Platinum anodes coated in molten cyanide baths	Headquarters: 3990 Concours, #425, Ontario, CA 91764, USA Tel.: +1-909-4665635 R&D Center: 240 Town Line Road, Southington, CT 06489, USA Tel.: +1-860-7934011 E-mail: sales@uyemura.com
Whizzo Science & Technology Development Co. Ltd	MMO, Ti/RuO_2, Ti/IrO_2	No. 83 Wencui Road, Shengyang, China Tel.: +86-24-24505855 Fax: +86-24-24503408 Email: whizzo@163.com URL: ► http://www.whizzo.com.cn

MMO mixed metal oxides

9.8 Electrochemical Galvanic Series

See ◘ Table 9.26.

9.9 Selected Standard Electrode Potentials

See ◘ Table 9.27.

9.10 Reference Electrodes Potentials

Selected electrochemical redox reactions with their standard electrode potentials are listed in ◘ Table 9.28.

◘ **Table 9.26** Galvanic series of metals and alloys in seawater

Corroded end (anodic or least noble)
Magnesium
Magnesium alloys
Zinc
Aluminum alloys 5052, 3004, 3003, 1100, 6053
Cadmium
Aluminum alloys 2117, 2017, 2024
Mild steel (AISI 1018), wrought iron
Cast iron, low-alloy high-strength steel
Chrome iron (active)
Stainless steel, AISI 430 series (active)
Stainless steels AISI 302, 303, 321, 347, 410, and 416 (active)
Ni-resist
Stainless steels AISI 316, 317 (active)
Carpenter 20Cb-3 (active)
Aluminum bronze (CA 687)
Hastelloy® C (active), Inconel® 625 (active), titanium (active)
Lead–tin solders
Lead
Tin
Inconel® 600 (active)
Nickel (active)

Table 9.26 (*continued*)

Corroded end (anodic or least noble)
60Ni-15Cr (active)
80Ni-20Cr (active)
Hastelloy® B (active)
Brasses
Copper (CDA 102)
Manganese bronze (CA 675), tin bronze (CA 903, CA 905)
Silicon bronze
Nickel silver
90Cu-10Ni
80Cu-20Ni
Stainless steel 430
Nickel, aluminum, bronze (CA 630, CA 632)
Monel® 400 and K500
Silver solder
Nickel 200 (passive)
60Ni-15Cr (passive)
Inconel® 600 (passive)
80Ni-20Cr (passive)
Cr–Fe (passive)
Stainless steel grades 302, 303, 304, 321, 347 (passive)
Stainless steel grades 316 and 317 (passive)
Carpenter 20 Cb-3 (passive), Incoloy® 825 and Ni-Mo-Cr-Fe alloy (passive)
Silver
Titanium (passive), Hastelloy® C276 (passive), Inconel® 625(passive)
Graphite
Zirconium
Gold
Platinum
Protected end (cathodic or noblest)

Table 9.27 Selected electrochemical redox reactions and standard electrode potential E_0

Electrochemical reaction	Standard electrode potential (V vs SHE)	Electrochemical reaction	Standard electrode potential (V vs SHE)
$N_2(g) + H^+ + e^- \rightarrow HN_3(aq)$	−3.090	$Ti^{3+} + 3e^- \rightarrow Ti(s)$	−1.210
$Li^+ + e^- \rightarrow Li(s)$	−3.0401	$Mn^{2+} + 2e^- \rightarrow Mn(s)$	−1.185
$N_2(g) + 4H_2O + 2e^- \rightarrow 2NH_2OH(aq) + 2OH^-$	−3.040	$Te(s) + 2e^- \rightarrow Te^{2-}$	−1.143
$Cs^+ + e^- \rightarrow Cs(s)$	−3.026	$V^{2+} + 2e^- \rightarrow V(s)$	−1.130
$Rb^+ + e^- \rightarrow Rb(s)$	−2.980	$Nb^{3+} + 3e^- \rightarrow Nb(s)$	−1.099
$K^+ + e^- \rightarrow K(s)$	−2.931	$Sn(s) + 4H^+ + 4e^- \rightarrow SnH_4(g)$	−1.070
$Ba^{2+} + 2e^- \rightarrow Ba(s)$	−2.912	$SiO_2(s) + 4H^+ + 4e^- \rightarrow Si(s) + 2H_2O$	−0.910
$La(OH)_3(s) + 3e^- \rightarrow La(s) + 3OH^-$	−2.900	$B(OH)_3(aq) + 3H^+ + 3e^- \rightarrow B(s) + 3H_2O$	−0.890
$Sr^{2+} + 2e^- \rightarrow Sr(s)$	−2.899	$TiO^{2+} + 2H^+ + 4e^- \rightarrow Ti(s) + H_2O$	−0.860
$Ca^{2+} + 2e^- \rightarrow Ca(s)$	−2.868	$2H_2O + 2e^- \rightarrow H_2(g) + 2OH^-$	−0.823
$Eu^{2+} + 2e^- \rightarrow Eu(s)$	−2.812	$Bi(s) + 3H^+ + 3e^- \rightarrow BiH_3$	−0.800
$Ra^{2+} + 2e^- \rightarrow Ra(s)$	−2.800	$Zn^{2+} + 2e^- \rightarrow Zn(Hg)$	−0.7628
$Na^+ + e^- \rightarrow Na(s)$	−2.710	$Zn^{2+} + 2e^- \rightarrow Zn(s)$	−0.7618
$La^{3+} + 3e^- \rightarrow La(s)$	−2.379	$Ta_2O_5(s) + 10H^+ + 10e^- \rightarrow 2Ta(s) + 5H_2O$	−0.750
$Y^{3+} + 3e^- \rightarrow Y(s)$	−2.372	$Cr^{3+} + 3e^- \rightarrow Cr(s)$	−0.740
$Mg^{2+} + 2e^- \rightarrow Mg(s)$	−2.372	$[Au(CN)_2]^- + e^- \rightarrow Au(s) + 2CN^-$	−0.600
$ZrO(OH)_2(s) + H_2O + 4e^- \rightarrow Zr(s) + 4OH^-$	−2.360	$Ta^{3+} + 3e^- \rightarrow Ta(s)$	−0.600
$Al(OH)_4^- + 3e^- \rightarrow Al(s) + 4OH^-$	−2.330	$PbO(s) + H_2O + 2e^- \rightarrow Pb(s) + 2OH^-$	−0.580
$Al(OH)_3(s) + 3e^- \rightarrow Al(s) + 3OH^-$	−2.310	$2TiO_2(s) + 2H^+ + 2e^- \rightarrow Ti_2O_3(s) + H_2O$	−0.560
$H_2(g) + 2e^- \rightarrow 2H^-$	−2.250	$Ga^{3+} + 3e^- \rightarrow Ga(s)$	−0.530
$Ac^{3+} + 3e^- \rightarrow Ac(s)$	−2.200	$U^{4+} + e^- \rightarrow U^{3+}$	−0.520
$Be^{2+} + 2e^- \rightarrow Be(s)$	−1.85	$H_3PO_2(aq) + H^+ + e^- \rightarrow P(white) + 2H_2O$	−0.508
$U^{3+} + 3e^- \rightarrow U(s)$	−1.660	$H_3PO_3(aq) + 2H^+ + 2e^- \rightarrow H_3PO_2(aq) + H_2O$	−0.499
$Al^{3+} + 3e^- \rightarrow Al(s)$	−1.660	$H_3PO_3(aq) + 3H^+ + 3e^- \rightarrow P(red) + 3H_2O$	−0.454
$Ti^{2+} + 2e^- \rightarrow Ti(s)$	−1.630	$Fe^{2+} + 2e^- \rightarrow Fe(s)$	−0.440

Table 9.27 (*continued*)

Electrochemical reaction	Standard electrode potential (V vs SHE)	Electrochemical reaction	Standard electrode potential (V vs SHE)
$ZrO_2(s) + 4H^+ + 4e^- \rightarrow Zr(s) + 2H_2O$	−1.553	$2CO_2(g) + 2H^+ + 2e^- \rightarrow H_2C_2O_4(aq)$	−0.430
$Zr^{4+} + 4e^- \rightarrow Zr(s)$	−1.450	$Cr^{3+} + e^- \rightarrow Cr^{2+}$	−0.420
$TiO(s) + 2H^+ + 2e^- \rightarrow Ti(s) + H_2O$	−1.310	$Cd^{2+} + 2e^- \rightarrow Cd(s)$	−0.400
$Ti_2O_3(s) + 2H^+ + 2e^- \rightarrow 2TiO(s) + H_2O$	−1.230	$GeO_2(s) + 2H^+ + 2e^- \rightarrow GeO(s) + H_2O$	−0.370
$Cu_2O(s) + H_2O + 2e^- \rightarrow 2Cu(s) + 2OH^-$	−0.360	$CO_2(g) + 2H^+ + 2e^- \rightarrow CO(g) + H_2O$	−0.110
$PbSO_4(s) + 2e^- \rightarrow Pb(s) + SO_4^{2-}$	−0.3588	$SnO(s) + 2H^+ + 2e^- \rightarrow Sn(s) + H_2O$	−0.100
$PbSO_4(s) + 2e^- \rightarrow Pb(Hg) + SO_4^{2-}$	−0.3505	$SnO_2(s) + 2H^+ + 2e^- \rightarrow SnO(s) + H_2O$	−0.090
$Eu^{3+} + e^- \rightarrow Eu^{2+}$	−0.350	$WO_3(aq) + 6H^+ + 6e^- \rightarrow W(s) + 3H_2O$	−0.090
$In^{3+} + 3e^- \rightarrow In(s)$	−0.340	$P(white) + 3H^+ + 3e^- \rightarrow PH_3(g)$	−0.063
$Tl^+ + e^- \rightarrow Tl(s)$	−0.340	$HCOOH(aq) + 2H^+ + 2e^- \rightarrow HCHO(aq) + H_2O$	−0.030
$Ge(s) + 4H^+ + 4e^- \rightarrow GeH_4(g)$	−0.290	$2H^+ + 2e^- \rightarrow H_2(g)$ (reference)	0.000
$Co^{2+} + 2e^- \rightarrow Co(s)$	−0.280	$AgBr(s) + e^- \rightarrow Ag(s) + Br^-$	+0.071
$H_3PO_4(aq) + 2H^+ + 2e^- \rightarrow H_3PO_3(aq) + H_2O$	−0.276	$S_4O_6^{2-} + 2e^- \rightarrow 2S_2O_3^{2-}$	+0.080
$V^{3+} + e^- \rightarrow V^{2+}$	−0.260	$Fe_3O_4(s) + 8H^+ + 8e^- \rightarrow 3Fe(s) + 4H_2O$	+0.085
$Ni^{2+} + 2e^- \rightarrow Ni(s)$	−0.250	$N_2(g) + 2H_2O + 6H^+ + 6e^- \rightarrow 2NH_4OH(aq)$	+0.092
$As(s) + 3H^+ + 3e^- \rightarrow AsH_3(g)$	−0.230	$HgO(s) + H_2O + 2e^- \rightarrow Hg(l) + 2OH^-$	+0.098
$AgI(s) + e^- \rightarrow Ag(s) + I^-$	−0.152	$Cu(NH_3)_4^{2+} + e^- \rightarrow Cu(NH_3)_2^+ + 2NH_3$	+0.100
$MoO_2(s) + 4H^+ + 4e^- \rightarrow Mo(s) + 2H_2O$	−0.150	$Ru(NH_3)_6^{3+} + e^- \rightarrow Ru(NH_3)_6^{2+}$	+0.100
$Si(s) + 4H^+ + 4e^- \rightarrow SiH_4(g)$	−0.140	$N_2H_4(aq) + 4H_2O + 2e^- \rightarrow 2NH_4^+ + 4OH^-$	+0.110
$Sn^{2+} + 2e^- \rightarrow Sn(s)$	−0.130	$H_2MoO_4(aq) + 6H^+ + 6e^- \rightarrow Mo(s) + 4H_2O$	+0.110
$O_2(g) + H^+ + e^- \rightarrow HO_2 \cdot (aq)$	−0.130	$Ge^{4+} + 4e^- \rightarrow Ge(s)$	+0.120

Table 9.27 (*continued*)

Electrochemical reaction	Standard electrode potential (V vs SHE)	Electrochemical reaction	Standard electrode potential (V vs SHE)
$Pb^{2+} + 2e^- \rightarrow Pb(s)$	−0.130	$C(s) + 4H^+ + 4e^- \rightarrow CH_4(g)$	+0.130
$WO_2(s) + 4H^+ + 4e^- \rightarrow W(s) + 2H_2O$	−0.120	$HCHO(aq) + 2H^+ + 2e^- \rightarrow CH_3OH(aq)$	+0.130
$P(red) + 3H^+ + 3e^- \rightarrow PH_3(g)$	−0.111	$S(s) + 2H^+ + 2e^- \rightarrow H_2S(g)$	+0.140
$CO_2(g) + 2H^+ + 2e^- \rightarrow HCOOH(aq)$	−0.110	$Sn^{4+} + 2e^- \rightarrow Sn^{2+}$	+0.150
$Se(s) + 2H^+ + 2e^- \rightarrow H_2Se(g)$	−0.110	$Cu^{2+} + e^- \rightarrow Cu^+$	+0.159
$HSO_4^- + 3H^+ + 2e^- \rightarrow SO_2(aq) + 2H_2O$	+0.160	$I_3^- + 2e^- \rightarrow 3I^-$	+0.530
$UO_2^{2+} + e^- \rightarrow UO_2^+$	+0.163	$[AuI_4]^- + 3e^- \rightarrow Au(s) + 4I^-$	+0.560
$SO_4^{2-} + 4H^+ + 2e^- \rightarrow SO_2(aq) + 2H_2O$	+0.170	$H_3AsO_4(aq) + 2H^+ + 2e^- \rightarrow H_3AsO_3(aq) + H_2O$	+0.560
$TiO^{2+} + 2H^+ + e^- \rightarrow Ti^{3+} + H_2O$	+0.190	$[AuI_2]^- + e^- \rightarrow Au(s) + 2I^-$	+0.580
$Bi^{3+} + 2e^- \rightarrow Bi^+$	+0.200	$MnO_4^- + 2H_2O + 3e^- \rightarrow MnO_2(s) + 4OH^-$	+0.590
$SbO^+ + 2H^+ + 3e^- \rightarrow Sb(s) + H_2O$	+0.200	$S_2O_3^{2-} + 6H^+ + 4e^- \rightarrow 2S(s) + 3H_2O$	+0.600
$AgCl(s) + e^- \rightarrow Ag(s) + Cl^-$	+0.222	$H_2MoO_4(aq) + 2H^+ + 2e^- \rightarrow MoO_2(s) + 2H_2O$	+0.650
$H_3AsO_3(aq) + 3H^+ + 3e^- \rightarrow As(s) + 3H_2O$	+0.240	$Quinoline + 2H^+ + 2e^- \rightarrow hydroxyquinoline$	+0.699
$GeO(s) + 2H^+ + 2e^- \rightarrow Ge(s) + H_2O$	+0.260	$O_2(g) + 2H^+ + 2e^- \rightarrow H_2O_2(aq)$	+0.700
$UO_2^+ + 4H^+ + e^- \rightarrow U^{4+} + 2H_2O$	+0.273	$Tl^{3+} + 3e^- \rightarrow Tl(s)$	+0.720
$Re^{3+} + 3e^- \rightarrow Re(s)$	+0.300	$PtCl_6^{2-} + 2e^- \rightarrow PtCl_4^{2-} + 2Cl^-$	+0.726
$Bi^{3+} + 3e^- \rightarrow Bi(s)$	+0.320	$H_2SeO_3(aq) + 4H^+ + 4e^- \rightarrow Se(s) + 3H_2O$	+0.740
$VO^{2+} + 2H^+ + e^- \rightarrow V^{3+} + H_2O$	+0.340	$PtCl_4^{2-} + 2e^- \rightarrow Pt(s) + 4Cl^-$	+0.758
$Cu^{2+} + 2e^- \rightarrow Cu(s)$	+0.340	$Fe^{3+} + e^- \rightarrow Fe^{2+}$	+0.770
$[Fe(CN)_6]^{3-} + e^- \rightarrow [Fe(CN)_6]^{4-}$	+0.360	$Ag^+ + e^- \rightarrow Ag(s)$	+0.800
$O_2(g) + 2H_2O + 4e^- \rightarrow 4OH^-(aq)$	+0.400	$Hg_2^{2+} + 2e^- \rightarrow 2Hg(l)$	+0.800
$H_2MoO_4 + 6H^+ + 3e^- \rightarrow Mo^{3+} + 2H_2O$	+0.430	$NO_3^-(aq) + 2H^+ + e^- \rightarrow NO_2(g) + H_2O$	+0.800
$Bi^+ + e^- \rightarrow Bi(s)$	+0.500	$[AuBr_4]^- + 3e^- \rightarrow Au(s) + 4Br^-$	+0.850
$CH_3OH(aq) + 2H^+ + 2e^- \rightarrow CH_4(g) + H_2O$	+0.500	$Hg^{2+} + 2e^- \rightarrow Hg(l)$	+0.850

Table 9.27 (*continued*)

Electrochemical reaction	Standard electrode potential (V vs SHE)	Electrochemical reaction	Standard electrode potential (V vs SHE)
$SO_2(aq) + 4H^+ + 4e^- \rightarrow S(s) + 2H_2O$	+0.500	$MnO_4^- + H^+ + e^- \rightarrow HMnO_4^-$	+0.900
$Cu^+ + e^- \rightarrow Cu(s)$	+0.520	$2Hg^{2+} + 2e^- \rightarrow Hg_2^{2+}$	+0.910
$CO(g) + 2H^+ + 2e^- \rightarrow C(s) + H_2O$	+0.520	$Pd^{2+} + 2e^- \rightarrow Pd(s)$	+0.915
$I_2(s) + 2e^- \rightarrow 2I^-$	+0.540	$[AuCl_4]^- + 3e^- \rightarrow Au(s) + 4Cl^-$	+0.930
$MnO_2(s) + 4H^+ + e^- \rightarrow Mn^{3+} + 2H_2O$	+0.950	β-$PbO_2(s) + 4H^+ + 2e^- \rightarrow Pb^{2+} + 2H_2O$	+1.460
$[AuBr_2]^- + e^- \rightarrow Au(s) + 2Br^-$	+0.960	α-$PbO_2(s) + 4H^+ + 2e^- \rightarrow Pb^{2+} + 2H_2O$	+1.468
$Br_2(l) + 2e^- \rightarrow 2Br^-$	+1.066	$2BrO_3^- + 12H^+ + 10e^- \rightarrow Br_2(l) + 6H_2O$	+1.480
$Br_2(aq) + 2e^- \rightarrow 2Br^-$	+1.087	$2ClO_3^- + 12H^+ + 10e^- \rightarrow Cl_2(g) + 6H_2O$	+1.490
$IO_3^- + 5H^+ + 4e^- \rightarrow HIO(aq) + 2H_2O$	+1.130	$MnO_4^- + 8H^+ + 5e^- \rightarrow Mn^{2+} + 4H_2O$	+1.510
$[AuCl_2]^- + e^- \rightarrow Au(s) + 2Cl^-$	+1.150	$HO_2\cdot + H^+ + e^- \rightarrow H_2O_2(aq)$	+1.510
$HSeO_4^- + 3H^+ + 2e^- \rightarrow H_2SeO_3(aq) + H_2O$	+1.150	$Au^{3+} + 3e^- \rightarrow Au(s)$	+1.520
$Ag_2O(s) + 2H^+ + 2e^- \rightarrow 2Ag(s) + H_2O$	+1.170	$NiO_2(s) + 4H^+ + 2e^- \rightarrow Ni^{2+} + 2OH^-$	+1.590
$ClO_3^- + 2H^+ + e^- \rightarrow ClO_2(g) + H_2O$	+1.180	$2HClO(aq) + 2H^+ + 2e^- \rightarrow Cl_2(g) + 2H_2O$	+1.630
$Pt^{2+} + 2e^- \rightarrow Pt(s)$	+1.188	$Ag_2O_3(s) + 6H^+ + 4e^- \rightarrow 2Ag^+ + 3H_2O$	+1.670
$ClO_2(g) + H^+ + e^- \rightarrow HClO_2(aq)$	+1.190	$HClO_2(aq) + 2H^+ + 2e^- \rightarrow HClO(aq) + H_2O$	+1.670
$2IO_3^- + 12H^+ + 10e^- \rightarrow I_2(s) + 6H_2O$	+1.200	$Pb^{4+} + 2e^- \rightarrow Pb^{2+}$	+1.690
$ClO_4^- + 2H^+ + 2e^- \rightarrow ClO_3^- + H_2O$	+1.200	$MnO_4^- + 4H^+ + 3e^- \rightarrow MnO_2(s) + 2H_2O$	+1.700
$O_2(g) + 4H^+ + 4e^- \rightarrow 2H_2O$	+1.230	$H_2O_2(aq) + 2H^+ + 2e^- \rightarrow 2H_2O$	+1.780
$MnO_2(s) + 4H^+ + 2e^- \rightarrow Mn^{2+} + 2H_2O$	+1.230	$AgO(s) + 2H^+ + e^- \rightarrow Ag^+ + H_2O$	+1.770
$Tl^{3+} + 2e^- \rightarrow Tl^+$	+1.250	$Co^{3+} + e^- \rightarrow Co^{2+}$	+1.820
$Cl_2(g) + 2e^- \rightarrow 2Cl^-$	+1.360	$Au^+ + e^- \rightarrow Au(s)$	+1.830
$Cr_2O_7^- + 14H^+ + 6e^- \rightarrow 2Cr^{3+} + 7H_2O$	+1.330	$BrO_4^- + 2H^+ + 2e^- \rightarrow BrO_3^- + H_2O$	+1.850
$CoO_2(s) + 4H^+ + e^- \rightarrow Co^{3+} + 2H_2O$	+1.420	$HSO_5^- + 2H^+ + 2e^- \rightarrow HSO_4^- + H_2O$	+1.850

Table 9.27 (*continued*)

Electrochemical reaction	Standard electrode potential (V vs SHE)	Electrochemical reaction	Standard electrode potential (V vs SHE)
$2NH_3OH^+ + H^+ + 2e^- \rightarrow N_2H_5^+ + 2H_2O$	+1.420	$Ag^{2+} + e^- \rightarrow Ag^+$	+1.980
$2HIO(aq) + 2H^+ + 2e^- \rightarrow I_2(s) + 2H_2O$	+1.440	$S_2O_8^{2-} + 2e^- \rightarrow 2SO_4^{2-}$	+2.010
$Ce^{4+} + e^- \rightarrow Ce^{3+}$	+1.440	$O_3(g) + 2H^+ + 2e^- \rightarrow O_2(g) + H_2O$	+2.075
$BrO_3^- + 5H^+ + 4e^- \rightarrow HBrO(aq) + 2H_2O$	+1.450	$HMnO_4^- + 3H^+ + 2e^- \rightarrow MnO_2(s) + 2H_2O$	+2.090
$F_2(g) + 2e^- \rightarrow 2F^-$	+2.870	$F_2(g) + 2H^+ + 2e^- \rightarrow 2HF(aq)$	+3.050
SHE standard hydrogen electrode			

Table 9.28 Selected reference electrode potentials

Electrochemical half-cell	Acronym	Electrode potential
Mercury/mercurous chloride (calomel)		
Hg/Hg_2Cl_2//KCl (saturated)	SCE	+0.24453 V/SHE
Hg/Hg_2Cl_2//NaCl (saturated)	NaSCE	+0.2360 V/SHE
Hg/Hg_2Cl_2//KCl (3.5 M)	n. a.	+0.2501 V/SHE
Hg/Hg_2Cl_2//KCl (1 N)	NCE	+0.2830 V/SHE
Hg/Hg_2Cl_2/KCl (0.1 N)	DNCE	+0.3356 V/SHE
Silver/silver chloride		
Ag/AgCl//KCl (saturated)	SSCE	+0.198 V/SHE
Ag/AgCl//NaCl (saturated)	NaSSCE	+0.197 V/SHE
Ag/AgCl//KCl (3.5 M)	n. a.	+0.205 V/SHE
Ag/AgCl//KCl (3.0 M)	n. a.	+0.208 V/SHE
Ag/AgCl//KCl (1 N)	NSCE	+0.22234 V/SHE
Ag/AgCl//KCl (seawater)	SWSSCE	+0.250 V/SHE
Ag/AgCl//KCl (0.1 N)	DNSSCE	+0.2881 V/SHE
Mercury/mercurous sulfate		
$Hg/Hg_2SO_4//K_2SO_4$ (saturated)	SMSE	+0.658 V/SHE
$Hg/Hg_2SO_4//H_2SO_4$ (30 wt%)	MSE	+0.635 V/SHE
$Hg/Hg_2SO_4//K_2SO_4$ (1 M)	MMSE	+0.674 V/SHE
$Hg/Hg_2SO_4//K_2SO_4$ (0.5 M)	NMSE	+0.682 V/SHE

Table 9.28 (*continued*)

Electrochemical half-cell	Acronym	Electrode potential
Silver/silver sulfate		
$Ag/Ag_2SO_4//K_2SO_4$ (saturated)	SSSE	+0.690 V/SHE
$Ag/_2SO_4//H_2SO_4$ (1 M)	MSSE	+0.710 V/SHE
$Ag/_2SO_4//H_2SO_4$ (0.5 M)	NSSE	+0.720 V/SHE
Mercury/mercuric oxide		
Hg/HgO//KOH (20 wt%)	MOE	+0.098 V/SHE
Hg/HgO//NaOH (1 M)	NaMOE	+0.140 V/SHE
Hg/HgO//NaOH (0.1 M)		+0.165 V/SHE
Copper/copper sulfate		
$Cu/CuSO_4$ (saturated)	SCSE	+0.316 V/SHE

DNCE decinormal calomel electrode, *DNSSCE* decinormal silver–silver chloride electrode, *MMSE* molar mercury sulfate electrode, *MOE* mercuric oxide electrode, *MSE* mercury sulfate electrode, *MSSE* molar standard silver sulfate electrode, *NaMOE* sodium mercuric oxide electrode, *NaSCE* sodium calomel electrode, *NCE* normal calomel electrode, *NMSE* normal mercury sulfate electrode, *NSSCE* normal silver–silver chloride electrode, *NSSE* normal silver sulfate electrode, *SCE* standard calomel electrode, *SCSE* standard copper sulfate electrode, *SHE* standard hydrogen electrode, *SMSE* standard mercury sulfate electrode, *SSCE* silver–silver chloride electrode, *SSSE* standard silver sulfate electrode, *SWSSCE* seawater silver–silver chloride electrode

9.11 Ampacity or Maximum Carrying Current

The ***maximum carrying current*** of an electrical conductor in the form of a wire or cable is called either the ***current rating*** or the ***ampacity*** by electrical engineers. Ampacities are closely related to the maximum temperature elevation the wire or cable can sustain without its electrical resistivity being affected and without the insulating material that forms the protective sheath being damaged. Therefore, the ampacity of a given conductor strongly depends on the intrinsic properties of the constituting material, such as its electrical resistivity, its thermal conductivity, its specific heat capacity, and its temperature of fusion, and also external factors, such as the nature of the insulating sheath materials and the type of external cooling (e.g., natural or forced cooling) provided.

The calculation of ampacities is extremely important for sizing the current collectors in the secondary circuit of a transformer as a large electric current of several thousand amperes circulates.

Primarily for reasons of safety, and mostly on the basis of practice and experiments, electrical engineers have developed guidance for selection of the proper wire or cable to carry safely an electric current and have established certain standards for electrical wiring, such as those specified in the National Electrical Code in the USA. Typical National Electrical Code wire ampacity tables will show allowable maximum currents for different sizes and applications of wire.

Although the melting point of copper theoretically imposes a limit on wire ampacity, the materials commonly used for insulating conductors melt at temperatures far below the melting point of copper, and so practical ampacity ratings are based on the thermal limits of the insulation. Voltage dropped as a result of excessive wire resistance is also a factor in

Table 9.29 Ampacities of conductors

Conductor type	Maximum ampacity (kA/m^2)	Empirical equation[a]
Self-baking Søderberg electrodes	40–50	$I = C_k(R_{ac}/R_{dc})^{-0.5}D^{3/2}$
Prebaked carbon electrode	60	
Graphite electrodes	280	$I = 170D^{1/2}$
Copper bus bars (air-cooled)	2820	
Copper bus bars (water-cooled)	4500	

[a] I is total electric current in kiloamperes, C_k is the electrode load factor (ranging 50–65 kA · m$^{2/3}$), R_{ac} and R_{dc} are the electrical resistances in milliohms for alternating current and direct current respectively, and D is the outer diameter in meters

sizing conductors for their use in circuits, but this consideration is better assessed through more complex means. It is not the intention in this handbook to disclose the ampacities of all types of conductors but the intention is rather to provide the reader with practical rules to evaluate the ampacities of bare copper conductors such as those used in electrochemical and electrothermal equipment.

For instance, for bare copper wires or cables, the **adopted value for a maximum carrying current** is given as 1 A for a wire with a cross section of **700 cmil** (i.e., a wire diameter of 0.0265 in); that is, a maximum current density of **2.82 A/mm^2**.

However, if the copper wire or cable is **water-cooled**, the ampacity can be increased up to 1 A for a wire with a cross section of **438.5 cmil** (i.e., a wire of diameter 0.021 in); that is, until a maximum current density of **4.50 A/mm^2**.

For large **graphite electrodes** such as those used in electric arc furnaces, the maximum carrying current adopted is usually **285 kA/m^2** (or **0.28 A/mm^2**). See also Table 9.29.

9.11.1 Maximum Frequency for Penetration

The depth of penetration (i.e., skin effect) produced by an alternating electric current circulating in a wire is given by the following equation.

$$\delta = (\rho/\pi\mu_0\mu_r f)^{1/2},$$

where δ is the depth of penetration in meters, μ_0 is the permeability of a vacuum in henries per meter, μ_r is the relative magnetic permeability, and f is the frequency in hertz.

Therefore, the maximum frequency to reach the core of the wire having a diameter D is given by

$$f = 4\rho/(\pi\mu_0\mu_r D^2).$$

For a bare and pure copper wire with diameter D, electrical resistivity of 1.7241 mW · cm, and a magnetic permeability of $4\pi \times 10^{-7}$ H/m, the maximum frequency is given by

$$f = 0.017469/D^2.$$

The ampacities, maximum frequencies, and linear resistance of pure copper wires for different American wire gauges are given ◘ Table 9.30.

9.11.2 Maximum Current and Cable Temperature

When a long wire of outer diameter D and length L, both in meters, made of a conducting metal or alloy with electrical resistivity ρ_e ($\Omega \cdot m$), mass density ρ_m (kg/m^3), specific heat capacity c_p ($J \cdot kg^{-1} \cdot K^{-1}$), and spectral emissivity ε is in thermal equilibrium with its surroundings at a temperature T_s (in kelvins), as soon an electric current I (in amperes), circulates through the circuit, Joule heating increases the wire temperature, while the wire exchanges heat with the surroundings concurrently by conduction, convection, and radiation.

When the steady state is reached, the wire exhibits the maximum temperature for the given electric current. The equation that governs the maximum temperature of the wire due to the passage of current as a function of the previous physical quantities and also based on the convection heat transfer coefficient is given by the overall energy balance per unit time; that is, the overall rate of energy change equals the energy produced within the system (i.e., Joule heating) less the rate of energy absorbed by the system less the rate of energy leaving the system due to losses by conduction, convection, and radiation:

9

$$dE/dt = dE/dt\,(\text{in}) - dE/dt\,(\text{out}) + S.$$

The rate at which energy is produced is mainly due to Joule heating, RI^2, with the electrical resistance for a cylindrical body given by $R = \rho_e(4L/\pi D^2)$, the rate at which energy is lost by convection follows Newton's convection equation, $h\pi LD(T - T_s)$, and the rate at which energy is lost by radiation is given by the Stefan–Boltzmann equation, $\varepsilon\sigma\pi LD(T^4 - T_s^4)$.

The overall energy balance per unit time is given by the following equation:

$$dE/dt = \rho_m(\pi LD^2/4)c_p\,d(T - T_0)/dt = RI^2 - h\pi LD(T - T_s) - \varepsilon\sigma\pi LD(T^4 - T_s^4).$$

Therefore, the temperature change per unit time is given by the following equation:

$$dT/dt = [\rho_e(4L/\pi D^2)I^2 - h\pi LD(T - T_s) - \varepsilon\sigma\pi LD(T^4 - T_s^4)]/[\rho_m(\pi LD^2/4)c_p].$$

These equations can be solved by numerical integration.

For most practical situations, once the steady state is reached, the right term becomes zero, and the temperature of the wire is maximum for the given current:

$$\rho_e(4/\pi^2 D^2)I^2 = hD(T_{max} - T_s) + \varepsilon\sigma D(T_{max}^4 - T_s^4).$$

To be even more rigorous, the temperature dependence of the resistivity for metals, $\rho_e(T) = \rho_e[1 + \alpha(T_{max} - T_s)]$, must be considered. Then it is possible to rewrite the equation in the steady-state condition as follows:

$$\rho_e[1 + \alpha(T_{max} - T_s)](4/\pi^2 D^2)I^2 = hD(T_{max} - T_s) + \varepsilon\sigma D(T_{max}^4 - T_s^4).$$

Table 9.30 Ampacities of electrical wire

AWG	Conductor outer diameter (in)	Conductor diameter (mm)	Linear resistance (Ω/1000 ft)	Linear resistance (Ω/km)	Maximum ampacity for chassis wiring (A)	Maximum ampacity for power transmission (A)	Maximum frequency 100% depth
0000	0.4600	11.6840	0.049	0.16072	380	302	125 Hz
000	0.4096	10.4038	0.0618	0.202704	328	239	160 Hz
00	0.3648	9.2659	0.0779	0.255512	283	190	200 Hz
0	0.3249	8.2525	0.0983	0.322424	245	150	250 Hz
1	0.2893	7.3482	0.1239	0.406392	211	119	325 Hz
2	0.2576	6.5430	0.1563	0.512664	181	94	410 Hz
3	0.2294	5.8268	0.197	0.64616	158	75	500 Hz
4	0.2043	5.1892	0.2485	0.81508	135	60	650 Hz
5	0.1819	4.6203	0.3133	1.027624	118	47	810 Hz
6	0.1620	4.1148	0.3951	1.295928	101	37	1100 Hz
7	0.1443	3.6652	0.4982	1.634096	89	30	1300 Hz
8	0.1285	3.2639	0.6282	2.060496	73	24	1650 Hz
9	0.1144	2.9058	0.7921	2.598088	64	19	2050 Hz
10	0.1019	2.5883	0.9989	3.276392	55	15	2600 Hz
11	0.0907	2.3038	1.26	4.1328	47	12	3200 Hz
12	0.0808	2.0523	1.588	5.20864	41	9.3	4150 Hz
13	0.0720	1.8288	2.003	6.56984	35	7.4	5300 Hz
14	0.0641	1.6281	2.525	8.282	32	5.9	6700 Hz
15	0.0571	1.4503	3.184	10.44352	28	4.7	8250 Hz
16	0.0508	1.2903	4.016	13.17248	22	3.7	11 kHz
17	0.0453	1.1506	5.064	16.60992	19	2.9	13 kHz
18	0.0403	1.0236	6.385	20.9428	16	2.3	17 kHz
19	0.0359	0.9119	8.051	26.40728	14	1.8	21 kHz
20	0.0320	0.8128	10.15	33.292	11	1.5	27 kHz
21	0.0285	0.7239	12.8	41.984	9	1.2	33 kHz
22	0.0254	0.6452	16.14	52.9392	7	0.92	42 kHz
23	0.0226	0.5740	20.36	66.7808	4.7	0.729	53 kHz
24	0.0201	0.5105	25.67	84.1976	3.5	0.577	68 kHz
25	0.0179	0.4547	32.37	106.1736	2.7	0.457	85 kHz
26	0.0159	0.4039	40.81	133.8568	2.2	0.361	107 kHz

Table 9.30 (*continued*)

AWG	Conductor outer diameter (in)	Conductor diameter (mm)	Linear resistance (Ω/1000 ft)	Linear resistance (Ω/km)	Maximum ampacity for chassis wiring (A)	Maximum ampacity for power transmission (A)	Maximum frequency 100% depth
27	0.0142	0.3607	51.47	168.8216	1.7	0.288	130 kHz
28	0.0126	0.3200	64.9	212.872	1.4	0.226	170 kHz
29	0.0113	0.2870	81.83	268.4024	1.2	0.182	210 kHz
30	0.0100	0.2540	103.2	338.496	0.86	0.142	270 kHz
31	0.0089	0.2261	130.1	426.728	0.7	0.113	340 kHz
32	0.0080	0.2032	164.1	538.248	0.53	0.091	430 kHz
Metric 2.0	0.0079	0.2000	169.39	555.61	0.51	0.088	440 kHz
33	0.0071	0.1803	206.9	678.632	0.43	0.072	540 kHz
Metric 1.8	0.0071	0.1800	207.5	680.55	0.43	0.072	540 kHz
34	0.0063	0.1600	260.9	855.752	0.33	0.056	690 kHz
Metric 1.6	0.0063	0.1600	260.9	855.752	0.33	0.056	690 kHz
35	0.0056	0.1422	329	1079.12	0.27	0.044	870 kHz
Metric 1.4	0.0055	0.1400	339	1114	0.26	0.043	900 kHz
36	0.0050	0.1270	414.8	1360	0.21	0.035	1100 kHz
Metric 1.25	0.0049	0.1250	428.2	1404	0.2	0.034	1150 kHz
37	0.0045	0.1143	523.1	1715	0.17	0.0289	1350 kHz
Metric 1.12	0.0044	0.1120	533.8	1750	0.163	0.0277	1400 kHz
38	0.0040	0.1016	659.6	2163	0.13	0.0228	1750 kHz
Metric 1	0.0039	0.1000	670.2	2198	0.126	0.0225	1750 kHz
39	0.0035	0.0889	831.8	2728	0.11	0.0175	2250 kHz
40	0.0031	0.0787	1049	3440	0.09	0.0137	2900 kHz

AWG American wire gauge

The preceding general equation can be rewritten as the biquadratic (i.e., quartic) equation

$$T_{\max}^4 + \{(h/\varepsilon\sigma) - [4\alpha\rho_e/(\varepsilon\sigma\pi^2 D^3)]I^2\}T_{\max} = [4\rho_e/(\varepsilon\sigma\pi^2 D^3)](1 - \alpha T_s)I^2 + T_s^4 + (h/\varepsilon\sigma)T_s.$$

Table 9.31 Biquadratic equations and maximum temperature for a chemically pure titanium wire

Electric current (*I*/A)	Biquadratic equation	Maximum temperature
100	$T_{max}^4 + 2.40 \times 10^8 T_{max} = 3.66 \times 10^{12}$	$T_{max} = 1352$ K = 1079 °C
50	$T_{max}^4 + 3.91 \times 10^8 T_{max} = 9.21 \times 10^{11}$	$T_{max} = 873$ K = 600 °C
25	$T_{max}^4 + 4.28 \times 10^8 T_{max} = 2.36 \times 10^{11}$	$T_{max} = 455$ K = 182 °C

Then in the simplified form, it becomes

$$T_{max}^4 + (A - BI^2)T_{max} = CI^2 + T_s^4 + AT_s,$$

with the constants $A = (h/\varepsilon\sigma)$, $B = [4\alpha\rho_e/(\varepsilon\sigma\pi^2 D^3)]$, and $C = [4\rho_e/(\varepsilon\sigma\pi^2 D^3)](1 - \alpha T_s)$.

Let us consider a chemically pure titanium wire slightly oxidized with a mass density of 4540 kg · m^{-3}, spectral emissivity of 0.80, electrical resistivity of 56 μΩ · cm with a temperature coefficient 5.42×10^{-5} K^{-1}, and an outer diameter of 2.38 mm in a surrounding atmosphere at 293.15 K with a natural convection heat transfer coefficient of 20 W · m^{-2} · K^{-1}. With a circulating current of 25, 50, and 100 A, we can then determine the two maximum temperatures of the wire by solving the following biquadratic equation by successive iterations:

$$T_{max}^4 + (4.41 \times 10^8 - 2 \times 10^4 I^2)T_{max} = 3.65 \times 10^8 I^2 + 7.83 \times 10^9.$$

The results are reported in Table 9.31.

9.11.3 Fusing Current

From the previous equation, assuming that for a maximum temperature equal to the temperature of fusion (i.e., melting point) of the metal or alloy, the corresponding current is called the ***fusing current***, I_{fusing} (in amperes), and it is obtained from

$$T_{fusion}^4 - T_s^4 - A(T_{fusion} - T_s) = (BT_{fusion} + C)I_{fusing}^2,$$
$$I_{fusing}^2 = [T_{fusion}^4 - T_s^4 - A(T_{fusion} - T_s)]/(BT_{fusion} + C).$$

As the two constants B and C are a function of D^{-3}, we can see that the fusing current is then a function of $D^{3/2}$.

$$I_{fusing}^2 = ((\varepsilon\sigma\pi^2/4\rho_e)\{[T_{fusion}^4 - T_s^4 - (h/\varepsilon\sigma)(T_{fusion} - T_s)]/(2 - \alpha T_s)\})D^3$$
$$I_{fusing} = ((\varepsilon\sigma\pi^2/4\rho_e)\{[T_{fusion}^4 - T_s^4 - (h/\varepsilon\sigma)(T_{fusion} - T_s)]/(2 - \alpha T_s)\})^{1/2} D^{3/2}$$

This dependence was obtained empirically from experiments that were conducted by H.W. Preece in 1884, and it is given in its simplest form as

$$I_{fusing} = k \times D^{3/2}$$